

**Experimental studies on the tumor
suppressor *p53*, the *myc* proto-oncogene
and tissue compatibility in the basal
metazoan phylum Placozoa**

Von der Naturwissenschaftlichen Fakultät
der Gottfried Wilhelm Leibniz Universität Hannover
zur Erlangung des Grades
Doktorin der Naturwissenschaften
Dr. rer. nat.
genehmigte Dissertation

von

Dipl.-Biol. Karolin Ursula Luise von der Chevallerie
geboren am 22. Dezember 1981 in Großburgwedel

2013

Referent: Prof. Dr. Bernd Schierwater
Korreferent: Prof. Dr. Dieter Steinhagen
Tag der Promotion: 12.12.2013

Dedicated to my family.

Zusammenfassung

Ein maßgeblicher Schritt der Evolution bestand im Zusammenschluss einzelliger Organismen (Protozoen) zu Vielzellern (Metazoen). Er ermöglichte die Ausdifferenzierung diverser Zelltypen und Gewebe, die dann für unterschiedlichste Ansprüche spezialisiert wurden. Die Entstehung einer solchen Komplexität brachte jedoch die Notwendigkeit mit sich, molekulare Instrumente zu entwickeln welche das zelluläre Gleichgewicht innerhalb eines Gewebes aufrechterhalten und die Integrität jedes Organismus schützen können. Der Zellzyklus (der periodische Ablauf von Ereignissen in einer sich teilenden Zelle) unterliegt strengen regulativen Einheiten und Netzwerken von immenser Komplexität. Defekte in zellzyklusrelevanten Genen sind häufig Ursache schwerwiegender Erkrankungen wie beispielsweise Krebs und stehen darum im zentralen Fokus vieler Forschungsprojekte.

Der kleine marine Invertebrat *Trichoplax adhaerens* gehört zum Stamm der Placozoa. Sein einfacher Bauplan, die simple Lebensweise und seine genetische Ausstattung legen den Schluss nahe, dass es sich bei ihm um den letzten noch lebenden gemeinsamen Vorfahren der Metazoen handelt. Gehen wir davon aus, dass *Trichoplax* dem evolutionsgeschichtlich ersten Vielzeller am ähnlichsten ist, können wir annehmen, dass die Mechanismen zur Zellzykluskontrolle in diesem Tier entsprechend einfach sind. Im Rahmen der vorliegenden Dissertation wurden zwei genetische Netzwerke in *Trichoplax adhaerens* untersucht, die einen erheblichen Einfluss auf die Kontrolle des Zellzyklus in höheren Tieren haben: (i) der Tumorsuppressor p53 sowie sein molekularer Gegenspieler Mdm2 und (ii) das Netzwerk der Myc/Max Transkriptionsfaktoren. Des Weiteren wurden (iii) Regenerationsexperimente durchgeführt, die die Vermischung verschiedener Placozoen- Linien beinhalteten und dazu beitragen, Verwandtschaftsverhältnisse innerhalb des Phylums aufzuklären.

(i) Die Verabreichung von Inhibitoren, die den p53-Anteil einer Zelle künstlich erhöhen, führte in *Trichoplax* zu einem signifikanten Anstieg der Apoptose- Rate. Des Weiteren veränderte sich das Mengenerhältnis von Rand- und Zentralgewebe der Tiere drastisch, was sich in ungewöhnlichen phänotypischen Ausprägungen äusserte. Die Ergebnisse unserer Studie lassen darauf schließen, dass die Funktion des p53/Mdm2 Netzwerkes der Placozoen ähnlich der von höheren Tieren ist und der Kontrolle des Zelltodes dient.

(ii) Die Funktionen der Transkriptionsfaktoren Myc und Max wurden mittels *in situ* Hybridisierung, Gen- "Knockdown", rekombinanter Proteinexpression und der Applikation von spezifischen Inhibitoren untersucht. Unsere Ergebnisse sprechen dafür, dass das

Netzwerk in *Trichoplax* unter anderem eine wichtige Funktion bei der Zelldifferenzierung übernimmt. Die Expression beider Gene variiert je nach Entwicklungsstadium der Tiere und die Abwesenheit der Proteine (erreicht durch "Knockdown" und Inhibitorapplikation) ist hochgradig letal.

(iii) Das Phylum Placozoa zeichnet sich durch eine überraschend hohe Diversität aus. Genetische und morphologische Analysen weltweit gesammelter Individuen beweisen, dass mindestens 19 verschiedene Placozoen-Linien (Haplotypen) existieren. Im Zuge dieser Dissertation wurden Regenerationsexperimente durchgeführt, bei denen Gewebestücke genetisch unterschiedlicher Linien zusammengefügt wurden. Je nach Kombination der verschiedenen Haplotypen verwuchsen die Transplantate gänzlich oder temporär, wurden desweilen aber auch sofort abgestoßen. Dieses Phänomen lässt darauf schließen, dass Placozoen in der Lage sind, eigenes von fremdem Gewebe zu unterscheiden. Außerdem bestätigen unsere Ergebnisse vorherige Resultate zur Phylogenie innerhalb der Placozoa, die auf der Analyse verschiedener molekularer Markersysteme fußen. Die beobachtete Verwachsungsrate hängt direkt mit dem genetisch ermittelten phylogenetischen Verwandtschaftsgrad zusammen, was als weiteres Argument dafür verstanden werden kann, dass es sich bei den unterschiedlichen Haplotypen womöglich um verschiedene Spezies, Gattungen und Familien des Phylums Placozoa handeln könnte.

Stichworte: Placozoa, *p53* und *mdm2*, *myc* und *max*, "Allorecognition"

Abstract

A crucial step within evolution was the fusion of unicellular organisms (Protozoa) to multicellular animals (Metazoa). This enabled the differentiation of diverse cell types and tissues, which then were specialized for various demands. The evolution of such a complexity, however, came along with the requirement to develop molecular instruments that were able to maintain cellular homeostasis within a tissue and to protect integrity of the organism. The cell cycle (the periodic procession of incidents in a dividing cell) underlies severe regulative units and networks of immense complexity. Defects in cell cycle relevant genes often are reason for serious diseases such as cancer and thus are main focus of diverse research projects.

The small marine invertebrate *Trichoplax adhaerens* belongs to the phylum Placozoa. Its simple bauplan characteristics, way of living and genetic equipment suggest that this organism represents the last recent common ancestor of the first multicellular animal. Proceeding from the assumption that it is most similar to the evolutionary first metazoan organism we can conclude that mechanisms for cell cycle control in this animal therefore are accordingly simple. In the course of the present thesis, two genetic networks in *Trichoplax adhaerens* were investigated which have a substantial influence on the control of the cell cycle in higher animals: (i) the tumor suppressor p53 and its molecular counterpart Mdm2 and (ii) the network of the Myc/Max transcription factors. Furthermore, (iii) regeneration experiments have been conducted that include the artificial fusion of different placozoan lineages and help to unravel relationships within the phylum.

(i) The application of inhibitors that artificially increase the amount of p53 in a cell, led to a significant increase of cells undergoing apoptosis in *Trichoplax*. Furthermore, the proportion of central and marginal tissue changed drastically which resulted in remarkable phenotypic characteristics. Results of the study suggest that the function of the p53/Mdm2 network in Placozoa are similar to its function in higher animals and serves the control of apoptosis.

(ii) The function of the transcription factors Myc and Max has been investigated by means of *in situ* hybridization, gene "knockdown", recombinant protein expression and application of specific inhibitors. Our results suggest that the network in *Trichoplax* has an important function, *inter alia*, in cellular differentiation. The expression of both genes varies depending on the developmental stage of the animal and absence of proteins (via

"knockdown" and inhibitor application) is highly lethal.

(iii) The phylum Placozoa is characterized by a surprisingly high diversity. Genetic and morphological analyses of worldwide sampled individuals prove the existence of at least 19 different placozoan lineages (haplotypes). In this thesis, regeneration experiments were conducted in which fractions of different genetic lineages were united. Depending on the combination of different haplotypes transplants merged completely or transitory whereas some were rejected instantly. This behavior pleads for the capability of the animal to distinguish own from foreign tissues. Our results furthermore confirm previous findings on the phylogeny of the Placozoa, which is relying on the analyses of different molecular marker systems. Observed intergrowth rate directly correlates with the genetically determined phylogenetic relationship what is yet another argument that haplotypes most probably correspond to different species, genera and families of the phylum Placozoa.

Keywords: Placozoa, *p53* and *mdm2*, *myc* and *max*, allorecognition

Contents

1 Introduction	14
2 Experimental Studies	32
2.1 Inhibitors of the p53-Mdm2 interaction in the placozoon <i>Trichoplax adhaerens</i>	33
2.2 The Myc/Max network at the base of the metazoan tree of life	46
2.3 Regeneration and self/non-self recognition in Placozoa	74
3 General Discussion	92
3.1 General Discussion	93
A Appendix	99
A.1 Inhibitors of the p53-Mdm2 interaction in the placozoon <i>Trichoplax adhaerens</i>	100
A.2 The Myc/Max network at the base of the metazoan tree of life	105
A.3 Regeneration and self/ non-self recognition in the phylum Placozoa	123
Curriculum Vitae	127
Acknowledgements	129
List of Publications	131

List of Figures

1.1	Placozoan morphology.	16
1.2	The p53-Mdm2 relationship.	18
1.3	The Myc/Max network.	19
1.4	Modes of allorecognition in <i>Hydractinia symbiolongicarpus</i>	21
2.1.1	Time course of population size and animal sizes after inhibitor treatment.	37
2.1.2	Phenotypic changes after inhibitor treatment.	38
2.1.3	Phenotypic abnormalities after inhibitor treatment.	39
2.1.4	TUNEL- and BrdU staining 72 h after inhibitor application.	40
2.2.1	Alignment of Myc and Max protein sequences.	56
2.2.2	Western blot analysis of expressed proteins.	57
2.2.3	Whole mount <i>in situ</i> hybridization of <i>tamyc</i> and <i>tamax</i>	58
2.2.4	Live imaging of transfected animals.	59
2.2.5	Time course of population and animal size during <i>tamyc</i> and <i>tamax</i> knockdown.	60
2.2.6	Amount of cell proliferation events after "knockdown" of <i>tamyc</i> and <i>tamax</i> .	61
2.2.7	Increase of apoptosis after <i>tamyc/tamax</i> gene knockdown.	62
2.2.8	Time course of population and animal size after treatment with the 10058-F4 inhibitor.	63
2.2.9	BrdU and TUNEL staining of inhibitor treated individuals after 24 h and 72 h.	64
2.3.1	Frequencies of transient tissue intergrowth.	80
2.3.2	Exemplary intergrowth and cell migration 24 hours after transplantation.	81
2.3.3	Xenografting can lead to morphological alterations in the acceptor tissue.	82
A.2.1	Gel filtration of the taMax-containing ÄKTA- fraction.	106
A.2.2	Light microscopy of "knockdown" individuals.	107
A.2.3	Animal population size after treatment with the 10058-F4 inhibitor. . .	109
A.2.4	Light microscopy of <i>Trichoplax</i> individuals after treatment with 10058-F4 inhibitor (5 μ M).	111
A.3.1	Grafting procedure exemplified by a <i>Trichoplax adhaerens</i> autograft. . .	123

List of Tables

2.2.1	Primer sequences used for insert amplification for the pETDuet-1 construct.	50
2.3.1	Haplotypes used in this study.	78
A.1.1	Raw data on animal population size after inhibitor treatment.	100
A.1.2	Raw data of animal sizes after inhibitor treatment.	102
A.1.3	Data on presence of abnormal <i>Trichoplax</i> phenotypes after inhibitor treatment.	103
A.1.4	Raw data on BrdU and TUNEL staining after inhibitor treatment.	104
A.2.1	Sequence information on taMyc and taMax.	105
A.2.2	Raw data of animal population sizes after "knockdown".	109
A.2.3	Raw data on animal sizes after "knockdown".	111
A.2.4	Raw data on BrdU signal after gene "knockdown".	113
A.2.5	Raw data on TUNEL staining 24h after initial <i>tamyc/tamax</i> gene "knockdown".	114
A.2.6	Statistical analyses on BrdU and TUNEL staining.	114
A.2.7	Raw data on population sizes after treatment with different concentrations of the 10058-F4 inhibitor.	116
A.2.8	Raw data on animal sizes after treatment with the 10058-F4 inhibitor.	120
A.2.9	Raw data on BrdU signal after treatment with the 10058-F4 inhibitor (5 μ M).	121
A.2.10	Raw data on TUNEL signal after treatment with the 10058-F4 inhibitor (5 μ M).	122
A.2.11	Statistical analyses on BrdU and TUNEL staining.	122
A.3.1	Primers used for genetic haplotype and clade identification.	124
A.3.2	Cross classification - Raw data of grafting experiments.	124
A.3.3	Data used for boxplot analyses.	125
A.3.4	Statistical analyses on donor/acceptor roles.	126
A.3.5	Results of PCR analyses.	126

Abbreviations

5'	five prime
3'	three prime
A	adenine
ARC	allorecognition complex
ASW	artificial seawater
bHLHL-Zip	basic helix-loop-helix leucine zipper
bp	base pairs
BrdU	bromodeoxyuridine
BSA	bovine serum albumin
C	cytosine
°C	degree Celsius
CDK	cycline dependent kinase
cDNA	complementary DNA
cf.	<i>confer</i> (compare)
DAPI	4',6-diamindino-2-phenylindole
ddH ₂ O	double distilled water
DEPC	diethylpyrocarbonate
DMSO	dimethyl sulfoxide
DNA	deoxyribonucleic acid
dUTP	deoxyuridine triphosphate
DTT	dithiothreitol
e.g.	<i>exempli gratia</i> (for example)
EDTA	ethylenediaminetetraacetic acid
EPEI	ethoxylated polyethylenimine
EtOH	ethanole
fig.	figure
FPLC	fast protein liquid chromatography
G	guanine
H	haplotype
h	hours
HCl	hydrochloric acid

HEPES	4-(2-hydroxyethyl)-1-piperazineethanesulfonic acid
HRP	horseradish peroxidase
i.e.	<i>id est</i> (that is)
IPTG	isopropyl- β -D-thiogalactoside
JGI	Joint Genome Institute
KD	knockdown
LB	lysogeny broth
M	molar
MB	Myc box
mg	milligram
min	minute
ml	milliliter
mM	millimolar
mm	millimeter
MO	morpholino oligonucleotide
μ g	microgram
μ l	microliter
μ m	micrometer
N	normal (chemically)
NaCl	sodium chloride
NCBI	National Center for Biotechnology Information
ng	nanogram
nm	nanometer
no.	number
OD	optical density
PCR	polymerase chain reaction
RACE	rapid amplification of cDNA ends
RNA	ribonucleic acid
rpm	rotations per minute
RT	room temperature
SDS	sodium dodecyl sulfate
sec	seconds
T	thymine
TBS	tris-buffered saline
TBST	tris-buffered saline +0.1% Tween-20
TBSTT	tris-buffered saline +0.1% Tween-20 +0.1% TritonX
TAME	p-toluenesulfonyl-L-arginine methyl ester
TPCK	tosyl phenylalanyl chloromethyl ketone

Tris	tris(hydroxymethyl)aminomethane
TSA	thyramide signal amplification
TUNEL	terminal deoxynucleotidyl transferase-mediated deoxyuridine triphosphate nick end labeling

1 Introduction

"In den Seewasseraquarien des Zoologischen Institutes der Universität Graz lebt ein bisher noch nicht beschriebenes Thier, dessen Organisation und Lebenserscheinung mir ein so gründliches und lange fortgesetztes Studium zu erfordern scheint, daß ich [...] voraussichtlich erst nach langer Zeit zum Abschluss meiner Untersuchungen über dasselbe gelangen werde..."

(Franz Eilhard Schulze, 1883)

The phylum Placozoa, a historical overview

In 1883 Franz Eilhard Schulze, a German zoologist described his observations on the simplest known metazoan animal thus far [1]. He discovered a small, disc shaped creature in a seawater aquarium in the University of Graz (Austria) and after closer investigation he named it after its obvious morphology *Trichoplax* (Greek ‘tricha’ = hair, ‘plax’ = plate) *adhaerens* (Latin ‘adhaere’ = to stick). Due to the absence of similarities to other known phyla, Schulze then proposed its phylogenetic position to be isolated and close to the root of the metazoan Tree of Life (ToL). After a more detailed description of the animal by Schulze in 1891 [2], the zoologist Thilo Krumbach erroneously claimed *Trichoplax* to be an aberrant hydrozoan larvae [3]. Even though Krumbachs theories had their critics [4, 5], the initial interest in *Trichoplax adhaerens* decreased drastically for a long period.

Karl Gottlieb Grell a German zoologist then brought *Trichoplax* back to discussion in the early seventies, introducing the new phylum ‘Placozoa’, named after Otto Bütschli’s ‘Placula Hypothesis’ about the origin of Metazoa [6, 7]. With Grell’s publications on the formation of egg cells [8] the interest in *Trichoplax* rekindled and substantial scientific efforts were made to unravel its morphology, biology and phylogenetic position in the following years (for review see [9]).

In recent years the phylum Placozoa turned out to be very diverse harboring several genetic lineages and species (termed haplotypes) distributed worldwide (cf. [10-15]). The phylogenetic position of Placozoa is close to the base of the metazoan tree of life and thus this animal can provide crucial insights into the evolution of multicellularity [16, 17]. The sequencing of the genome of *Trichoplax adhaerens*, the so far only described representative of the phylum Placozoa [18] revealed a remarkable conservation of the genetic repertoire from Placozoa to higher animals and highlights Placozoa as a model system for different areas of science including applied research (e.g. [19-22]).

Placozoan morphology and ecology

The marine invertebrate *Trichoplax adhaerens* represents the simplest organized animal known thus far with the simplest known bauplan characteristics [1, 2]. It has an average size of a few millimeter in diameter and comprises of only five different somatic cell types forming three distinct layers: the upper and the lower epithelium which encloses a loose formation of interconnected fiber cells (fig. 1.1 and references therein). The animal dispenses any axis has no defined shape and is evocative of an amoeba [1, 2, 23, 24]. The lack of organs, neuronal and muscular cells a basal lamina or an extracellular matrix suggests its evolutionary origin to be close to the base of Metazoa and recent overall analysis suggests the Placozoa to be the best surrogate for the ‘Urmetazoon’, while the

1 Introduction

relationship of animal phyla at the base of the tree of life remain heavily discussed (cf. [9, 16, 17, 25-29]).

The upper epithelium of *Trichoplax* consists of monociliated, flattened cover cells with interspersed highly refractive structures, the so-called ‘shiny spheres’. The function of these degenerated cells is not clear yet but investigations give hints for a probable defensive function [31]. The lower epithelium is much more dense, overtakes a nutritive function and is responsible for the movement of the animal. It is made up of ciliated cylinder cells responsible for locomotion as well as ingestion of food via pinocytosis [32-35], and flask-shaped gland cells excreting enzymes for extracellular digestion [36]. Sandwiched in between the epithelia, the fiber cells are interconnecting the upper and lower epithelium forming a loose syncytial network [37, 38]. The continuous change of shape during movement of the animal is coordinated by contraction of these cells [39, 40]. The multipotent stem cells, the postulated fifth cell type, are located at the margin of the animal. They mark the boundary of the upper and lower epithelium and differentiate during development of the animal [41].

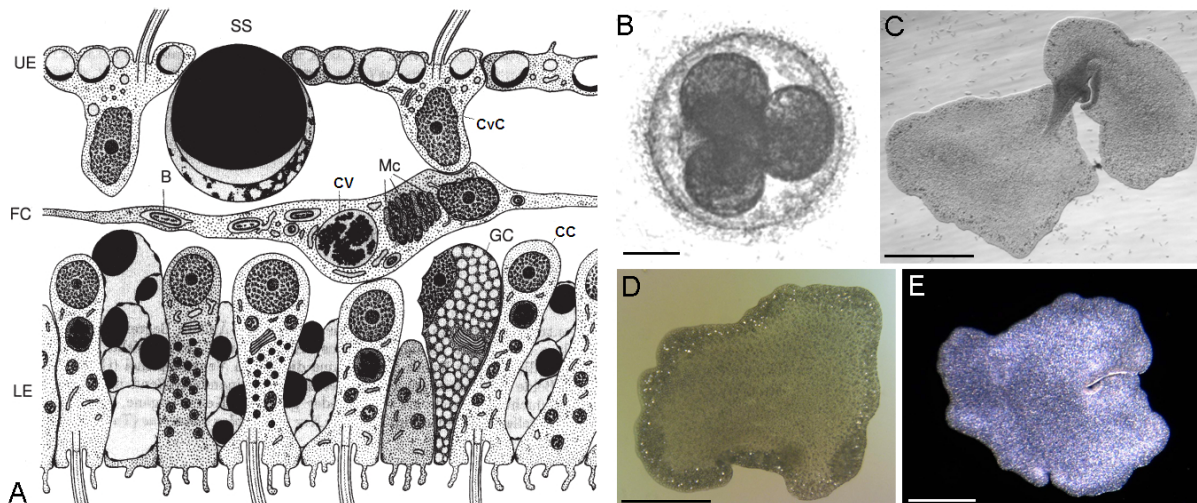


Figure 1.1: Placozoan morphology.

(A) Schematic cross section of *T. adhaerens* (modified after [7]) upper epithelium (UE), lower epithelium (LE) fiber cells (FC) cover cell (CvC), shiny sphere (SS), bacteria (B), concretment vacuole (Cv), mitochondrial complex (Mc), gland cell (GC) and cylinder cell (CC).

(B) Egg cell in the 4-cell stage.

(C) Vegetative reproduction via binary fission.

(D) Birefringent granules at the margin of a *Trichoplax* individual,

(E) *Trichoplax adhaerens* in the stereomicroscope.

Scale bar in (B) marks 20 μm , bar in (C, D, E) marks 100 μm .

The phylum Placozoa is much more diverse than initially thought [10]. Extensive taxon sampling revealed the existence of at least 19 different genetic lineages (haplotypes) distributed worldwide in the littoral of predominantly tropical and subtropical oceans [13, 15]. The recent finding of a placozoan species in the Atlantic Ocean in the north of

France (Roscoff) however demonstrates the animals' ability to adapt also to cold water [42]. Morphological analysis and genome sequencing has revealed taxonomic diversity and tissue grafting between diverse haplotypes (as described in this thesis) confirms that different genetic lineages likely represent different species and higher taxonomic units. [13, 14]. A comprehensive revision of the taxonomy of the phylum Placozoa thus is an important field of current research.

Under standardized laboratory conditions Placozoa mainly reproduce vegetatively via binary, respectively, multiple fission [43]. They can also form spherical swarmers which are choked off the upper epithelium of a mother individual. This mostly occurs under suboptimal culturing conditions and likely serves the distribution of animals to conquest new habitats in nature [44]. The formation of egg cells under certain conditions suggests the existence of sexual reproduction, however under laboratory conditions embryos are dying aback after reaching the 128-cell stage [8, 30, 45-47]. While molecular data imply the existence of sexual reproduction [47, 48], the life cycle of Placozoa remains unclear.

Observations on the way of living of placozoan species are solely based on laboratory cultures and material sampled from the ocean (e.g. stones or mussel shells). The reason is that the animals are too small and translucent to be observable in the wild. Placozoans are found in company of other marine invertebrates such as cnidarians or sponges, but no interaction has been observed so far [12]. Despite the lack of organs and neurons *Trichoplax adhaerens* shows directed movement towards light sources, i.e. positive phototaxis [49-51]. Analysis of the *Trichoplax* genome revealed the presence of genes encoding for G-protein coupled receptor proteins found in photoreceptor cells (opsins) and regulatory genes important in embryonic eye development (Pax genes) suggests the existence of a primitive photoreceptor cell in the Placozoa [52, 53]. Recent findings also indicate a positive reaction to temperature gradients whereas the individuals preferred warmer temperatures when exposed to a gradient of 15 °C – 20 °C [54]. All together these results show that *Trichoplax* is able to convert external stimuli and respond with coordinated behavior. It is likely that the reaction is coordinated by dint of fiber cells, which could therefore be seen as proto-neuronal/muscular cells [55].

The tumor suppressor p53 and its ubiquitin ligase Mdm2

p53 is deemed to be one of the most important genes to study in the context of cancerous diseases as more than 50% of all human malignancies are accompanied by a mutations in this gene [56]. Simultaneously discovered by Albert DeLeo, Sir David Lane and Alberto Levine in 1979 [57-59], it soon was clear that the gene product of *p53*, the p53 protein plays an important role in modulating cellular transformation of tumor cells. Now fittingly known as the 'guardian of the genome' [60], p53 is renowned to resume an essential function in the regulation of cell growth, division and apoptosis as well as in differentiation and

1 Introduction

development (for review see e.g. [61-63]).

Under unstressed conditions the level of p53 in the cell is relatively low and the protein is held inactive by its negative regulator Mdm2, an ubiquitin ligase that binds to the p53 protein. Mdm2 has an ubiquitin ligase activity and thereby marks the protein for subsequent degradation by the proteasome (cf. [64]). The p53 pathway is activated in response to various stress signals as e.g. DNA damage leading to an interruption of p53-Mdm2 interaction by means of posttranscriptional modifications [65]. The p53 protein then transcriptionally activates the expression of target genes. Activated genes are responsible for cell cycle arrest, respectively, senescence induced e.g. by the cyclin dependent kinase inhibitor p21 [66], or apoptosis e.g. by the Bcl-2 homology domain 3-only protein PUMA (p53-upregulated modulator of apoptosis, [67]) to name but a few. Beside this transcriptional-dependent function, p53 can also induce apoptosis by affecting the survival of mitochondrial proteins, microRNA processing or DNA repair [68-70].

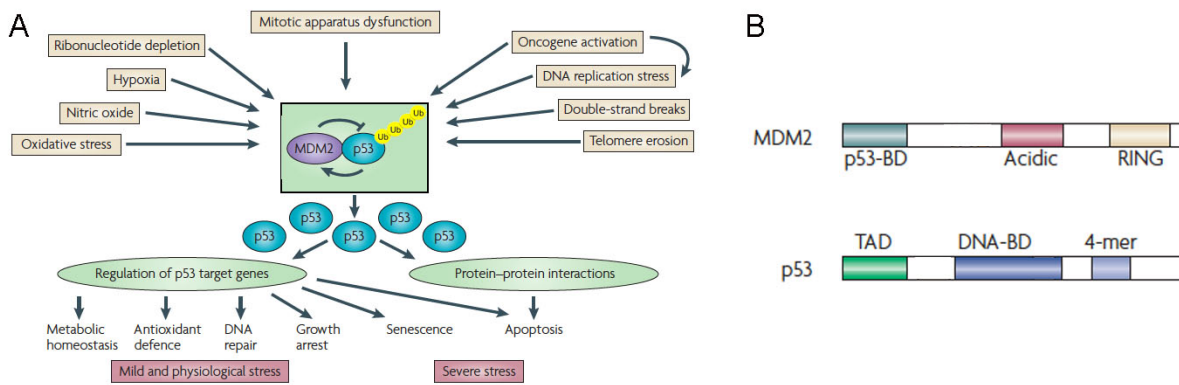


Figure 1.2: The p53-Mdm2 relationship.

(A) Various cellular stress signals lead to the disruption of p53-Mdm2 interaction activating the p53 pathway. Target genes now regulate stress responses such as senescence or apoptosis (modified after [62]).

(B) Structure of the Mdm2 and p53 protein: p53 binding domain (p53-BD), acidic- and RING finger domain in Mdm2; transactivation domain (TAD), DNA binding domain (DNA-BD) and oligomerization domain (4-mer) in p53 (modified after [63]).

The human p53 protein has, as the name implies, a size of 53kDa. It contains an N-terminal transactivation domain responsible for binding to interacting proteins such as the negative regulator Mdm2. The central DNA-binding domain mediates sequence specific binding of the protein to corresponding DNA regions. As human p53 forms a tetramer to bind to the DNA, the oligomerization domain (4mer) is structurally conserved. The human Mdm2 protein consists of 149 amino acids with a N-terminal domain to specifically bind the p53 protein. The central part of the protein contains an acidic region conterminous to a zinc finger region responsible for binding to various regulatory factors. The ubiquitin ligase activity of Mdm2 is mediated by the C-terminal RING finger domain (cf. fig. 1.2 and references within).

A recent publication of Lane in 2010 revealed that the genome of *Trichoplax adhaerens* encodes for both a p53- and an Mdm2-like protein [71]. The *Trichoplax* p53 and Mdm2 do possess all necessary functional domains known from their human homologues. In this thesis, first experimental approaches for unraveling the role of *p53* and *Mdm2* in Placozoa have been conducted. The application of two inhibitors of p53-Mdm2 interaction (roscovitine and nutlin-3 [72, 73]) provides first insights into the function of a possible p53/Mdm2 network in Placozoa and highlights its importance for the organism.

The Myc/Max transcription factor network

Cell behavior, such as the initiation of proliferation, apoptosis, differentiation or quiescence has to be tightly regulated in all Metazoa. The *c-myc* proto-oncogene encodes a transcription factor (Myc) that has a high impact on the control of these incidents (cf. [74]). Originally identified as a nucleotide sequence that "may encode the oncogenic potential of the avian virus MC29" [75] the *myc* gene soon achieved ambiguous fame as its deregulation contributes to a large number of human tumors. It belongs to the family of *myc* genes whereas *c-myc*, *L-myc* and *N-myc* are known to cause malignancies if deregulated (for review see e.g. [76]). Later on the Max protein (Myc associated factor X) was discovered to overtake the central function in a transcriptional network that also includes other basic-helix-loop-helix zipper (bHLHLZip) proteins [77]. Myc and Max belong to the bHLHLZip transcription factors and form heterodimers that specifically bind to enhancer sequences (E-boxes with the specific sequence CA C/T GTG) of the DNA causing transcriptional activation or respectively repression of target genes [78, 79].

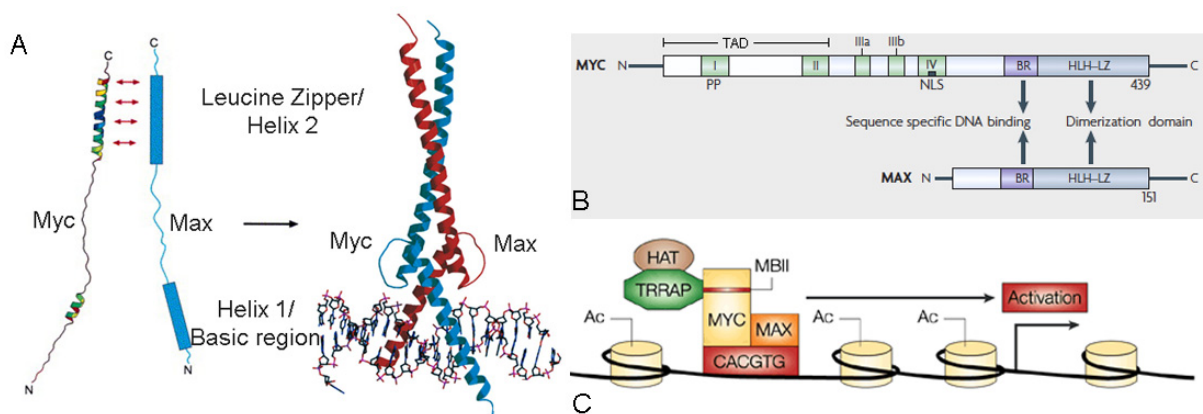


Figure 1.3: The Myc/Max network.

- (A) Organization of Myc and Max; both proteins are forming a fork-like structure and bind to the major groove of the DNA (modified after [80, 81]).
- (B) Conserved domains of Myc and Max; Myc-boxes I-IV in green, the basic region in violet and the helix-loop-helix-leucine zip in blue. The transactivation domain (TAD) phosphorylation sites (PP) the region encoding for nuclear localization signal (NLS) are indicated (modified after [74]).
- (C) Myc and Max transcriptionally can activate target genes by recruiting TRRAP for regulation of histone acetylation (modified after [82]).

With a size of ~49 kilo Dalton (kDa) the human c-Myc Protein comprises of a N-terminal basic domain and a C-terminal leucine zipper both forming two separated alpha helices. The C-terminal leucine zipper of Myc is the nucleus of Myc/Max dimerization and the N-terminal part of the protein is responsible for DNA binding. The conserved Myc homology boxes (I-IV) are essential for Myc function [83]. The Myc interacting protein Max has a size of ~18 kDa in human and is build up of a basic DNA binding domain and a bHLHLZip Zip region (fig. 1.3 and references within). The Myc protein is an important transcriptional regulator that may translocate to the nucleus for binding to Max and subsequently to the DNA. Genes targeted by the Myc/Max complex are mainly involved in cell cycle progression including apoptosis and cellular metabolism. A cleavage product of the Myc protein lacking the nuclear localization signal site is functional in the cytoplasm and has an impact on cellular differentiation as well as on cytoplasmic organization. Alterations in Myc protein distribution within a cell also seem to be an important regulative element of the Myc/Max network [84]. Recent analyses additionally suggest Myc to have a Max-independent function that activates RNA polymerase III-dependent transcription [85] making the Myc/Max network even more complex. The genes regulated by the Myc/Max network are manifold (e.g. p53) constituting about 15% of all human genes [86]. *Myc* expression itself is regulated by mitogenic factors triggered by cellular growth signals and also via posttranscriptional phosphorylation in the transactivation domain [87]. Regulation of gene expression by Myc can be carried out via transcriptional activation or repression and is often associated with the recruitment of histone acetyltransferases by the nuclear cofactor TRRAP (transformation/transcription domain-associated protein [88]). Deregulation of *myc* by means of insertional mutagenesis, chromosomal translocation and gene amplification [74] are involved in tumor formation.

Homologues of Myc and its binding partner Max have been found in all metazoan lineages and in two unicellular relatives: the choanoflagellate *Monosiga brevicollis* and the ophisthokont *Capsaspora ovczarzaki* [88]. The Myc protein of *Monosiga* furthermore was proven to interact with Max for binding to E-box sequences [89, 90]. This finding indicates the origin of the Myc/Max network to predate the evolution of Metazoa. Research on this important network in the simplest animal, *Trichoplax adhaerens*, will help to further elucidate the function of these transcriptional factors in course of evolution and their role in cell cycle regulation. Experiments conducted in course of this thesis underline the evolutionary preservation of the network and also highlight Placozoa as a model system for applied cancer research.

Placozoa and allorecognition

The skill to discriminate between ‘self’ tissue and tissues of genetically different individuals of the same species is a capability termed allorecognition. With the evolution of the

immune system, organisms became capable of differentiating between distant relationship and close kinship [91].

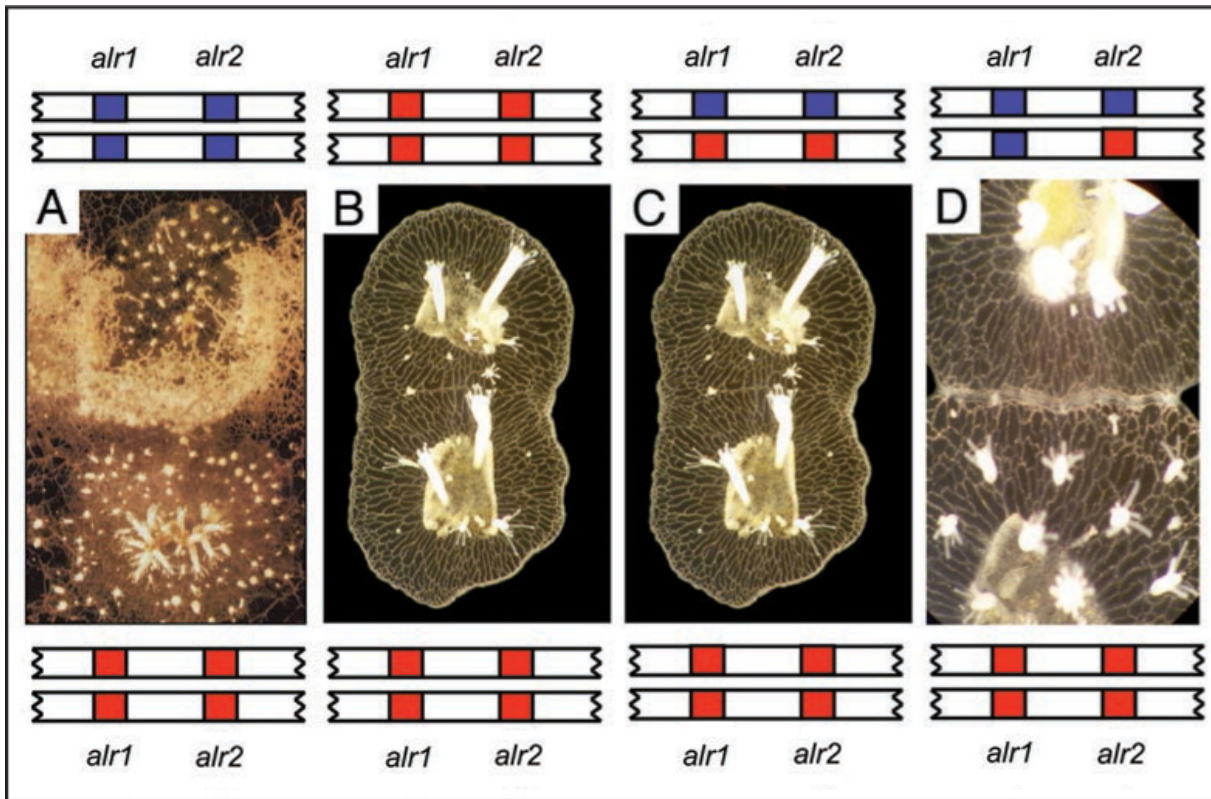


Figure 1.4: Modes of allorecognition in *Hydractinia symbiolongicarpus*.

Drawing represents allorecognition loci on chromosomes, colors indicate analogy of alleles (modified after [91]).

(A) Rejection occurs when no haplotype is shared by the colonies.

(B), (C) Colonies fuse if they share at least one haplotype.

(D) If one allele is shared colonies undergo transitory fusion.

Allorecognition is a mechanism displayed by all major invertebrate taxa like sponges, cnidarians or tunicates [92-94]. In sessile marine invertebrates the mechanism is important for the maintenance of colonial integrity, as different genetic lineages compete for limited habitats. Representative for this mechanism is the hydroid *Hydractinia symbiolongicarpus* that inhabits shells carried by hermit crabs [95]. While colonies of the same genetic lineage fuse, unrelated colonies actively ‘fight’ about space. Competing colonies thereby discharge nematocytes to the contact zone with intend to destroy the foreign tissue. Transitory fusion occurs between closely related colonies and is characterized by the occurrence of a necrotic band with a subsequent rejection of tissue approximately 12-24 hours after initial fusion. The mechanism controlling the identification of own and foreign tissue in *Hydractinia* is determined in two gene loci, allorecognition 1 (*alr1*) and *alr2* that encode a putative transmembrane protein [96]. Individuals sharing at least one haplotype of these loci undergo fusion whereas the lack of a mutual haplotype results in rejection of tissue.

Only individuals with an identical allele perform transitory fusion (fig. 1.4 and references therein).

In 1984 Schwartz first demonstrated regeneration ability in *Trichoplax* by grafting of tissue between two animals [23]. In this thesis, grafting experiments between different placozoan lineages have been performed. Fusion, rejection and transitory fusion has been observed in course of investigations suggesting the presence of a primitive allorecognition system also within the Placozoa. These experiments could qualify *Trichoplax* as a model for the evolution of the allorecognition machinery and could furthermore help to unravel the taxonomic relationship within the Placozoa.

Placozoa as a model organism

With the evolution of a metazoan life form from a unicellular ancestor came the requirement to control the progression of cell division and cell death (apoptosis) within a tissue [97, 98]. Imbalances in the regulation of these processes inevitably lead to a reduced fitness of tissue and may even result in serious disorders such as cancer [99]. The molecular mechanisms controlling cell cycle events in Metazoa are very complex and even though they are permanent focus of extensive state-of-the-art research, there are still many crucial questions. Besides well-known invertebrate model organisms such as *Drosophila melanogaster* and *Caenorhabditis elegans* [100, 101], non-Bilaterians like Poriferans, Cnidaria and Ctenophores are needed to unravel the emergence of developmental or physiological traits as well as the underlying complex molecular processes for cell cycle control [102]. Due to its simple anatomy the fresh water polyp *Hydra* (Cnidaria) for example turned out to be a good model for answering a broad range of questions concerning the evolution of Metazoa [103]. Placozoa are presumably a even better model system because of their basal phylogenetic position and their extreme simple morphology [17]. Given the ancestral features of the placozoan genome it is beyond doubt that this phylum will soon become an important model system not only for evolutionary biology but also for applied research.

The aim of this thesis is to highlight the applicability of placozoans as a model system to address questions concerning cell cycle control, regeneration and the evolution of the immune system. *Trichoplax* fulfills all of the demands for classical model systems. The way of cultivating Placozoa is straightforward, they have a short generation time and the genome has been sequenced [17, 18, 24]. Additionally, the flat and translucent morphology of Placozoa make them resemble a ‘crawling cell culture’ permitting the application of standard methods to whole organisms. *Trichoplax* has a remarkable ability for regeneration. After cutting an individual the wound closes within approximately 20 minutes and even grafting of tissue between two individuals is possible [23]. This characteristic opens diverse prospects for experimental designs. Looking at the genome it is conspicuous that despite its simple morphology many genes controlling complex mechanisms in higher animals are

1 Introduction

conserved within the Placozoa [18, 22]. To unravel the function of the genetic equipment necessary to control essential functions such as the regulation of cell cycle and cellular homeostasis, differentiation or regeneration in this simple animal, will provide unique insights into the evolution of multicellularity and will help to better understand the origin of diseases caused by deregulations of these processes as it is the case in cancer.

References

1. Schulze, F.E. (1883). *Trichoplax adhaerens*, nov. gen., nov. spec. Zool Anz 6, 92-97.
2. Schulze, F.E. (1892). *Über Trichoplax adhaerens*. In Abhandlungen der Königlichen Preuss. Akademie der Wissenschaften zu Berlin. (Berlin: Verlag der königlichen Akademie der Wissenschaften), pp. 1-23.
3. Krumbach, T. (1907). *Trichoplax, die umgewandelte Planula einer Hydromedusae*. Zool Anz 31, 450-454.
4. Schubotz, H. (1912). *Ist Trichoplax die umgewandelte Planula einer Hydromeduse?* Zool Anz 39, 582-585.
5. Schulze, F.E. (1914). *Einige kritische Bemerkungen zu neueren Mitteilungen über Trichoplax*. Zoolog. Anz. 64, 33-35.
6. Bütschli, O. (1884). *Bemerkungen zur Gastraea-Theorie*. Morph Jahrb 9, 415-427.
7. Grell, K.G. (1971). *Trichoplax adhaerens* F.E. Schulze und die Entstehung der Metazoen. Naturw. Rdsch. 24, 160-161.
8. Grell, K.G. (1971). *Embryonalentwicklung bei Trichoplax adhaerens* F. E. Schulze. Naturwiss 58, 570.
9. Syed, T., and Schierwater, B. (2002). *Trichoplax adhaerens: discovered as a missing link, forgotten as a hydrozoan, re-discovered as a key to metazoan evolution*. Vie Milieu 52, 177-187.
10. Voigt, O., Collins, A.G., Pearse, V.B., Pearse, J.S., Ender, A., Hadrys, H., and Schierwater, B. (2004). *Placozoa - no longer a phylum of one*. Curr Biol 14, R944-945.
11. Signorovitch, A.Y., Dellaporta, S.L., and Buss, L.W. (2006). *Caribbean placozoan phylogeography*. Biol Bull 211, 149-156.
12. Pearse, V.B., and Voigt, O. (2007). *Field biology of placozoans (Trichoplax): distribution, diversity, biotic interactions*. In *Symposium on Key Transitions in Animal Evolution*. (Phoenix, AZ), pp. 677-692.
13. Eitel, M., and Schierwater, B. (2010). *The phylogeography of the Placozoa suggests a taxon-rich phylum in tropical and subtropical waters*. Mol Ecol 19, 2315-2327.
14. Guidi, L., Eitel, M., Cesarini, E., Schierwater, B., and Balsamo, M. (2011). *Ultrastructural analyses support different morphological lineages in the phylum Placozoa Grell, 1971*. J Morphol 272, 371-378.

15. Eitel, M., Osigus, H.-J., DeSalle, R., and Schierwater, B. (2013). *Global diversity of the Placozoa*. PLoS One, 8(4): e57131. doi:10.1371/journal.pone.0057131.
16. Schierwater, B., de Jong, D., and Desalle, R. (2009). *Placozoa and the evolution of Metazoa and intrasomatic cell differentiation*. Int J Biochem Cell Biol 41, 370-379.
17. Schierwater, B., Eitel, M., Jakob, W., Osigus, H.J., Hadryns, H., Dellaporta, S.L., Kolokotronis, S.O., and DeSalle, R. (2009). *Concatenated Analysis Sheds Light on Early Metazoan Evolution and Fuels a Modern 'Urmetazoon' Hypothesis*. Plos Biology 7, 36-44.
18. Srivastava, M., Begovic, E., Chapman, J., Putnam, N.H., Hellsten, U., Kawashima, T., Kuo, A., Mitros, T., Salamov, A., Carpenter, M.L., et al. (2008). *The Trichoplax genome and the nature of placozoans*. Nature 454, 955-960.
19. de Jong, D., Eitel, M., Jakob, W., Osigus, H.J., Hadryns, H., DeSalle, R., and Schierwater, B. (2009). *Multiple Dicer Genes in the Early-Diverging Metazoa*. Molecular Biology and Evolution 26, 1333-1340.
20. Loenarz, C., Coleman, M.L., Boleininger, A., Schierwater, B., Holland, P.W., Ratcliffe, P.J., and Schofield, C.J. (2011). *The hypoxia-inducible transcription factor pathway regulates oxygen sensing in the simplest animal, Trichoplax adhaerens*. EMBO Rep 12, 63-70.
21. Vij, S., Rink, J.C., Ho, H.K., Babu, D., Eitel, M., Narasimhan, V., Tiku, V., Westbrook, J., Schierwater, B., and Roy, S. (2012). *Evolutionarily ancient association of the FoxJ1 transcription factor with the motile ciliogenic program*. PLoS Genet 8, e1003019.
22. Ringrose, J.H., van den Toorn, H.W., Eitel, M., Post, H., Neerincx, P., Schierwater, B., Maarten Altelaar, A.F., and Heck, A.J. (2013). *Deep proteome profiling of Trichoplax adhaerens reveals remarkable features at the origin of metazoan multicellularity*. Nat Commun 4, 1408.
23. Schwartz, V. (1984). *The radial polar pattern of differentiation in Trichoplax adhaerens F.E. Schulze (Placozoa)*. Z. Naturforsch. 39c, 818-832.
24. Schierwater, B. (2005). *My favorite animal, Trichoplax adhaerens*. Bioessays 27, 1294-1302.
25. Grell, K.G. (1981). *Trichoplax adhaerens and the origin of Metazoa*. In Origine dei Grandi Phyla dei Metazoi, Convegno Intern. pp. 107-121.

26. Miller, D.J., and Ball, E.E. (2005). *Animal evolution: the enigmatic phylum placozoa revisited*. *Curr Biol* 15, R26-28.
27. Schierwater, B., Desalle, R., Jakob, W., Schroth, W., Hadryns, H., and Dellaporta, S. (2006). *Total evidence analysis identifies Placozoa as basal to extant Metazoa*. *Integrative and Comparative Biology* 46, E126-E126.
28. Schierwater, B., and Desalle, R. (2007). *Can we ever identify the Urmetazoan?* *Integr Comp Biol* 47, 670-676.
29. Osigus, H.J., Eitel, M., and Schierwater, B. (2013). *Chasing the urmetazoon: Striking a blow for quality data?* *Mol Phylogenet Evol* 66, 551-557.
30. Grell, K.G. (1972). *Eibildung und Furchung von Trichoplax adhaerens F.E.Schulze (Placozoa)*. *Z Morph Tiere* 73, 297-314.
31. Jackson, A.M., and Buss, L.W. (2009). *Shiny spheres of placozoans (Trichoplax) function in anti-predator defense*. *Invertebrate Biology* 128, 205-212.
32. Kuhl, W., and Kuhl, G. (1963). *Bewegungsphysiologische Untersuchungen an Trichoplax adhaerens F. E. Schulze*. *Zool. Anz. Suppl.* 26, 460-469.
33. Kuhl, W., and Kuhl, G. (1966). *Untersuchungen über das Bewegungsverhalten von Trichoplax adhaerens F.E.Schulze*. *Zeitschr Ökolog u Morph Tiere* 56, 417-435.
34. Kuhl, W. (1971). *Bewegungsverhalten von Trichoplax adhaerens (Motor Behaviour of Trichoplax adhaerens)*. W. Kuhl, ed. (Göttingen: IWF Wissen und Medien gGmbH (<http://www.iwf.de>), Nonnenstieg 72, D-37075 Göttingen).
35. Ueda, T., Koya, S., and Maruyama, Y.K. (1999). *Dynamic patterns in the locomotion and feeding behaviors by the placozoan Trichoplax adhaerens*. *Biosystems* 54, 65-70.
36. Grell, K.G., and Ruthmann, A. (1991). *Placozoa*. In *Microscopic Anatomy of Invertebrates, Placozoa, Porifera, Cnidaria, and Ctenophora*, Volume Vol. 2, F.W. Harrison, Westfall, J.A., ed. (New York: Wiley-Liss), pp. 13-28.
37. Grell, K.G., and Benwitz, G. (1981). *Ergänzende Untersuchungen zur Ultrastruktur von Trichoplax adhaerens F.E. Schulze (Placozoa)*. *Zoomorphology* 98, 47-67.
38. Buchholz, K., and Ruthmann, A. (1995). *The mesenchyme-like layer of the fibre cells of Trichoplax adhaerens: A syncytium*. *Z Naturforsch [C]* 50c, 282-285.
39. Behrendt, G., and Ruthmann, A. (1986). *The cytoskeleton of the fiber cells of Trichoplax adhaerens (Placozoa)*. *Zoomorphology* 106, 123-130.

40. Thiemann, M., and Ruthmann, A. (1989). *Microfilaments and microtubules in isolated fiber cells of Trichoplax adhaerens (Placozoa)*. Zoomorphology 109, 89-96.
41. Jakob, W., Sagasser, S., Dellaporta, S., Holland, P., Kuhn, K., and Schierwater, B. (2004). *The Trox-2 Hox/ParaHox gene of Trichoplax (Placozoa) marks an epithelial boundary*. Dev Genes Evol 214, 170-175.
42. von der Chevallerie, K., Eitel, M., and Schierwater, B. (2010). *Focus on an unexpected discovery in Roscoff - a warm water species of the phylum Placozoa*. Cah Biol Mar 212, 21.
43. Thiemann, M., and Ruthmann, A. (1991). *Alternative modes of sexual reproduction in Trichoplax adhaerens (Placozoa)*. Zoomorphology 110, 165-174.
44. Thiemann, M., and Ruthmann, A. (1988). *Trichoplax adhaerens Schulze, F. E. (Placozoa) - The formation of swarmers*. Z. Naturforsch. 43, 955-957.
45. Grell, K.G. (1973). *Trichoplax adhaerens (Placozoa). Eizellen und Furchungsstadien*. In Encyclopaedia Cinematographica. (Inst. wiss. Film, Göttingen, Film E 1920).
46. Grell, K.G., and Benwitz, G. (1974). *Elektronenmikroskopische Beobachtungen über das Wachstum der Eizelle und die Bildung der 'Befruchtungsmembran' von Trichoplax adhaerens F.E.Schulze (Placozoa)*. Z Morph Tiere 79, 295-310.
47. Eitel, M., Guidi, L., Hadrys, H., Balsamo, M., and Schierwater, B. (2011). *New insights into placozoan sexual reproduction and development*. PLoS One 6, e19639.
48. Signorovitch, A.Y., Dellaporta, S.L., and Buss, L.W. (2005). *Molecular signatures for sex in the Placozoa*. Proc Natl Acad Sci USA 102, 15518-15522.
49. Bergmann, T. (2007). *Experimentelle Studien zur Expression und Funktion von Opsin-Genen in Trichoplax adhaerens.*, Master thesis
50. von der Chevallerie, K. (2008). *First experimental approaches to vision, proliferation and apoptosis in Trichoplax adhaerens.*, Master thesis
51. Cramm, M. (2009). *Experimentelle und genetische Studien zur Phototaxis in Trichoplax adhaerens.*, Master thesis
52. Sagasser, S. (2011). *On development and evolution of Trichoplax adhaerens (Placozoa)*, PhD thesis
53. Hadrys, T., DeSalle, R., Sagasser, S., Fischer, N., and Schierwater, B. (2005). *The Trichoplax PaxB gene: a putative Proto-PaxA/B/C gene predating the origin of nerve and sensory cells*. Mol Biol Evol 22, 1569-1578.

54. Reinke, P. (2011). *Verhaltensgenetische Studien an dem Placozoon Trichoplax adhaerens.*, Bachelor thesis
55. Schierwater, B., Kolokotronis, S.O., Eitel, M., and DeSalle, R. (2009). *The Diploblast-Bilateria Sister hypothesis: parallel evolution of a nervous systems may have been a simple step.* Commun Integr Biol 2, 403-405.
56. Joerger, A.C., and Fersht, A.R. (2007). *Structure-function-rescue: the diverse nature of common p53 cancer mutants.* Oncogene 26, 2226-2242.
57. DeLeo, A.B., Jay, G., Appella, E., Dubois, G.C., Law, L.W., and Old, L.J. (1979). *Detection of a transformation-related antigen in chemically induced sarcomas and other transformed cells of the mouse.* Proc Natl Acad Sci U S A 76, 2420-2424.
58. Lane, D.P., and Crawford, L.V. (1979). *T antigen is bound to a host protein in SV40-transformed cells.* Nature 278, 261-263.
59. Linzer, D.I., and Levine, A.J. (1979). *Characterization of a 54K dalton cellular SV40 tumor antigen present in SV40-transformed cells and uninfected embryonal carcinoma cells.* Cell 17, 43-52.
60. Lane, D.P. (1992). *Cancer. p53, guardian of the genome.* Nature 358, 15-16.
61. Vousden, K.H., and Prives, C. (2009). *Blinded by the Light: The Growing Complexity of p53.* Cell 137, 413-431.
62. Levine, A.J., and Oren, M. (2009). *The first 30 years of p53: growing ever more complex.* Nat Rev Cancer 9, 749-758.
63. Meek, D.W. (2009). *Tumour suppression by p53: a role for the DNA damage response?* Nat Rev Cancer 9, 714-723.
64. Momand, J., Zambetti, G.P., Olson, D.C., George, D., and Levine, A.J. (1992). *The mdm-2 oncogene product forms a complex with the p53 protein and inhibits p53-mediated transactivation.* Cell 69, 1237-1245.
65. Manfredi, J.J. (2010). *The Mdm2-p53 relationship evolves: Mdm2 swings both ways as an oncogene and a tumor suppressor.* Genes Dev 24, 1580-1589.
66. Macleod, K.F., Sherry, N., Hannon, G., Beach, D., Tokino, T., Kinzler, K., Vogelstein, B., and Jacks, T. (1995). *p53-dependent and independent expression of p21 during cell growth, differentiation, and DNA damage.* Genes Dev 9, 935-944.
67. Nakano, K., and Vousden, K.H. (2001). *PUMA, a novel proapoptotic gene, is induced by p53.* Mol Cell 7, 683-694.

68. Suzuki, H.I., Yamagata, K., Sugimoto, K., Iwamoto, T., Kato, S., and Miyazono, K. (2009). *Modulation of microRNA processing by p53*. Nature 460, 529-533.
69. Moll, U.M., Wolff, S., Speidel, D., and Deppert, W. (2005). *Transcription-independent pro-apoptotic functions of p53*. Curr Opin Cell Biol 17, 631-636.
70. Ahn, J., Poyurovsky, M.V., Baptiste, N., Beckerman, R., Cain, C., Mattia, M., McKinney, K., Zhou, J., Zupnick, A., Gottifredi, V., et al. (2009). *Dissection of the sequence-specific DNA binding and exonuclease activities reveals a superactive yet apoptotically impaired mutant p53 protein*. Cell Cycle 8, 1603-1615.
71. Lane, D.P., Cheok, C.F., Brown, C., Madhumalar, A., Ghadessy, F.J., and Verma, C. (2010). *Mdm2 and p53 are highly conserved from placozoans to man*. Cell Cycle 9, 540-547.
72. Lu, W., Chen, L., Peng, Y., and Chen, J. (2001). *Activation of p53 by roscovitine-mediated suppression of MDM2 expression*. Oncogene 20, 3206-3216.
73. Vassilev, L.T., Vu, B.T., Graves, B., Carvajal, D., Podlaski, F., Filipovic, Z., Kong, N., Kammlott, U., Lukacs, C., Klein, C., et al. (2004). *In vivo activation of the p53 pathway by small-molecule antagonists of MDM2*. Science 303, 844-848.
74. Meyer, N., and Penn, L.Z. (2008). *Reflecting on 25 years with MYC*. Nat Rev Cancer 8, 976-990.
75. Sheiness, D., Fanshier, L., and Bishop, J.M. (1978). *Identification of nucleotide sequences which may encode the oncogenic capacity of avian retrovirus MC29*. J Virol 28, 600-610.
76. Nilsson, J.A., and Cleveland, J.L. (2003). *Myc pathways provoking cell suicide and cancer*. Oncogene 22, 9007-9021.
77. Blackwood, E.M., and Eisenman, R.N. (1991). *Max: a helix-loop-helix zipper protein that forms a sequence-specific DNA-binding complex with Myc*. Science 251, 1211-1217.
78. Grandori, C., and Eisenman, R.N. (1997). *Myc target genes*. Trends Biochem Sci 22, 177-181.
79. Blackwell, T.K., Kretzner, L., Blackwood, E.M., Eisenman, R.N., and Weintraub, H. (1990). *Sequence-specific DNA binding by the c-Myc protein*. Science 250, 1149-1151.
80. Nair, S.K., and Burley, S.K. (2003). *X-ray structures of Myc-Max and Mad-Max recognizing DNA. Molecular bases of regulation by proto-oncogenic transcription factors*. Cell 112, 193-205.

81. Fieber, W., Schneider, M.L., Matt, T., Krautler, B., Konrat, R., and Bister, K. (2001). *Structure, function, and dynamics of the dimerization and DNA-binding domain of oncogenic transcription factor v-Myc*. J Mol Biol 307, 1395-1410.
82. Pelengaris, S., Khan, M., and Evan, G. (2002). *c-MYC: more than just a matter of life and death*. Nat Rev Cancer 2, 764-776.
83. Stone, J., de Lange, T., Ramsay, G., Jakobovits, E., Bishop, J.M., Varmus, H., and Lee, W. (1987). *Definition of regions in human c-myc that are involved in transformation and nuclear localization*. Mol Cell Biol 7, 1697-1709.
84. Craig, R.W., Buchan, H.L., Civin, C.I., and Kastan, M.B. (1993). *Altered cytoplasmic/nuclear distribution of the c-myc protein in differentiating ML-1 human myeloid leukemia cells*. Cell Growth Differ 4, 349-357.
85. Gallant, P., and Steiger, D. (2009). *Myc's secret life without Max*. Cell Cycle 8, 3848-3853.
86. Dang, C.V., O'Donnell, K.A., Zeller, K.I., Nguyen, T., Osthus, R.C., and Li, F. (2006). *The c-Myc target gene network*. Semin Cancer Biol 16, 253-264.
87. Lutterbach, B., and Hann, S.R. (1994). *Hierarchical phosphorylation at N-terminal transformation-sensitive sites in c-Myc protein is regulated by mitogens and in mitosis*. Mol Cell Biol 14, 5510-5522.
88. Bouchard, C., Dittrich, O., Kiermaier, A., Dohmann, K., Menkel, A., Eilers, M., and Luscher, B. (2001). *Regulation of cyclin D2 gene expression by the Myc/Max/Mad network: Myc-dependent TRRAP recruitment and histone acetylation at the cyclin D2 promoter*. Genes Dev 15, 2042-2047.
89. Sebe-Pedros, A., de Mendoza, A., Lang, B.F., Degnan, B.M., and Ruiz-Trillo, I. (2011). *Unexpected repertoire of metazoan transcription factors in the unicellular holozoan Capsaspora owczarzaki*. Mol Biol Evol 28, 1241-1254.
90. King, N., Westbrook, M.J., Young, S.L., Kuo, A., Abedin, M., Chapman, J., Fairclough, S., Hellsten, U., Isogai, Y., Letunic, I., et al. (2008). *The genome of the choanoflagellate Monosiga brevicollis and the origin of metazoans*. Nature 451, 783-788.
91. Sherman, L.A., and Chattopadhyay, S. (1993). *The molecular basis of allorecognition*. Annu Rev Immunol 11, 385-402.

92. Kuznetsov, S.G., and Bosch, T.C. (2003). *Self/nonself recognition in Cnidaria: contact to allogeneic tissue does not result in elimination of nonself cells in Hydra vulgaris*. *Zoology (Jena)* 106, 109-116.
93. Ben-Shlomo, R. (2008). *The molecular basis of allorecognition in ascidians*. *Bioessays* 30, 1048-1051.
94. Gauthier, M., and Degnan, B.M. (2008). *Partitioning of genetically distinct cell populations in chimeric juveniles of the sponge Amphimedon queenslandica*. *Dev Comp Immunol* 32, 1270-1280.
95. Rosengarten, R.D., and Nicotra, M.L. (2011). *Model systems of invertebrate allorecognition*. *Curr Biol* 21, R82-92.
96. Lakkis, F.G., Dellaporta, S.L., and Buss, L.W. (2008). *Allorecognition and chimerism in an invertebrate model organism*. *Organogenesis* 4, 236-240.
97. Ameisen, J.C. (2002). *On the origin, evolution, and nature of programmed cell death: a timeline of four billion years*. *Cell Death Differ* 9, 367-393.
98. Grosberg, R.K., and Strathmann, R.R. (2007). *The Evolution of Multicellularity: A Minor Major Transition?* *Annu. Rev. Ecol. Evol. Syst.* 38, 621-654.
99. Kastan, M.B., and Bartek, J. (2004). *Cell-cycle checkpoints and cancer*. *Nature* 432, 316-323.
100. Beckingham, K.M., Armstrong, J.D., Texada, M.J., Munjaal, R., and Baker, D.A. (2005). *Drosophila melanogaster—the model organism of choice for the complex biology of multi-cellular organisms*. *Gravit Space Biol Bull* 18, 17-29.
101. Brenner, S. (2009). *In the beginning was the worm*. *Genetics* 182, 413-415.
102. Collins, A.G., Cartwright, P., McFadden, C.S., and Schierwater, B. (2005). *Phylogenetic context and Basal metazoan model systems*. *Integr Comp Biol* 45, 585-594.
103. Galliot, B. (2012). *Hydra, a fruitful model system for 270 years*. *Int J Dev Biol* 56, 411-423.

2 Experimental Studies

2.1 Inhibitors of the p53-Mdm2 interaction increase apoptosis and produce abnormal phenotypes in the placozoon *Trichoplax adhaerens* (F.E. Schulze)

von der Chevallerie K.¹

Rolfes S.¹

Schierwater B.^{1,2}

¹ Division of Ecology and Evolution, Stiftung Tierärztliche Hochschule Hannover, Germany

² Department of Molecular, Cellular and Developmental Biology, Yale University, New Haven, Connecticut, United States of America

Abstract

Recent identification of genes homologous to human p53 and Mdm2 in the basal phylum Placozoa raised the question whether the network overtakes the same functions in the most primitive metazoan organism as it does in higher animals. We here describe inhibition experiments on p53/Mdm2 interaction in *Trichoplax adhaerens* by applying the inhibitors nutlin-3 and roscovitine. Both inhibitors had a strong impact on the animals' health by significantly increasing apoptotic events. Treatment with roscovitine also decreased cell proliferation, which likely is reducible to its function as cyclin-dependent kinase (CDK) inhibitor. Phenotypic abnormalities have been observed during long-term application of both inhibitors and either treatment is highly lethal in *Trichoplax adhaerens*. The findings of this study suggests a conserved role of the p53/Mdm2 network for apoptosis since the origin of the Metazoa and advocate the deployment of Placozoa as a model for p53, apoptosis and possibly cancer research.

Keywords: Placozoa, p53, Mdm2, nutlin-3, roscovitine

Introduction

Trichoplax adhaerens, the only described species of the basal phylum Placozoa offers peculiar opportunities to investigate complex mechanisms such as the control of apoptosis at the base of the metazoan tree of life (cf. [1-3]). Sequencing of the *Trichoplax* genome in 2008 revealed a surprisingly high diversity of protein coding genes, which look like an apparent discrepancy to its extremely simple bauplan [4-7].

The tumor suppressor p53 and its ubiquitin ligase Mdm2 have lately been shown to be conserved from Placozoa to human [8]. In higher animals p53 has been shown to have a protective function that ensures the integrity of a cell. In case of cellular stress or DNA damage, the protein is able to induce the transcription of target genes important for repair mechanisms or to provoke entrance into the apoptotic pathway (for review cf. [9, 10]). The negative regulator of p53, Mdm2, is antagonizing p53 in case of normal conditions [11]. In invertebrates, protein homologues to Mdm2 have yet been identified for seven species only. This suggests the early evolution of p53 regulation on the one hand but also supports the hypothesis of an ancient Mdm2-independent p53 modulation [12, 13]. P53 is indispensable for the retention of a tissues fitness conspicuously coherent regarding the fact that 50% of all known human tumors are a result of p53 deregulation [14]. The p53/Mdm2 interplay hence is an area of intense research. It is particularly extraordinary that Mdm2 is missing in well-known invertebrate model systems like *Caenorhabditis* or *Drosophila* [15, 16]. This information pleads for a derived function of the network in these

2.1 Inhibitors of the p53-Mdm2 interaction in the placozoon *Trichoplax adhaerens*

organisms, which likely evolved an Mdm2-independent way of p53 regulation. However, the lack of Mdm2 in *Caenorhabditis* and *Drosophila* makes it questionable whether these species can be appropriate models for p53 research [12, 17].

Knowledge on the presence of p53 and Mdm2 in Placozoa has so far been based on sequence analyses only [8]. We here describe the first experimental approaches to unravel functions of p53/Mdm2 interaction in the primitive animal *Trichoplax adhaerens*. The application of two inhibitors, nutlin-3 and roscovitine, was used to find out whether these proteins overtake functions in Placozoa that are analogous to the ones known in higher animals. Nutlin-3 is a cis-imidazoline that chemically obstructs the p53/Mdm2 interface and thus their interaction [18]. The purine roscovitine, commonly known as cyclin-dependent kinase (CDK) inhibitor, has also been shown to have an effect on Mdm2 expression on mRNA and protein level [19]. Both inhibitors cause imbalances in the p53/Mdm2 network by accumulation of p53 [20]. Besides observations of treated *Trichoplax* individuals via light microscopy, cell proliferation and apoptosis during treatment was monitored by means of Bromodesoxyuridine- (BrdU) incorporation and terminal deoxynucleotidyl transferase-mediated deoxyuridine triphosphate nick end labeling (TUNEL) essays. The results of our experiments reinforce the assumption that the p53/Mdm2 interplay has a fundamental impact on the progression of programmed cell death in *Trichoplax adhaerens*.

Material and Methods

Animal material

Trichoplax adhaerens (Haplotype 1, the “Grell” strain) was cultured as previously described in [21]. The animals were fed with *Pyrenomonas helgolandii* and *Chlorella salina* ad libitum. Experiments were performed with individuals of different sizes that were preliminary checked for not showing phenotypic irregularities.

Inhibitor treatment

The inhibitors were dissolved in dimethyl sulfoxide (DMSO) and were diluted in artificial seawater (ASW, salinity 35 ‰) up to 10 μ M (nutlin-3, Calbiochem) and 20 μ M (roscovitine, Calbiochem). Control experiments were performed with 0.1 % DMSO in ASW and ASW only. Animals were kept in one well glass chamber slides (one well cell culture chamber, Sarstedt, 2 ml volume) for daily counting and microscopic observations. The ASW containing the appropriate concentration of inhibitor and food solution respectively was changed every 48 hours (h) to avoid osmotic stress due to evaporation of water. Four individual experiments have been performed.

For subsequent BrdU or TUNEL staining as described below, the previous application of inhibitors was done in glass culture dishes (50 ml volume) in the same concentrations as used before. In these experiments an ASW control was not necessary since physiological

2.1 Inhibitors of the p53-Mdm2 interaction in the placozoon *Trichoplax adhaerens*

data had already revealed that DMSO application has no impact on the animals' fitness (unpublished data).

The BrdU essay

For the detection of cell proliferation after inhibitor treatment animals were treated each with roscovitine (20 μ M), nutlin-3 (10 μ M) or DMSO (0.1 % control) for 72 hours. Individuals were then fed with BrdU (Sigma, 50 ng/ml) for 4 h. After fixation in *Lavdowsky* fixative (Ethanol/TBS/Acetic Acid/Formaldehyde: 11/11/1/2) for one hour at room temperature the samples were permeabilized in TBS (pH 7.5) containing 0.5 % Tween-20 (TBST) for 12 h at 4 °C. The tissue was further permeabilized by proteinase K digestion (4 ng/ml) in TBST for 5 min. After stopping the reaction with glycine (1 mg/ml) two more washes with TBST were performed. Animals were then rinsed in 2 N HCL (in TBST) for 30 min and after three further washing steps in TBST, the tissue was quenched with 3 % H₂O₂. Samples were washed afterwards with TBST two more times and then blocked in 0.1 % Bovine Serum Albumin (BSA, Sigma) in TBST for 30 min. For detection of incorporated BrdU, a horseradish peroxidase labeled polyclonal sheep BrdU antibody (Abcam) was diluted 1:100 in TBST+BSA (0.1 %) and samples were incubated three hours at room temperature. The detection of the antibody was performed using the Thyramide Signal Amplification Kit #23 (TSA ®, Invitrogen) following the manufacturers protocol. Nuclei were subsequently counterstained with 1x 4',6-diamino-2-phenylindole (DAPI) in TBST for 10 min and after two terminal washes in TBS samples were mounted with Vectashield (Vector Labs) for microscopy.

The TUNEL essay

Animals were treated with inhibitors, fixed and permeabilized as described above. Apoptotic cells were then labeled using the ApopTag ® red *in situ* Kit (Chemicon International) following the manufacturers instructions. Subsequently nuclei were counterstained with 1x DAPI in TBST for 10 min, as described for BrdU staining, and samples were mounted on slides with Vectashield.

Microscopy

All microscopic pictures were made with a Zeiss Axiovert 200M connected to a digital camera (Zeiss, Axio Cam MRn). Zeiss Filter sets used for fluorescence pictures were 02 (DAPI) and 25 (Alexa Fluor 546). Pictures were modified using the Adobe Photoshop Elements 8.0 program to increase contrast only. Animal sizes and amount of proliferative or respectively apoptotic cells has been estimated utilizing the ImageJ software version 1.44. The proportions of proliferating (BrdU) and dying cells (TUNEL) have been estimated by counting the DAPI signals and calculate the relation to signal from BrdU and TUNEL.

2.1 Inhibitors of the p53-Mdm2 interaction in the placozoon *Trichoplax adhaerens*

Statistics

T-test analyses were conducted in Excel[®] (Microsoft Office[®] 2007) for all experiments. To compare animal sizes after inhibitor treatment, both controls (ASW and 0.1% DMSO) were compared with the experiments (nutlin-3 or roscovitine) independently and mutually. For analyses of apoptotic, respectively proliferating cells, values of experiments were compared with the DMSO control only as no ASW control was performed.

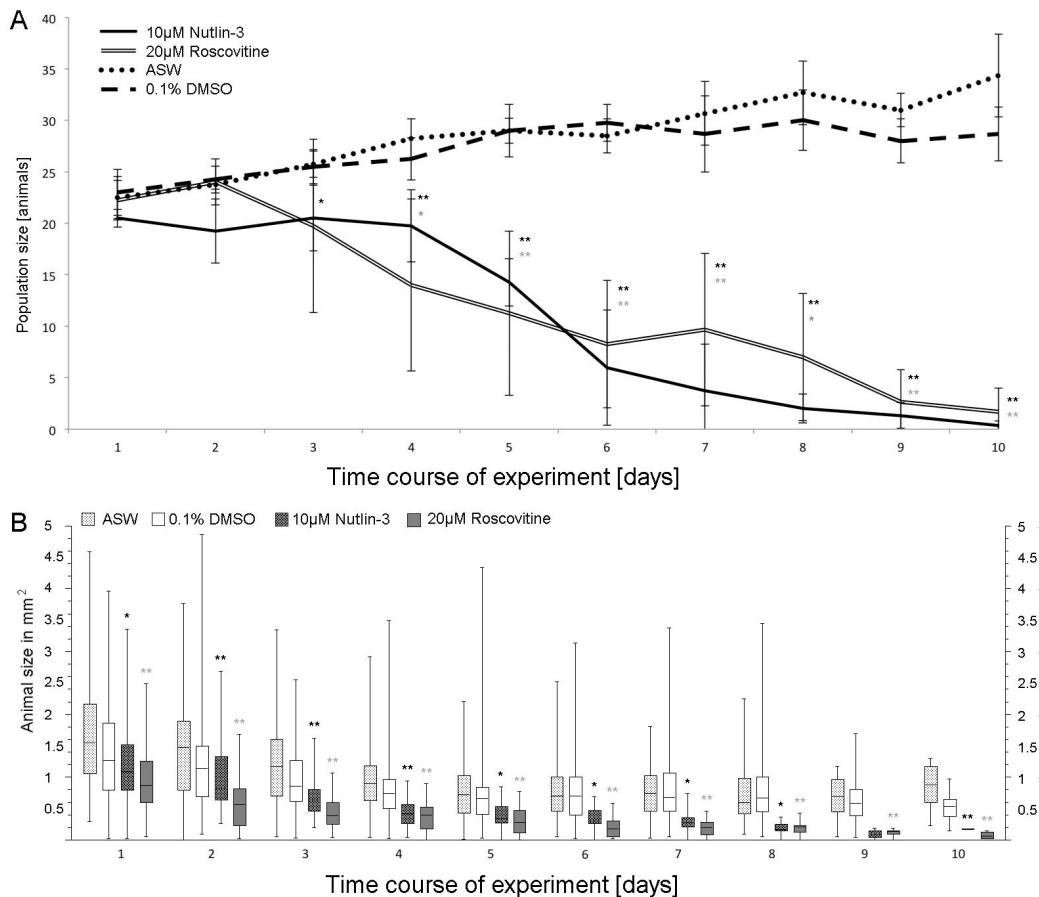


Figure 2.1.1: Time course of population size and animal sizes after inhibitor treatment.

The application of 10 μM nutlin-3 and 20 μM roscovitine was lethal within 11 days of treatment. All animals treated with the inhibitors were dead at day 11 (here not indicated).

(A) The number of animals decreases over time and significantly differs from the controls (ASW and 0.1% DMSO) after 3 days of nutlin-3 treatment and four days after initial roscovitine application.

(B) An overall reduction of size was observed directly after initial treatment for both inhibitors. Whiskers mark minimum and maximum body size, the box represents the upper and the lower quartile and the horizontal line indicates the median. Asterisks mark significances for nutlin-3 (black) and roscovitine (grey) treatment. $p < 0.05 = *$, $p < 0.01 = **$ and $p < 0.001 = ***$.

For raw data and statistics see table A.1.1 and A.1.2.

2.1 Inhibitors of the p53-Mdm2 interaction in the placozoon *Trichoplax adhaerens*

Results

Both inhibitors have a strong impact on the animals' physiology.

Long-term application of the inhibitors led to severe stress for the animals, which was observed after application of nutlin-3 as well as roscovitine.

The overall number of 10 μM nutlin-3 treated animals was significantly reduced after 3 days ($p < 0.05$) compared to DMSO and ASW controls. The 20 μM roscovitine treated animal population significantly decreased even after 4 days ($p < 0.05$). Treatment was lethal to all individuals latest after 11 days (cf. fig. 2.1.1 A and 1B). Death of treated individuals was generally preceded by decrease of size (fig. 2.1.1 B) whereas this was instantly significant the day after initial treatment ($p < 0.05$ for nutlin-3 treatment and $p < 0.01$ for roscovitine application; cf. fig. 2.1.1 B and fig. 2.1.2). The control experiments in ASW and 0.1% DMSO did show a reduction in animal size but not in population size (fig. 2.1.1 A and B).

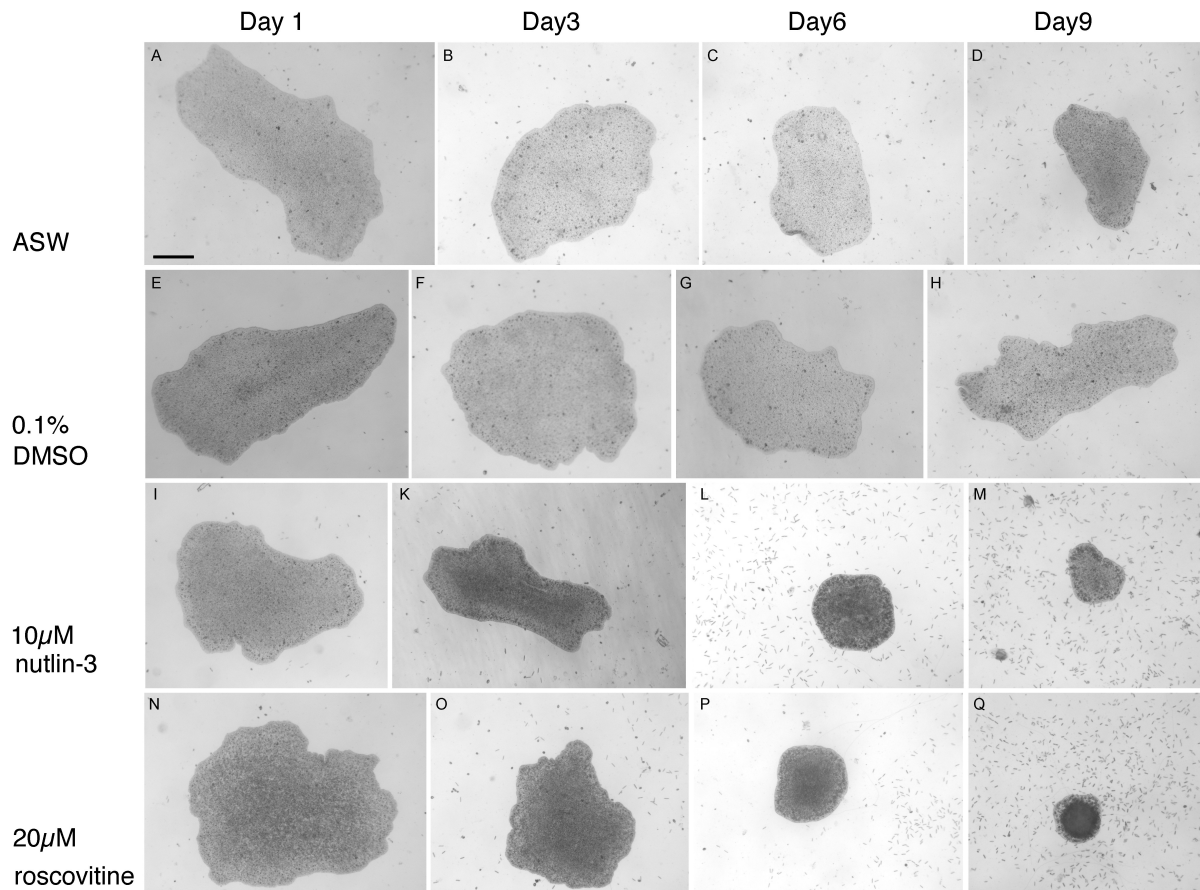


Figure 2.1.2: Phenotypic changes after inhibitor treatment.

Light microscopy of animals treated with 10 μM nutlin-3 (I-M) and 20 μM roscovitine (N-Q) as well as ASW only (A-D) and 0.1% DMSO (E-H). Day 1 (A,E,I,N), day 3 (B,F,K,O), day 6 (C,G,L,P) and day 9 (D,H,M,Q) after initial treatment. ASW and DMSO control animals do not show phenotypic conspicuities whereas nutlin-3 and roscovitine treatment was accompanied by a reduction of size. Size bar in A marks 100 μm for all pictures.

2.1 Inhibitors of the p53-Mdm2 interaction in the placozoon *Trichoplax adhaerens*

A certain proportion (up to 21.4% in case of nutlin-3 and up to 19.6% for roscovitine) of individuals reproducibly showed distinct changes in body shape within the first six days of treatment (fig. 2.1.3). In three out of four experiments the expression of fringed hunches at the animals' margin happened after application of both inhibitors respectively and holes in the center of animals were observed in two of four experiments with roscovitine (fig. 2.1.3, A-C). Control experiments and lower concentrations of inhibitors did not result in any of such shape changes (data not shown).

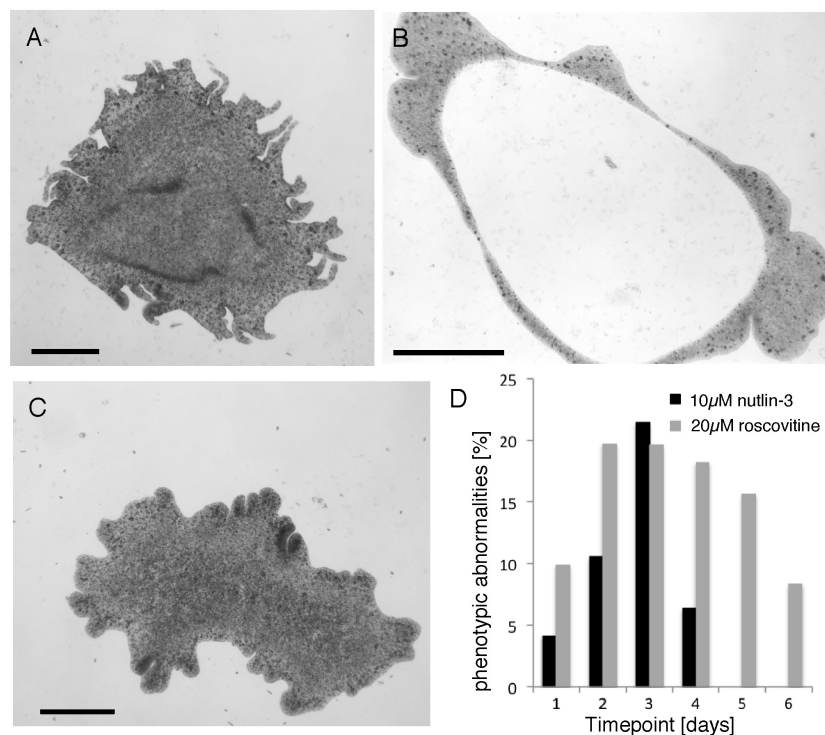


Figure 2.1.3: Phenotypic changes after inhibitor treatment.

Abnormalities were observed within the first six days of treatment with both inhibitors: fringed hunches and central holes after roscovitine treatment (A, day 2; and B, day 3) and fringes only after nutlin-3 application (C, day 2). The overall percentages of animals with phenotypic changes (D) affirm an impact of inhibitor treatment on the animals' physical appearance. However, the observed effects turned out to be not significant ($p > 0.05$ for all experiments). The size bar marks 100 μm (A and C) and 200 μm (B). For raw data and statistics on phenotypes see table A.1.3.

Inhibitor treatment increases apoptosis and roscovitine has an impact on cell proliferation.

Besides the abnormal phenotypic effects resulting from inhibitor treatment, outcomes of BrdU and TUNEL staining indicate that treatment with nutlin-3 and roscovitine significantly affects programmed cell death (fig. 2.1.4). After 72 h of nutlin-3 treatment, the average amount of apoptotic cells increased by 3.8% compared to the DMSO control.

2.1 Inhibitors of the p53-Mdm2 interaction in the placozoon *Trichoplax adhaerens*

Roscovitine treatment for the same interval resulted in an increase of apoptotic cells by 1.9% compared to the control. Both values differ significantly from the DMSO control ($p < 0.001$). Nutlin-3 treatment in contrast did not significantly affect cell proliferation. Although average cell proliferation rate in each approach was equally reduced by $\sim 10\%$ after application of the particular inhibitors, merely the decrease caused by roscovitine turned out to be significant ($p < 0.05$).

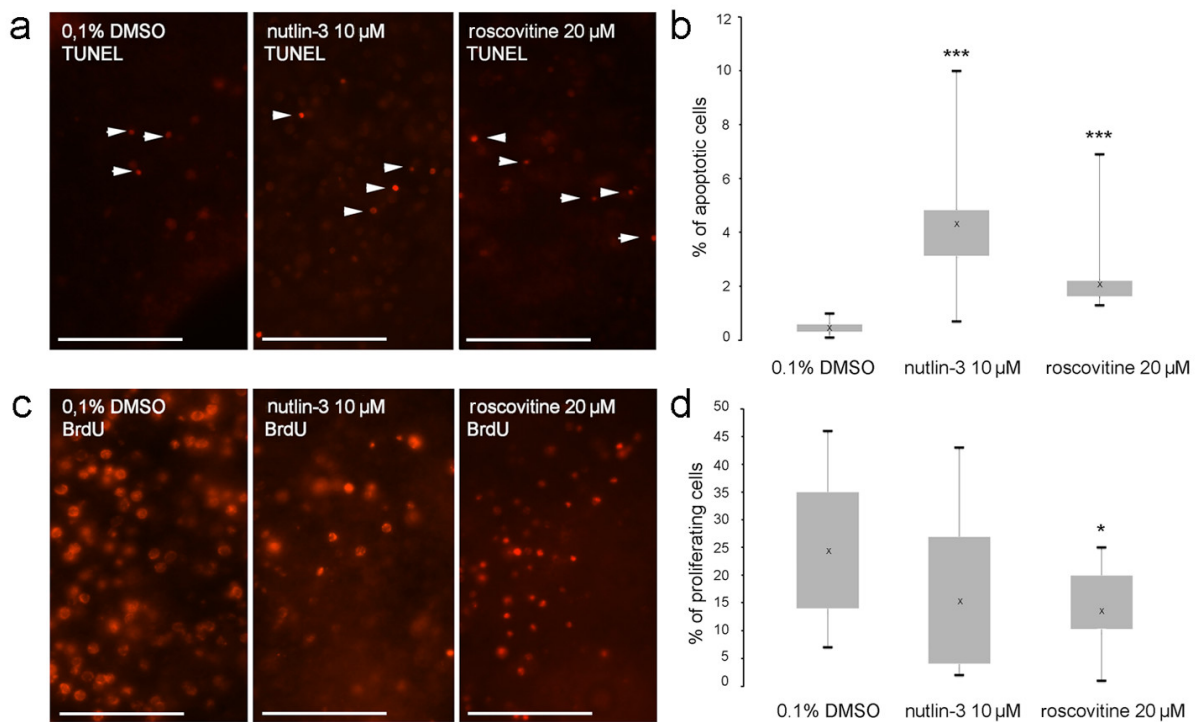


Figure 2.1.4: TUNEL- and BrdU staining 72h after inhibitor application.

Apoptotic- (TUNEL, upper panel) and proliferating cells (BrdU, lower panel). Apoptosis was highly significant increased after treatment with both, 10 μM nutlin-3 and 20 μM roscovitine ($p < 0.001$) respectively whereas proliferation was significantly decreased ($p < 0.05$) after treatment with 20 μM roscovitine only. Boxplot shows maximum and minimum (whiskers), upper and lower quartile (box) and the average (cross). Asterisks mark significant deviations from the DMSO control. The size bars marks 20 μm . For raw data and statistics see table A.1.4.

Discussion

Nutlin-3 and roscovitine have been known to induce the accumulation of p53 in a cell leading to p53-induced apoptosis (cf.[20]). Despite intense research efforts, many functions of the vertebrate p53/Mdm2 interaction and their targets still remain a closed book. Thus, knowledge of the network in different animal phyla, especially in lower metazoans, will provide crucial insights from disparate perspectives. So far known functions of p53 in invertebrates are related to the protection of genome integrity in early embryos as well as in germ-line cells but also to the regulation of stem-cell proliferation and development [15, 22-24].

2.1 Inhibitors of the p53-Mdm2 interaction in the placozoon *Trichoplax adhaerens*

Inhibition of p53/Mdm2 interaction triggers apoptosis and is lethal in Placozoa.

Nutlin-3 is known to bind to the human Mdm2 protein and thereby prevent its role as a p53 antagonist [18]. This may also be the case in Placozoa particularly since the *Trichoplax* Mdm2 protein has been shown to be able to bind to human p53 [17]. The observed increase of apoptosis in nutlin-3 treated animals could be caused by p53 accumulation in line with p53-induced programmed cell death. The usage of roscovitine in the laboratory mainly addresses questions concerning its function as a cyclin dependent kinase (CDK) inhibitor but its role in down regulation of Mdm2 has previously been demonstrated [19, 25]. Augmentation of apoptosis due to roscovitine treatment of *Trichoplax* individuals can be a result of both; CDK as well as Mdm2 inhibition.

Roscovitine treatment affects cell proliferation and both inhibitors produce abnormal phenotypes.

Nutlin-3 treatment of *Trichoplax* individuals did not affect cell cycle progression as monitored by the BrdU essay. This stays in contrast to the effect triggered by roscovitine application: Treatment with roscovitine caused a significant decrease in cell proliferation. This effect could be related to its function as CDK inhibitor since roscovitine treatment is known to cause cell cycle arrest (cf. [25]). The amount of cell proliferation events differs significantly between *Trichoplax* individuals, depending on the animals' developmental stage (means: swarmer, before/after fission) and size (unpublished data). This explains the high variance of BrdU signal (fig. 2.1.4) and leads us to the speculation that an average reduction of signal (~10%) may point to an effect on cell cycle progression induced by both inhibitor treatments. The reduction of body size during long-term inhibitor treatment further supports the assumption that cell proliferation is affected by both inhibitor treatments. ASW and DMSO control also showed a decrease in size that, however, likely is a consequence of suboptimal culturing conditions during the experiment and differs significantly from the treatments. Abnormal phenotypes have been observed after treatment with both inhibitors whereas the effect caused by roscovitine was stronger. The described phenotypes provide strong evidence for a disturbance of animals' development: The enlarged margin, respectively the central hole, suggests an imbalance in the control of central to marginal tissue growth ratio which usually is tightly regulated in placozoans [26]. It may be the case that the inhibitor treatment also has an influence on stem cell proliferation that was not detectable in our experiments, as proliferation of epithelial cells is frequent and possibly masks signal from cells with a lower proliferation rate. Altered stem cell proliferation as a consequence of inhibitor treatment could explain the enlargement of the animals' margin, since placozoan stem cells are known to be located in the area close to the margin and control the animals' growth and division rate [27].

2.1 Inhibitors of the p53-Mdm2 interaction in the placozoon *Trichoplax adhaerens*

Conclusion

The overall results of this study provide evidence for a p53/Mdm2 network in Placozoa that has similar functions to the ones found in higher animals and which is also involved in developmental processes. Future studies on p53 and Mdm2 in Placozoa will help to understand this network from a very basal point of view and thus will help to encourage research also on the evolution of human malignancies.

Acknowledgements

K. vdC. was funded by an Evangelische Studienwerk Villigst e.V. PhD fellowship, an "Otto Bütschli" scholarship from the Tierärztliche Hochschule Hannover and a travel grant from Boehringer Ingelheim Fonds. We are grateful to Dr. Ismail M. Hanif for providing the inhibitors and for coming up with the initial idea for the experiments.

2.1 Inhibitors of the p53-Mdm2 interaction in the placozoon *Trichoplax adhaerens*

References

1. Schierwater, B., de Jong, D., and Desalle, R. (2009). *Placozoa and the evolution of Metazoa and intrasomatic cell differentiation*. Int J Biochem Cell Biol 41, 370-379.
2. Schierwater, B., Eitel, M., Jakob, W., Osigus, H.J., Hadryns, H., Dellaporta, S.L., Kolokotronis, S.O., and DeSalle, R. (2009). *Concatenated Analysis Sheds Light on Early Metazoan Evolution and Fuels a Modern "Urmetazoon" Hypothesis*. Plos Biology 7, 36-44.
3. Osigus, H.J., Eitel, M., and Schierwater, B. (2013). *Chasing the urmetazoon: Striking a blow for quality data?* Mol Phylogenet Evol 66, 551-557.
4. Srivastava, M., Begovic, E., Chapman, J., Putnam, N.H., Hellsten, U., Kawashima, T., Kuo, A., Mitros, T., Salamov, A., Carpenter, M.L., et al. (2008). *The Trichoplax genome and the nature of placozoans*. Nature 454, 955-960.
5. Ringrose, J.H., van den Toorn, H.W., Eitel, M., Post, H., Neerincx, P., Schierwater, B., Maarten Altelaar, A.F., and Heck, A.J. (2013). *Deep proteome profiling of Trichoplax adhaerens reveals remarkable features at the origin of metazoan multicellularity*. Nat Commun 4, 1408.
6. de Jong, D., Eitel, M., Jakob, W., Osigus, H.J., Hadryns, H., DeSalle, R., and Schierwater, B. (2009). *Multiple Dicer Genes in the Early-Diverging Metazoa*. Molecular Biology and Evolution 26, 1333-1340.
7. Eitel, M., Osigus, H.-J., DeSalle, R., and Schierwater, B. (2013). *Global diversity of the Placozoa*. PLoS One, accepted.
8. Lane, D.P., Cheok, C.F., Brown, C., Madhumalar, A., Ghadessy, F.J., and Verma, C. (2010). *Mdm2 and p53 are highly conserved from placozoans to man*. Cell Cycle 9, 540-547.
9. Levine, A.J., and Oren, M. (2009). *The first 30 years of p53: growing ever more complex*. Nat Rev Cancer 9, 749-758.
10. Vousden, K.H., and Prives, C. (2009). *Blinded by the Light: The Growing Complexity of p53*. Cell 137, 413-431.a
11. Manfredi, J.J. (2010). *The Mdm2-p53 relationship evolves: Mdm2 swings both ways as an oncogene and a tumor suppressor*. Genes Dev 24, 1580-1589.
12. Momand, J., Villegas, A., and Belyi, V.A. (2011). *The evolution of MDM2 family genes*. Gene 486, 23-30.

2.1 Inhibitors of the p53-Mdm2 interaction in the placozoon *Trichoplax adhaerens*

13. Muttray, A.F., O'Toole, T.F., Morrill, W., Van Beneden, R.J., and Baldwin, S.A. (2010). *An invertebrate mdm homolog interacts with p53 and is differentially expressed together with p53 and ras in neoplastic Mytilus trossulus haemocytes*. *Comp Biochem Physiol B Biochem Mol Biol* 156, 298-308.
14. Joerger, A.C., and Fersht, A.R. (2007). *Structure-function-rescue: the diverse nature of common p53 cancer mutants*. *Oncogene* 26, 2226-2242.
15. Jin, S., Martinek, S., Joo, W.S., Wortman, J.R., Mirkovic, N., Sali, A., Yandell, M.D., Pavletich, N.P., Young, M.W., and Levine, A.J. (2000). *Identification and characterization of a p53 homologue in Drosophila melanogaster*. *Proc Natl Acad Sci U S A* 97, 7301-7306.
16. Derry, W.B., Putzke, A.P., and Rothman, J.H. (2001). *Caenorhabditis elegans p53: role in apoptosis, meiosis, and stress resistance*. *Science* 294, 591-595.
17. Lane, D.P., and Verma, C. (2012). *Mdm2 in evolution*. *Genes Cancer* 3, 320-324.
18. Vassilev, L.T., Vu, B.T., Graves, B., Carvajal, D., Podlaski, F., Filipovic, Z., Kong, N., Kammlott, U., Lukacs, C., Klein, C., et al. (2004). *In vivo activation of the p53 pathway by small-molecule antagonists of MDM2*. *Science* 303, 844-848.
19. Lu, W., Chen, L., Peng, Y., and Chen, J. (2001). *Activation of p53 by roscovitine-mediated suppression of MDM2 expression*. *Oncogene* 20, 3206-3216.
20. Brown, C.J., Lain, S., Verma, C.S., Fersht, A.R., and Lane, D.P. (2009). *Awakening guardian angels: drugging the p53 pathway*. *Nat Rev Cancer* 9, 862-873.
21. Schierwater, B. (2005). *My favorite animal, Trichoplax adhaerens*. *Bioessays* 27, 1294-1302.
22. Pankow, S., and Bamberger, C. (2007). *The p53 tumor suppressor-like protein nvp63 mediates selective germ cell death in the sea anemone Nematostella vectensis*. *PLoS One* 2, e782.
23. Jessen-Eller, K., Kreiling, J.A., Begley, G.S., Steele, M.E., Walker, C.W., Stephens, R.E., and Reinisch, C.L. (2002). *A new invertebrate member of the p53 gene family is developmentally expressed and responds to polychlorinated biphenyls*. *Environ Health Perspect* 110, 377-385.
24. Pearson, B.J., and Sanchez Alvarado, A. (2010). *A planarian p53 homolog regulates proliferation and self-renewal in adult stem cell lineages*. *Development* 137, 213-221.

2.1 Inhibitors of the p53-Mdm2 interaction in the placozoon *Trichoplax adhaerens*

25. Meijer, L., Borgne, A., Mulner, O., Chong, J.P., Blow, J.J., Inagaki, N., Inagaki, M., Delcros, J.G., and Moulinoux, J.P. (1997). *Biochemical and cellular effects of roscovitine, a potent and selective inhibitor of the cyclin-dependent kinases cdc2, cdk2 and cdk5*. Eur J Biochem 243, 527-536.
26. Schwartz, V. (1984). *The radial polar pattern of differentiation in Trichoplax adhaerens F.E. Schulze (Placozoa)*. Z. Naturforsch. 39c, 818-832.
27. Jakob, W., Sagasser, S., Dellaporta, S., Holland, P., Kuhn, K., and Schierwater, B. (2004). *The Trox-2 Hox/ParaHox gene of Trichoplax (Placozoa) marks an epithelial boundary*. Dev Genes Evol 214, 170-175.

2.2 The Myc/Max network at the base of the metazoan tree of life

von der Chevallerie K.¹

Topf A.²

Sagasser S.^{1,3}

Tsiavaliaris G.²

Schierwater B.^{1,4}

¹ Division of Ecology and Evolution, Stiftung Tierärztliche Hochschule Hannover, Germany

² Institute for Biophysical Chemistry, OE4350, Hannover Medical School, 30623 Hannover, Germany

³ Department of Cell and Molecular Biology, Karolinska Institutet, Stockholm, Sweden

⁴ Department of Molecular, Cellular and Developmental Biology, Yale University, New Haven, Connecticut, United States of America

This manuscript is an authors version of a manuscript to be submitted to *Molecular Biology and Evolution*.

Abstract

The Myc/Max network of transcription factors is well conserved throughout animal kingdom. By binding to specific DNA sequence motifs, the bHLHL-Zip proteins are involved in the regulation of cell cycle, metabolism, apoptosis and differentiation. Deregulations of the *c-myc* gene are reason for a large proportion of known malignancies. Placozoa hold a pivotal role regarding the evolution of multicellularity as they are most closely related to the hypothetical "Urmetazoon". The sequencing of the *Trichoplax* genome in 2008 revealed the presence of Myc/Max homologues and has led us to investigate their role in this simple animal. By means of *in situ* hybridization and Myc/Max gene inhibition studies we got first insights of this important network at the very base of the metazoan tree of life. In this study, first experimental approaches were done to unravel the function of the Myc/Max network in the basal phylum Placozoa. By means of both, gene inhibition and RNA expression studies, we gained insights into function of these genes in Placozoa. The gene knockdown of *tamyc* and *tamax* as well as the chemical inhibition of Myc/Max dimerization by the small-molecule inhibitor 10058-F4 significantly increased the amount of cells undergoing apoptosis. Chemical inhibition of Myc/Max interaction did not influence cell proliferation in *Trichoplax*. In contrast, knockdown of *tamyc/tamax* decreases the amount of cell division events after shorter time and did up regulate proliferation rate a longer time after initial knockdown. As the lack of *tamyc* function results in an increase of apoptosis in the animals' marginal area and the expression pattern of *tamyc* and *tamax* furthermore did reveal prominent gene activity in this region, where the Placozoan stem cells are presumed to be located, our results suggests that the function of *tamyc* possibly is involved in differentiation processes.

Keywords: Myc/Max network, Placozoa, development

Introduction

About 30 % of all known human malignancies are induced or at least accompanied by a deregulation of the *myc* gene. Genes of the *myc* proto-oncogene family (*c-myc*, *L-myc* and *N-myc*) are known to be involved in the regulation of various mechanisms affecting cell cycle control including metabolism, protein biosynthesis, cell adhesion and differentiation to name but a few. Point mutations in the *myc* gene or translocations respectively duplication of the gene regions can result in an overexpression of the gene as well as an increased Myc protein stability. For example Burkitt's lymphoma is a cancer of the lymphatic system

2.2 The Myc/Max network at the base of the metazoan tree of life

caused by chromosomal translocation of the *myc* gene that displaces the gene proximal to an immunoglobulin enhancer leading to massive overexpression of the gene [1].

Myc belongs to the basic helix-loop-helix-leucine-zipper (bHLHL-Zip) proteins and together with the bHLHL-Zip protein Max, Myc is proceeding in a network whereas the switch between Max-Max and Myc-Max dimerization represses or activates the transcription of target genes (for review see e.g. [2-4]). By binding to specific E-box sequences of the DNA (consensus sequence CACGTG) and subsequent recruitment of co-regulators Myc's scope as transcription factor is known to comprise 10-15 % of all gene loci found in mammals and *Drosophila melanogaster* which makes it a critical master control gene [5, 6]. Homologues of the *myc* gene have been found in all metazoan lineages including the cnidarian *Hydra vulgaris* in which it is active in rapidly proliferating cells of the interstitial stem cell system [7, 8]. In the unicellular organism *Monosiga brevicollis* the Myc protein has been demonstrated to interact with Max suggesting a similar role as in multicellular organisms [9]. We now investigated the Myc/Max network at the very base of the metazoan tree of life.

Trichoplax adhaerens is the up to now only described representative of the phylum Placozoa [10, 11]. With only five different somatic cell types forming three distinct layers, this organism possesses the simplest known animal bauplan. Monociliated cover cells with interspersed likely degenerated cells, the shiny spheres, form the upper epithelium and likewise ciliated cylinder cells together with gland cells make up the lower epithelium. Enclosed by both epithelia, the fiber cells form a syncytial network (cf. [12]). The marginal region of the organism inhabits the multipotent stem cells, known to be essential for the animals' development [13]. As Placozoa represent the best living surrogate for the most basal metazoan phylum, regulative mechanisms controlling complex incidents like the cell cycle may be the most primitive and thus possibly the simplest [14, 15]. The genetic equipment of Placozoa is much more diverse as it would be expected, relatively speaking compared to its simple bauplan characteristics [16]. Understanding the role of an important regulatory network as the Myc/Max network in Placozoa will clearly help to better understand the role of this system also in higher animals.

Here we describe first experimental approaches to unravel the function of *myc/max* homologues in *Trichoplax adhaerens* (*tamyc* and *tamax*). Whole mount *in situ* hybridization experiments display the expression patterns in this ancient animal. A gene knockdown (KD) of both: *tamyc* and *tamax* by means of morpholino oligonucleotides (MO) has been conducted as well as the chemical inhibition of taMyc/taMax dimerization by the small-molecule inhibitor 10058-F4 [17]. Effects of this treatment have been monitored via light microscopy and fluorescent staining of cell proliferation (BrdU) and apoptosis (TUNEL). First experimental efforts to express taMyc/taMax proteins have been conducted and lay the foundation for further research in this field. Results of our study indicate an

involvement of *tamyc/tamax* in the control of developmental processes. Inhibition of taMyc by means of MO knockdown as well as inhibitor treatment is lethal and causes an increase of apoptosis whereas cell proliferation affected by KD but not by the inhibitor. The outcome of *tamyc/tamax* expression studies by *in situ* hybridization furthermore suggests that the genes are active mainly in the *Trichoplax* stem cell lineage suggesting their role to be crucial for animal growth and development. The usage of Placozoa as a model system for further research on the Myc/Max network will substantially extend our knowledge on the evolution of cell cycle regulation.

Material and Methods

Animal material

Trichoplax adhaerens (the "Grell" strain [18]) was used in this study. Culturing conditions were standardized as described before [10]. Animals were fed *ad libitum* with the unicellular algae *Pyrenomonas helgolandii* and *Chlorella salina*.

Total RNA isolation and full-length cDNA synthesis

Approximately 100 individuals have been picked and rinsed in artificial seawater (ASW). After 18 h starvation, animals have been homogenized in 500 μ l homogenization buffer (HomI buffer: 0.1 M Tris HCl pH 8, 0.01 M ethylenediaminetetraacetic acid (EDTA) pH 8, 0.1 M NaCl, 0.025 M dithiothreitol (DTT) and 0.5 % sodium dodecyl sulfate (SDS) in ddH₂O) with 25 μ l ProteinaseK (10 mg/ml, Carl Roth, Germany) at 55 °C for 30 min. Nucleic acids then have been isolated with phenol-chlorophorm isoamylalcohol (Roti® Aqua- Phenol/C/I, Carl Roth, Germany) and a subsequent isopropanol precipitation. The pellet has been resuspended in diethylpyrocarbonate-treated (DEPC, Carl Roth, Germany) water and DNA then was digested with DNaseI (Fermentas) following the manufacturer's instructions. Quality of RNA has been determined by gel electrophoresis and total RNA (~ 100 ng) has then been used for full-length cDNA preparation using the Gene Racer™ Core Kit (Invitrogen) according to the manufacturer's instructions.

5' RACE amplification of cDNA ends

Comparative Blast searches were done for identification of *myc* and *max* homologues in *Trichoplax adhaerens* (NCBI: *tamyc*, GenBank accession no XM_002113921.1 and *tamax* GenBank accession no XM_002107825.1. To obtain information on the 5' end of the *tamyc* and *tamax* genes for subsequent MO design, a gene-specific primer (*tamyc* 5'-CAGCAATACATAACTGATACTTCATC-3'; *tamax* 5'-AAGAGCCCATCATAACGCTTTGGAGCG -3') has been combined with the 5' Race Primer of the Kit (Gene Racer™ Core Kit, Invitrogen) and 1 μ l of the full-length cDNA (diluted 1:10) was used in a final volume of 25 μ l. The fragments have been amplified with the BioTaq™ DNA Polymerase (Bioline)

2.2 The Myc/Max network at the base of the metazoan tree of life

system using the following "Touch Down" PCR conditions: initial denaturation 5 min at 95 °C, 5 circles of 30 sec at 95 °C, 30 sec at 72 °C, 1 min at 72 °C, 5 circles of 30 sec at 95 °C, 30 sec at 70 °C, 1 min- 72 °C, 25 circles of 30 sec - 95 °C, 30 sec - 68 °C, 1 min - 72 °C and a final elongation step for 7 min at 72 °C. Fragments have been precipitated and were subsequently cloned into the pGemT vector system (Promega). Ligation then has been transformed into Top10 competent cells and after selection of positive clones via blue-white screening the plasmid has been isolated with the Miniprep Kit (Wizard ® Plus SV Minipreps, Promega) following the manufacturers protocol and sequenced (LIGHTrun, GATC).

No.	Gene	Trivial Name	Primer	Restriction site	Primer sequence
1	<i>tamax</i>	max_fw_hind	HindIII	<i>gc aagctt</i>	ATG AGT GAC GAA GAT AAG TAC
2	<i>tamax</i>	max_rv_not	NotI	<i>ga gcg gcc gct</i>	CTC TGC TTT GAC CTT TTT AGT
3	<i>tamyc</i>	myc_fw_SgfI_His	SgfI	<i>ga gcgatcgc</i>	<u>tcaccatcaccac</u> ATG GCA GTT CAT GCG GAA GCC
4	<i>tamyc</i>	myc_rv_Xho	XhoI	<i>ga ctgag</i>	ATT TCT TTT GCT CTT TAA AAT

Table 2.2.1: Primer sequences used for insert amplification for the pETDuet-1 construct.

Restriction sites used for ligation are indicated in italic. The His-tag sequence in primer no. 3 is underlined. The base pairs 'gc' (in primer no.1) and 'ga' (primer 2 - 4) were added to protect restriction sites from degradation. Reverse primer sequences are specified in reverse complement direction.

Amplification of full-length tamyc and tamax fragments for sequence analysis and construction of tamyc/tamax/pETDuet-1 plasmids for protein expression.

Full-length fragments of *tamyc/tamax* were amplified for cloning into the bicistronic vector pETDuet-1 (Novagen). The primers for amplification of full-length fragments have been equipped with flanking 5' and 3' restriction sites for each multiple cloning site of the vector respectively (table 2.2.1). The *tamyc* fragment additionally was provided with a 5' His Tag sequence for later precipitation of the protein. Fragments have been amplified from full-length cDNA using the KAPAHiFi™ DNA polymerase (PeqLab) with the following PCR conditions: 5 min -95 °C, 40 cycles of (30 sec - 95 °C, 30 sec - 60 °C, 1 min - 72 °C) and 4 min - 72 °C. Products have been precipitated and cloned into the pGemT vector system for sequencing as described before. Sequences were used for analyses (described below) and after identification of appropriate clones, full-length *tamyc* and *tamax* have been cut out of the vector by using the respective restriction sites. Fragments were gel-purified and subsequently cloned into the expression vector. The pETDuet™ -1 vector has been cut with HindIII (Fermentas) and NotI (Fermentas) and the *max* fragment was ligated first. After transformation of the *tamax/pETDuet™ -1* construct into *Escherichia coli* (One Shot ® TOP10F' Chemically Competent *E. coli*, Invitrogen), colonies were selected by means of ampicillin resistance and plasmids have been checked for correct insertion of *tamax* fragment via PCR using the same *tamax* gene specific primer set as above (table 2.2.1, primer 1 and 2). Plasmids with the correct insert then have been cut

2.2 The Myc/Max network at the base of the metazoan tree of life

with the restriction enzymes SgfI (Promega) and XhoI (Fermentas) for subsequent ligation of *tamyc*. Transformation has been performed and colonies were selected by means of ampicillin resistance. Success of incorporation of both inserts into the petDuet-1 vector later on was checked with the forward primer of the *tamax* fragment combined with the reverse primer of *tamyc* (table 2.2.1, primer 1 and 4). Elongation time for this PCR approach has been prolonged to 90 sec, beside conditions were maintained as described above.

Expression and purification of taMyc and taMax proteins

Constructs of petDuet-1 with the full-length *tamyc/tamax* fragments were transformed into Rosetta (BL21), F-ompT hsdSB(rB- mB-) gal dcm pRARE (*Cam^R*). Bacteria were grown in a preparatory culture over night at 37 °C and were inoculated into a 4 liter culture in (LB broth with ampicillin 75 ng/ml) at 20 °C after induction of protein expression. Expression was induced at an optical density (OD) of 0.4 - 0.8 (measured at 600 nm) with isopropyl- β -D-thiogalactoside (IPTG, 0.1 mM) and lasted 16 h. Cells were pelletized and resuspended in lysis buffer (50 mM 4-(2-hydroxyethyl)-1-piperazineethanesulfonic acid (HEPES), pH 7.4 and 500 mM NaCl and 3 mM 2-Mercaptoethanol) with proteinase inhibitors (cOmplete EDTA free, Roche, Mannheim; 10 μ g/ml p-toluenesulfonyl-L-arginine methyl ester (TAME), 8 μ g/ml tosyl phenylalanyl chloromethyl ketone (TPCK), 0.2 μ g/ml pepstatin, 0.5 μ g/ml leupeptin, 0.1 mM phenylmethanesulfonylfluoride) and with 5 mg/100 ml lysozyme. After 30 min incubation on ice the suspension was sonicated on ice for 3 min in total (Branson Sonifier 250, Heinemann Ultraschall und Labortechnik, Schwäbisch Gmünd). Benzonase (5000 units, Sigma) then was added and the mixture was incubated 30 min on ice. The sample has been centrifuged at 30.000 rpm (Ti70 Rotor, Beckmann Coulter Optima XPN-90) for 60 min at 4 °C and the cleared supernatant was loaded on a nickel NTA column (Ni-NTA Superflow, Quiagen Hilden). Affinity chromatography was done at 4 °C in a ÄKTA purifier (FPLC system ÄKTA purifier 10, GE Healthcare, Freiburg). After equilibration of the column with buffer A (50 mM HEPES, pH 7.4, 500 mM NaCl, 3 mM 2-Mercaptoethanol, flow rate 3 ml/min, 6 column volumes, CV) the proteins were injected (0.5 ml/min) and the column was washed with buffer A (50 mM HEPES, pH 7.4, 500 mM NaCl, 3 mM 2-Mercaptoethanol, flow rate 3 ml/min, 6 CV), and subsequently with buffer B (50 mM HEPES, pH 7.4, 1 M NaCl, 3 mM 2-Mercaptoethanol, flow rate 3 ml/min, 6 CV). The column then was washed 3 CV with buffer A containing 5 % elution buffer (50 mM HEPES pH 7.4, 500 mM NaCl, 500 mM imidazole, 3 mM 2-Mercaptoethanol), and with 5 CV of buffer A including 10 % elution buffer. Elution of proteins was carried out in a gradient of buffer A with elution buffer whereas the proportion of elution buffer finally is 100 %. Fractions (collected with Frac-900, GE Healthcare, Freiburg) were checked on a SDS-polyacrylamide gel and the proteins were further purified via gel-filtration (using the ÄKTA system, mentioned above) on a high load 26/60 Superdex

2.2 The Myc/Max network at the base of the metazoan tree of life

200 prepgrade (GE, Healthcare, Freiburg) column equilibrated in storage buffer (50 mM TrisHCl pH 7.4, 500 mM NaCl, 2 mM EDTA, 1 mM DTT, 3 mM benzamidine and 3 % Sucrose). Fractions were checked on a SDS gel, purified taMyc/taMax was concentrated with Vivaspin 20 centrifugal concentrators with a polyethersulfone membrane (Sartorius Stedim Biotech, Göttingen). The proteins were frozen in liquid nitrogen and stored at -80°C . After gel purification, proteins also were subjected on SDS-polyacrylamide gel and subsequently blotted to a nitrocellulose membrane (SuperSignal[®] West Dura Extended Duration Substrate, Thermo scientific) in a blotting machine (Trans-Blot Semi-Dry Electrophoretic Transfer cell, Biorad, Munich). The membrane then was blocked in 1xTBS-T Puffer (50 mM Tris HCl pH 7.5; 150 mM NaCl, 0,05 % Tween-20) containing 5 % milk powder for 30 min and incubated in $0.2\ \mu\text{g}/\mu\text{l}$ Penta-His antibody (Quiagen). A secondary anti-mouse (HRP, Thermo scientific) antibody was used to detect proteins of interest and coloration of membrane was performed with the SuperSignal[®] West Dura Extended Duration Substrate kit (Thermo Scientific, Rockford, USA) and the blot was imaged with a digital imaging system (ImageQuant LAS 4000, GE Healthcare). Calculations on protein sizes were made with the "Protein Molecular Weight Calculator" (www.sciencegateway.org).

Sequence analyses

Sequences obtained from full-length gene amplification described before have been compared to predicted protein sequences in NCBI. Protein sequences then were aligned using the in Seaview version 4.12.12 with subsequent manual modifications in compliance to [8]. Besides *Trichoplax* proteins, sequences included in this analysis were taken from human (huMyc/huMax, GenBank accession no NP_002458 / NP_002373), chicken (ckMyc/ckMax, GenBank accession no NP_001026123 / P52162) and *Hydra vulgaris* (hyMyc/hyMax, GenBank accession no GQ856264 / GQ856264).

Probe synthesis for RNA in situ hybridization

Gene fragments for RNA *in situ* probe synthesis were amplified from the full length- cDNA using the primer pairs 5'-GCGGAAGCCTTTTCAAATAA-3'/5'-GGTTAACACGAACGTTA-3' (*tamyc*) and 5'-AGTACTTGGACGTCGATATTGAC-3'/5'-CAATCGGACGGTAA CGTGAAC-3' (*tamax*). PCR conditions were: initial denaturation for 5 min at 95°C , 35 cycles of 30 sec - 95°C , 30 sec - 60°C , 1 min - 72°C , and a final elongation step for 4 min at 72°C . Fragments had a size of 449 base pairs (bp) (*tamax*) and 348 bp (*tamyc*). After purification, the fragments have been ligated into the pGemT vector system and subsequent cloning and plasmid isolation were done as described before. After sequencing of the fragments (ABI Prism 310 Genetic Analyzer) the plasmids were diluted 1:100 and used as DNA template for a total volume of $25\ \mu\text{l}$ per PCR-reaction utilizing the SP6/T7 primer sites of the pGemT vector for amplification of fragments. PCR conditions were: 5

2.2 The Myc/Max network at the base of the metazoan tree of life

min - 95 °C, 35 cycles of (30 sec - 95 °C, 30 sec - 52 °C, 1 min - 72 °C) and a final elongation step for 4 min at 72 °C. *Tamyc*- and *tamax*- fragments were subsequently precipitated and RNA probes were transcribed using digoxigenin- (Dig) or fluorescein-labeled dUTPs (Roche) and SP6/T7 Polymerase (Roche) following the manufacturers protocol. Probes were purified by lithium chloride precipitation and solved in DEPC-treated water (Roth, Germany). Sense probes of respective fragments were used as negative controls.

Whole mount RNA in situ hybridization

Animals were fixed in Lavdowsky fixative (44 % EtOH, 44 % TBS, 8 % formaldehyde, 4 % acetic acid) and permeabilized in Tris buffered saline (TBS, 150 mM NaCl, 0.1 M Tris HCl pH 7.5) containing 0.5 % Tween-20 (Carl Roth, Germany) and 0.5 % TritonX (Carl Roth, Germany) hereafter termed TBSTT. *In situ* hybridization was subsequently performed using a protocol modified after Jakob et al. 2004 [13]. Hybridization of probes was done at 60 °C for at least 12 h in hybridization buffer containing 50 % formamide, 5x saline-sodium citrate (SSC), 0.1 % Tween, 500 µg/ml tRNA (Sigma) and 0,092 M citric acid. After hybridization, samples were washed with SSC (containing 1 % SDS) in declining concentrations (2x SSC, 1x SSC, 0.2x SSC, 0.1x SSC) each step for 15 min at 60 °C. Samples stained with fluorescein were then terminally washed with TBSTT at RT. After rinsing in TBS samples were mounted with Vectashield (Vector Labs) for microscopy. Dig-labeled samples were incubated in blocking solution (TBSTT with 0.1 % BSA, Sigma) for 30 min after the last wash with SSC buffer. The anti-Dig antibody (Roche) was diluted 1:1000 in the blocking buffer and samples were incubated for one h at RT. After several washing steps with TBSTT and terminally with *ddH₂O*, the antibody was detected by application of BM Purple (Roche). After coloration of tissue (after approximately 30 min at RT) the solution was removed by several washes in *ddH₂O* and samples were mounted for microscopy as described above.

Gene "Knockdown" via morpholino oligonucleotides (MO)

Sequences for MO design have been taken from the 5'ends of *tamyc/tamax* amplified and sequenced as described above. MO's for *tamyc* and *tamax* were obtained from Gene Tools, LLC and delivered into cells following the "Special Delivery" protocol provided by the manufacturer. For this, Special Delivery MO's were prepared by hybridization of oligonucleotides (26mer: 16 bases complementary to the 3' End of the MO and a 10 bases adenine overhang; MO: DNA equals 1.4 : 1) for 10 min at RT. The Special Delivery MO/DNA stock solution had a final concentration of 0.5 mM. The transfection solution then was prepared by mixing 5.6 µl of the 0.5 mM Special Delivery MO/DNA stock solution with 188.8 µl *ddH₂O* and a subsequent addition of 5.6 µl of the 200 µM ethoxylated polyethylenimine (EPEI, Gene Tools, LLC) Special Delivery solution. After

2.2 The Myc/Max network at the base of the metazoan tree of life

vortexing, the mixture was incubated 20 min at RT and then was applied to the animals in 2 ml ASW (final concentration of MO in ASW: 1.4 μM). After 18 h, several washing steps with ASW served to remove the chemical and success of transfection was subsequently monitored via fluorescence microscopy. Fresh MOs were then added at a concentration of 1.25 μM to maintain gene KD. Control experiments were performed by omission of oligonucleotides (ASW control) and the application of a MO, specific for the Cnidarian Hox gene *Cnox-2* (*Cnox-2* control, [19]) which is not present in the *Trichoplax* genome. Long-term experiments were conducted in glass chamber slides (one well cell culture chamber, Sarstedt) to enable daily observations of the animal's condition via bright field microscopy. Individuals were cultured under standard laboratory conditions (light/dark 12 h/12 h and 24 °C) and were fed ad libitum. To avoid osmotic stress due to higher salt concentrations caused by evaporation of liquid, the ASW/MO mixture was changed every 48 h. Physiological changes were monitored every 24 h via bright field microscopy and population size was gathered by counting of animals. To monitor a possible influence on cell proliferation and cell death, animals were also used for BrdU (24 h and 72 h) and TUNEL (24 h) -staining after initial gene KD.

Inhibition of Myc/Max dimerization through application of the 10058-F4 inhibitor.

To further validate the gene KD approach, the inhibitor 10058-F4 (Sigma) was applied to the animals. The small molecule inhibitor was diluted in ASW up to indicated concentrations. Control animals were kept in ASW only and in ASW containing 0.1 % DMSO. Animals were fed *ad libitum* and cultured in glass chamber slides under culturing conditions described above. The ASW/inhibitor mixture was changed every second day, as described above for KD analyses. Samples were observed daily via bright field microscopy and animals were counted to estimate population sizes. For the observation of proliferation and apoptosis of cells during treatment animals were also used for BrdU- and TUNEL-staining 24 h and 72 h after initial application of inhibitor.

Detection of Bromodeoxyuridine (BrdU) incorporation by means of Tyramide Signal Amplification (TSA)

Detection of cell proliferation after blocking taMyc and taMax expression (via KD) or inhibition of Myc/Max interaction (10058-F4 inhibitor) was performed by means of the Bromodeoxyuridine (BrdU) staining method. Before fixation of *Trichoplax* individuals in Lavdowsky fixative as described before, BrdU (Sigma) was diluted to a concentration of 50 ng/ml in culture medium and fed to the previously treated (KD /inhibitor) animals for 6 h. The samples were then fixed in Lavdowsky fixative as described before and permeabilized by washing four times 15 min in TBS (pH 7.5) containing 0.5 % Tween-20 (TBST). The tissue was further permeabilized with 4 ng/ml ProteinaseK for 10 min at RT. The reaction

2.2 The Myc/Max network at the base of the metazoan tree of life

was stopped with 1 mg/ml glycine in several washing steps. Samples were then rinsed in TBST two times for five min. Afterwards, animals were incubated in 2 N HCL (in TBST) for 30min and after three further washing steps in TBST, the tissue then was quenched with 3 % H_2O_2 (in TBST) to ensure specificity of the afterwards applied thymidine signal amplification (TSA) staining method. Samples were subsequently rinsed in TBST two more times and blocked in 0.1 % bovine serum albumin (BSA, Sigma) in TBST for 30 min. For detection of incorporated BrdU a horseradish peroxidase labeled polyclonal sheep BrdU antibody (Abcam) was diluted 1:100 in blocking solution and Samples were incubated two h at RT. Detection of the antibody was performed using the TSA Kit #23 (Invitrogen) following the manufacturers protocol. Nuclei were subsequently counterstained with 4',6-diamidino-2-phenylindole (DAPI, 1x in TBS) for 10 min. After two terminal washing steps in TSB samples were mounted with Vectashield (Vector Labs) for microscopy.

Terminal deoxynucleotidyl transferase-mediated deoxyuridine triphosphate nick end labeling (TUNEL) staining

After the initial steps of fixation and permeabilization as described before, apoptotic cells were detected via the TUNEL staining method using the ApopTag® Red *In Situ* Apoptosis Kit (Chemicon International) following manufacturers protocol. After DAPI staining as described above, samples were terminally washed in TBS and mounted for microscopy with Vectashield (Vector Labs).

Microscopy and statistical analyses

Animal fitness, signal of BrdU and TUNEL assay, success of transfection with MO's and results of RNA *in situ* hybridization were examined via fluorescence microscopy and light microscopy respectively (Zeiss, Axiovert 200M using the filter sets 09 for fluorescein, 02 for DAPI and 25 for TSA) pictures were taken with a digital camera (Zeiss, Axio Cam MRn and ICc3). Images were subsequently edited by usage of Adobe Photoshop Elements 8.0 to improve contrast only. Animal sizes for KD analyses and inhibitor treatment as well as the amount of proliferating and apoptotic cells were estimated by usage of ImageJ version 1.44. Cell numbers were estimated by counting nuclear DAPI signals and values were put into relation to counted TUNEL/BrdU signals. For statistical analyses, a student's t-test has been performed in Excel® (Microsoft Office® 2007). Control experiments were summed up and were compared with the experiments.

Results

1. Sequence analyses

Sequencing of the 5' RACE PCR product exhibited a 135 bp (*tamyc*) and a 150 bp (*tamax*) fragment. Both 5' untranslated regions (UTRs) do contain an intron with a size of 4125 bp (*tamyc*) and 437 bp (*tamax*). The *tamyc* 5' end further includes an alternative start methionine 33 bp prior to the predicted start. Analyses of the full-length coding sequence showed that predictions [20] are in accordance to the *tamyc/tamax* fragments sequenced in this study. Three variable nucleic acids have been found: in *tamyc* (position 285: C/T and 289: T/C) and one in *tamax* (position 132: T/C) whereas the detected substitutions however do not result in changes of protein sequence (cf. table A.2.1). Analyses of the *Trichoplax* protein sequence did show an overall sequence similarity of 24.8 % to the human Myc protein, 27.88 % to chicken and 21.02 % to *Hydra vulgaris* (fig. 2.2.1). The highest sequence similarities were found in the C-terminal Myc-boxes (MB I-IV and in the N-terminal bHLHL-Zip region (MB I: 59 %, MB II: 47 %, MB IIIa 75 %, MB IIIb 54 %, MB IV 27 % and the bHLHL-Zip 56.5 % similarity *Trichoplax* to human c-Myc respectively). The intron-exon sites of the Myc protein are conserved whereas the *Trichoplax* protein has an additional intron also found in the *Hydra vulgaris* sequence. In contrast to the human, chicken or the *Hydra* Myc protein, one of the octameric leucines is missing in the bHLHL-Zip region and is replaced by a glutamic acid. The *Trichoplax* Max protein is even more conserved than taMyc with an overall similarity of 44 % to human 42.05 % to *Hydra* and 46.58 % to chicken. The highest degree of homology was found in the bHLHL-Zip (46 % identical to human Max).

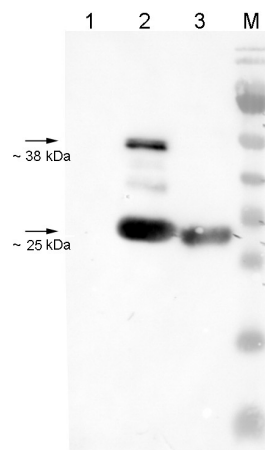


Figure 2.2.2: Western blot analysis of expressed proteins.

Shown is: before induction (1), concentrated protein (2), ÄKTA taMax fraction (3) and the marker (M) Two protein products (Myc and Max) are visible at ~ 38 kilo Dalton (kDa) and ~ 22 kDa. The ÄKTA fraction of the taMax protein (3) was used for further gel filtration purification.

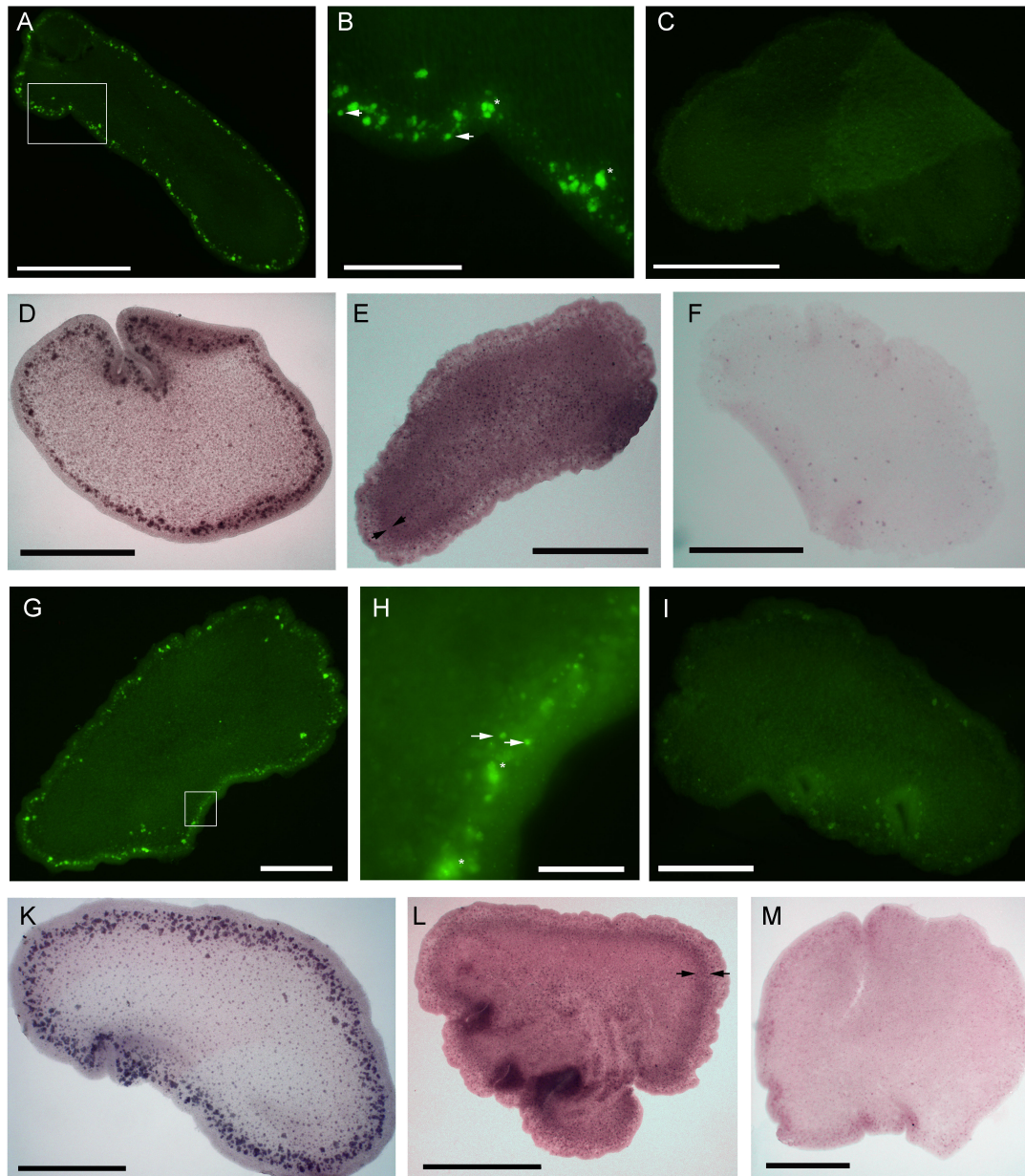


Figure 2.2.3: Whole mount *in situ* hybridization of *tamyc* and *tamax*.

RNA *in situ* hybridization of the *tamyc* (A-F) and *tamax* (G-M) genes. Fluorescein signal (A) and the higher magnification of the inlet (B) shows strong *tamyc* gene expression in small cells (arrowheads in B) and cell clusters (asterisks in B) of the animals' marginal region. The same pattern can be observed in (D). The staining in (E) shows a different pattern and the signal is distributed evenly over the whole animal. *Tamax* gene expression shows a similar pattern as *tamyc*: signal can be found in small cells (arrowheads in H, higher magnification of the inlet in G) and big cells or clusters (asterisks in H), in the marginal region of *Trichoplax adhaerens* (G and K) or distributed ubiquitous with higher signal density in the region close to the margin (L). Sense probe negative controls (C, F, I and M) show no distinct but low background signal, which however differs from real signal. The size bar marks 100 μm (A, C-G, I-M), 50 μm (B) and 20 μm (H).

2.2 The Myc/Max network at the base of the metazoan tree of life

2. Recombinant protein expression of *taMyc* and *taMax*

Previously calculated protein sizes of the constructs are 37.36 kDa for *taMyc* and 19.97 kDa for *taMax*. Expression of *taMyc* and *taMax* proteins was successful (fig. 2.2.2). The *Max* protein turned out to be stable and well solvable. Fractions can be used for binding studies and antibody production. But even after further purification via gel filtration, the *taMax* protein contains certain contaminations (fig. A.2.1). Most of the *taMyc* protein remains in the bacterial pellet what drastically reduce protein yield (data not shown).

3. Whole mount *in situ* hybridization

In situ hybridization of both, *tamyc* and *tamax*, did reveal strong similarities whereas expression pattern of both genes is found in two distinct manifestations: Signal either (i) is found in the outer margin of the animal in small cells as well as cell clusters (fig. 2.2.3 A, D, G and K, small cells indicated by arrows and clusters by asterisks in fig. 3 B and H), or it is (ii) distributed evenly over the whole animal with a ring of slightly stronger expression near to the margin (fig. 2.2.3 E and L, area of higher expression is implied by arrows) whereas expression is restricted to smaller cells. Sense controls did not give specific but weak background signal (fig. 2.2.3 C, F, I and M).

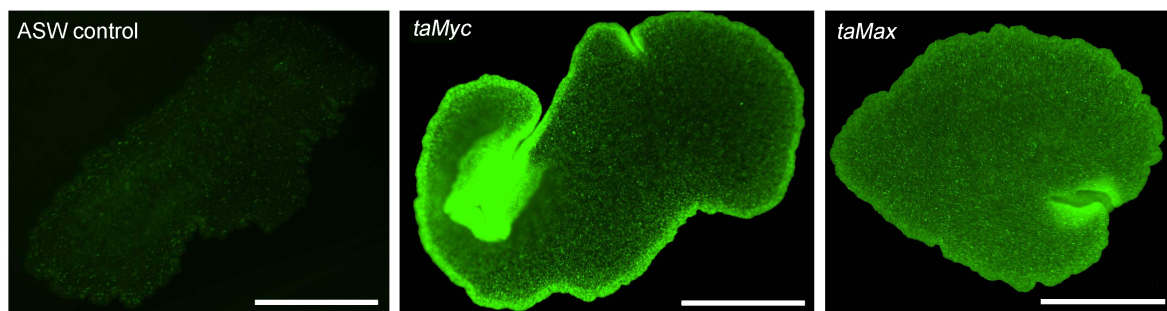


Figure 2.2.4: Live imaging of transfected animals.

18 h after transfection with fluorescent MOs of *tamyc* and *tamax*, signal can be detected equally distributed in the animals. The area of supposedly higher signal intensity in the *tamyc*-transfected animal is due to folding of the animal and apparently higher signal intensity at the animals' margin can be explained with higher cell density in this area. The ASW control does not show any signal, but a low amount of autofluorescence. The bar marks 100 μm .

4. Gene "Knockdown" via morpholino oligonucleotides (MO)

Fluorescence microscopy of living transfected animals does show a uniformly distribution of signal given by the fluorescein-labeled MO's in contrast to control animals (fig. 2.2.4). Folding of the animal while movement and higher cell densities in the marginal region (both visible in fig. 2.2.4 B) give the impression of higher signal strength in this area, which however is not the case.

2.2 The Myc/Max network at the base of the metazoan tree of life

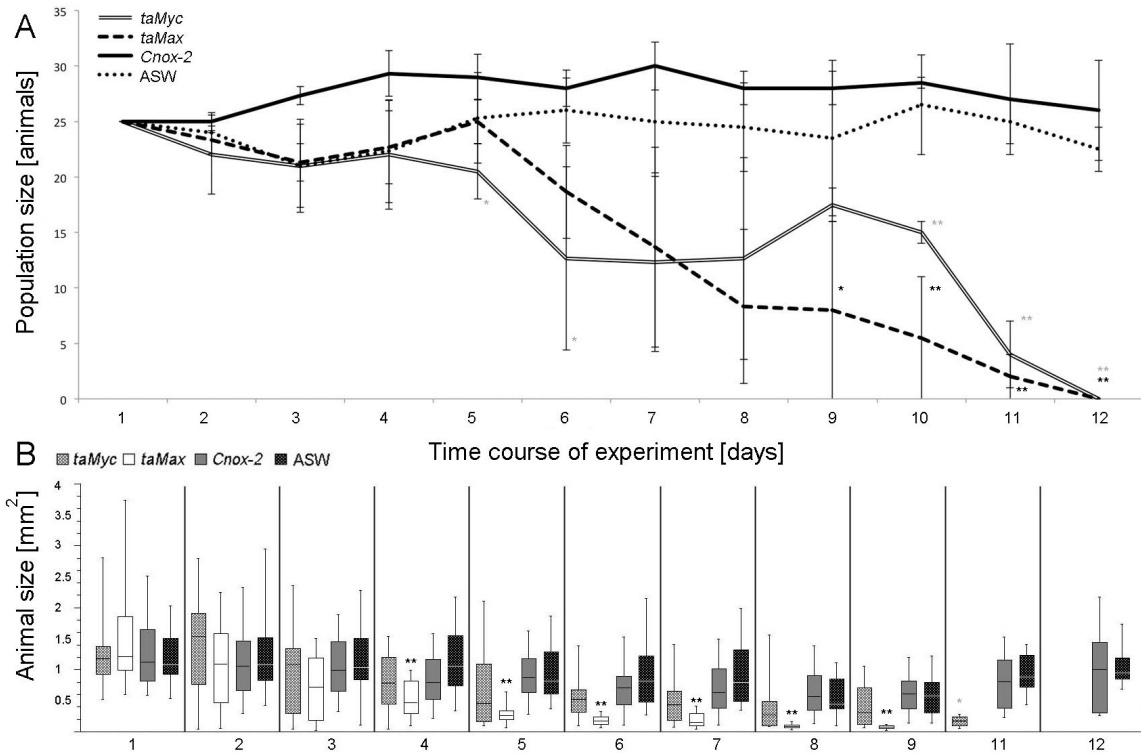


Figure 2.2.5: Time course of population and animal size during *tamyc* and *tamax* "knockdown".

Upper graph: Population sizes of *tamyc* and *tamax* KD animals decrease in course of experiment. The amount of *tamyc* KD animals significantly differs from the controls at day four of experiment whereas the amount of *tamax* KD individuals significantly deviate from controls at day five. Bars indicate the standard deviation, for raw data see table A.2.2 A.

Lower graph: Animal sizes of treated individuals are reduced during treatment. Sizes of animals transfected with *tamax* MO is significantly reduced after three days and transfection with *tamyc* MO results in smaller animal size significant after five days. Boxplot shows whiskers (minimum and maximum values), upper and lower quartile of values (box) and the median (dash in box). For raw data on boxplot analyses see table A.2.3 A.

Significances in A and B are denoted by asterisks (grey for *tamyc* and black for *tamax*, $p < 0.05$ *, $p < 0.01$ **, $p < 0.001$ ***), for statistical calculations see table A.2.2 B and A.2.3 B.

4.1 Observations on animal fitness

In all experiments, KD of *tamyc* and *tamax* was lethal latest after 11 days (fig. 2.2.5A). Death of individuals was accompanied with a reduction in size (fig. 2.2.5B). Beside, shrinkage together with a globular form of treated animals, no phenotypic abnormalities could be observed during the experiments (fig. A.2.2). Control individuals were stable in population- and animal-size over the indicated experimental period.

2.2 The Myc/Max network at the base of the metazoan tree of life

4.2 BrdU and TUNEL assay

Cell proliferation monitored with the BrdU assay did result in a significant decrease of proliferation 24 h and an increase of cell division events 72 h after initial KD ($p < 0.05$). Overall proliferation monitored by BrdU was distributed evenly over the whole animal. Experimental time points generally exhibit an overall change in proliferation rate. (fig. 2.2.6).

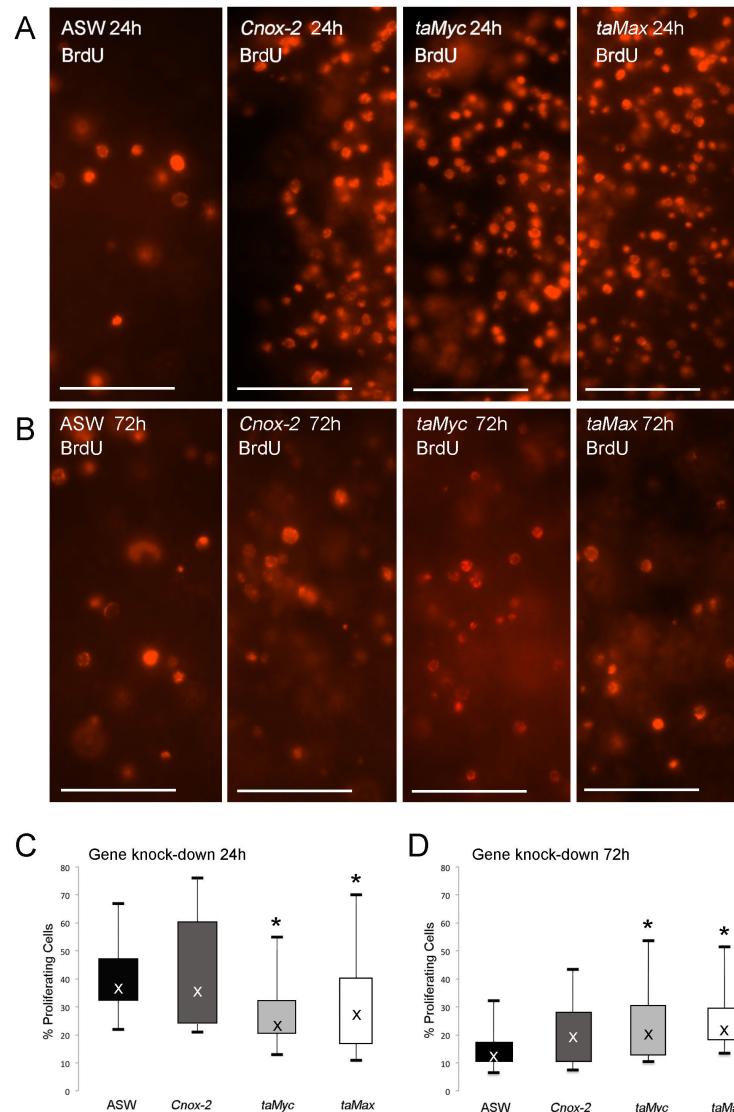


Figure 2.2.6: Amount of cell proliferation events after "knockdown" of *tamyc* and *tamax*.

The upper panels show cell proliferation by means of the BrdU assay 24 h after KD (A) and 72 h after KD (B). Boxplot depiction of data reveals that proliferation is affected by *tamyc/tamax* gene KD and firstly results in a significant decrease (after 24 h, C) and subsequently in a significant increase of cell proliferation 72 h (D) after initial transfection ($p < 0.05$). Signal of proliferating cells (red) is found ubiquitously in all cell types. The bars mark $20 \mu\text{m}$. Boxplots show whiskers (minimum and maximum values), upper and lower quartile of values (box) and the median (dash in box). For raw data, statistics and boxplot analyses see table A.2.4 and A.2.6.

2.2 The Myc/Max network at the base of the metazoan tree of life

The TUNEL assay revealed a significant increase of apoptotic cells 24 h after initial KD of both: *tamyc* and *tamax*. The occurrence of programmed cell death roughly was tripled (fig. 2.2.7). Cell death was augmented from an average of 0.57 % (ASW) and 0.66 % (*Cnox-2*) of apoptotic cells in control experiments to an average of 1.5 % in *tamyc* and 1.8 % of dying cells in *tamax* KD experiments.

5. Inhibition of Myc/Max dimerization through application of the 10058-F4 inhibitor

Different concentrations of the 10058-F4 inhibitor have been tested. Concentrations higher than 5 μM turned out to be lethal shortly after application and thus 5 μM turned out to be appropriate for treatment (cf. fig. A.2.3).

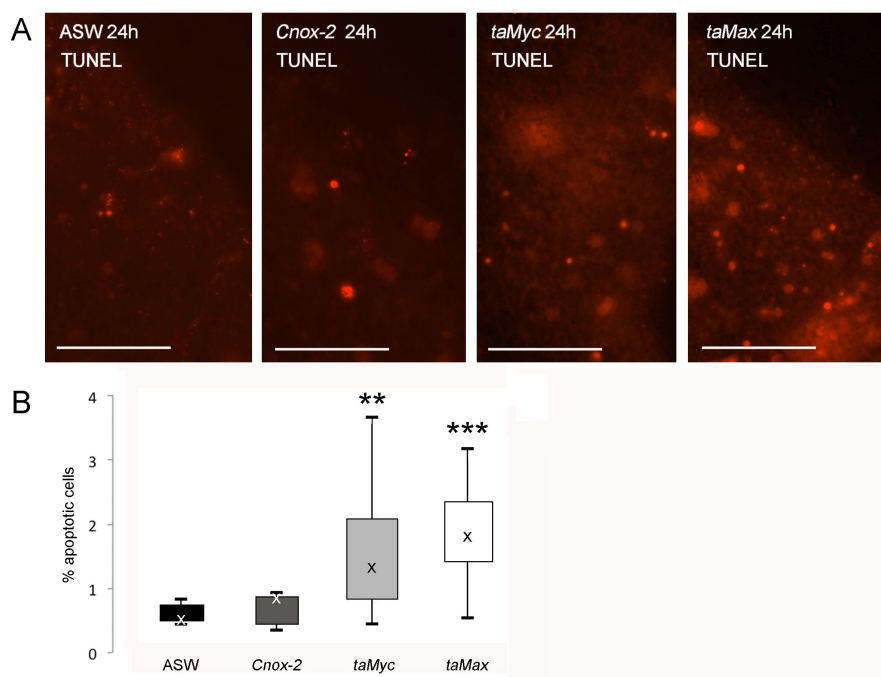


Figure 2.2.7: Increase of apoptosis after *tamyc/tamax* gene "knockdown".

The amount of cells undergoing apoptosis (arrowheads in A) is significantly increased 24 h after initial gene KD (B, $p < 0.01$ **, $p < 0.001$ ***). The bars mark 20 μm . Boxplot indicates whiskers (minimum and maximum values), upper and lower quartile of values (box) and the median (dash in box). For raw data, statistics and boxplot analyses see table A.2.5 and A.2.6.

5.1 Observations on animal fitness

As already observed in *tamyc/tamax* knockdown experiments, chemical interruption of Myc/Max interaction is also lethal for *Trichoplax* individuals. Animals died latest after 8 days of inhibitor treatment (5 μM , fig. 2.2.8, upper panel). As observed in KD experiments, the size of individuals significantly decreased before death (fig. 2.2.8, lower panel) and shrinkage comes along with a globular form of treated animals. Phenotypic abnormalities were not observed (fig. A.2.4).

2.2 The Myc/Max network at the base of the metazoan tree of life

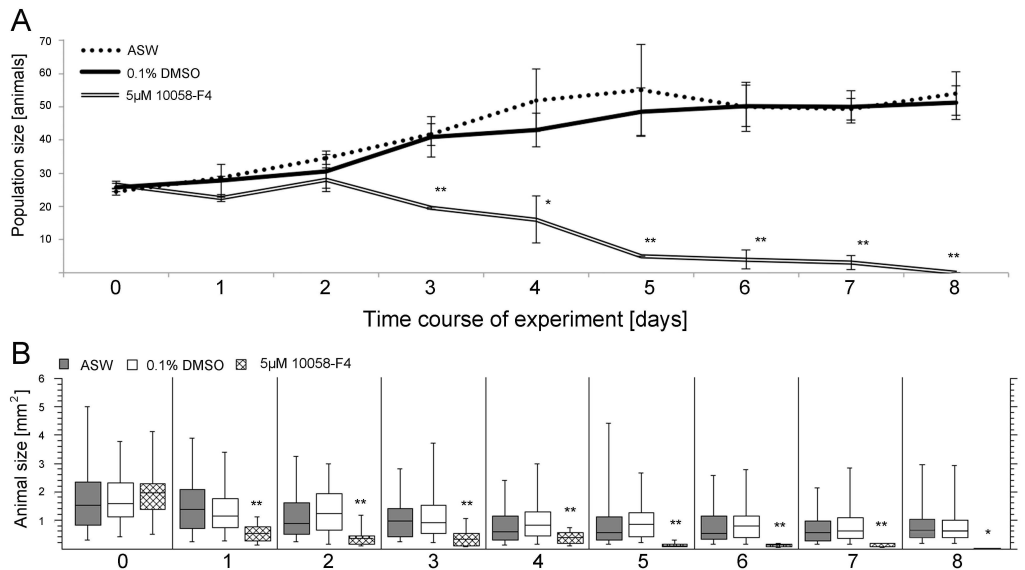


Figure 2.2.8: Time course of population and animal size after treatment with the 10058-F4 inhibitor.

Animal population size (A) and animal size (B) decreases after initial treatment with the 10058-F4 inhibitor (5 μ M). Significances are indicated by asterisks ($p < 0.05^*$, $p < 0.01^{**}$). Boxplot shows whiskers (minimum and maximum values), upper and lower quartile of values (box) and the median (dash in box). For raw data, boxplot data and statistics see table A.2.7 and A.2.8.

5.2 BrdU and TUNEL assay

Similar to KD results, inhibitor treatment did significantly increase the amount of apoptosis in *Trichoplax* compared to the DMSO controls whereas increase was even stronger after inhibitor treatment than after KD, 24 h (1.07 % in DMSO control and 3.89 % after inhibitor treatment) and 72 h (1.3 % in DMSO control and 2.9 % after inhibitor treatment). Cell proliferation however was not affected by inhibitor treatment (cf. fig. 2.2.9), which stays in contrast to the results of performed KD experiments.

Discussion

The Myc/Max proteins are conserved within the Metazoa

Conserved motifs are found within the *Trichoplax* Myc and Max proteins suggesting similarities in functions known from higher animals, namely dimerization and binding to E-box sequences (e.g. [21]). The substitution of one critical leucine by glutamic acid in the C-terminal bHLHL region may probably influence the dimerization capacity of the *Trichoplax* Myc protein and thus their function as transcription factor. However, one substitution merely, if at all, reduces and not prohibits binding capacity [22]. The role of amino acid composition of proteins will be further examined by protein binding essays.

Information on 5' UTR of *tamyc* and *tamax* gained in course of this study and 5' UTRs sequences from transcriptome analyses differ in length, which however does not change the respective open reading frames (unpublished data, for information on genomic scaffolds cf.

2.2 The Myc/Max network at the base of the metazoan tree of life

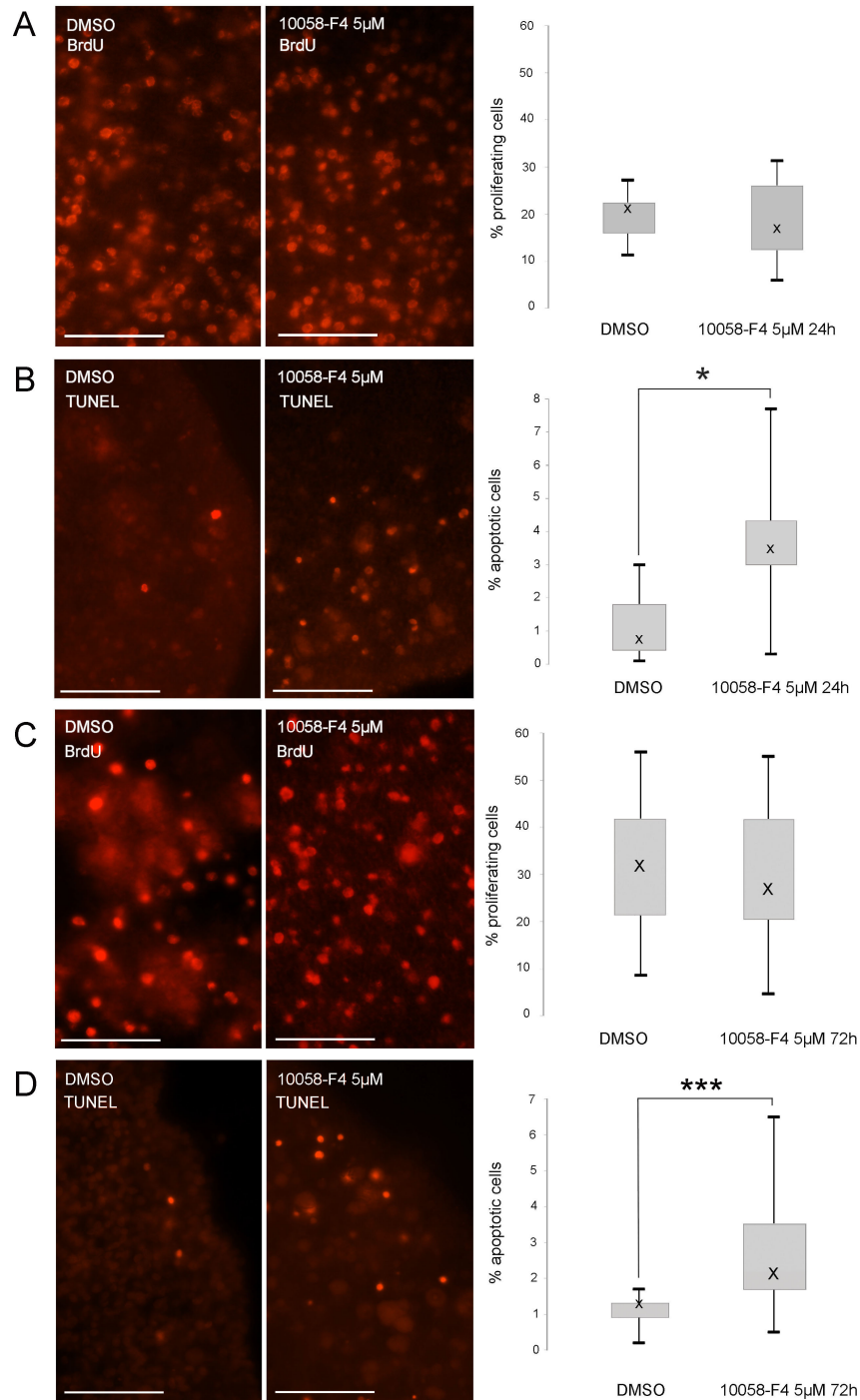


Figure 2.2.9: BrdU and TUNEL staining of inhibitor treated individuals after 24 h and 72 h.

Cell proliferation (A and C, monitored via BrdU) is not affected by treatment with the 10058-F4 inhibitor. In contrast, the amount of apoptosis (B and D, monitored by the TUNEL assay) is significantly increased after 24 h (B, $p < 0.05$, indicated by asterisks) and 72 h (D, $p < 0.001$). Boxplot indicates whiskers (minimum and maximum values), upper and lower quartile of values (box) and the median (dash in box). For raw data, statistics and boxplot analyses see table A.2.9, A.2.10 and A.2.11. The bars mark 20 μm .

2.2 The Myc/Max network at the base of the metazoan tree of life

A.2.1B). The large intron in the 5' UTR of *tamyc* and the additional start methionine prior to the predicted start of *tamyc* further plead for different protein isoforms and could be an incidence for different modes of gene expression control [23, 24]. Sequence information on the protein-coding region gained in course of this study nonetheless gives proper knowledge on protein structure, as conserved *myc/max* motifs indispensable for protein function are present.

Expression of taMyc/taMax proteins will enable additional approaches to further shed light on the myc/max network in Placozoa.

Experiments performed so far revealed that the expression of full-length *tamyc* is associated with poor solubility. Future experiments should include the expression of shorter Myc transcripts. Former studies on the protein demonstrated that expression of the C-terminal part of the protein only (containing the DNA binding domain and the motif indispensable for dimerization with taMax) will enable experimental binding approaches as well (as e.g. in [25]), and extraction of protein will likely be more frugal. Nevertheless, crystallization studies on the full-length taMyc protein provide innovative insights into the biochemistry of the transcription factor and thus further approaches should be conducted. The usage of different tags for immune precipitation of proteins to probably increase solubility and pureness [26].

The taMax protein was expressed successfully. However, even after gel-filtration of the protein contaminations still are visible on SDS page and western blot. Optical measurements of the protein further revealed a high amount of DNA and other background impurities (data not shown). For perspective approaches the usage of a FLAG-tag instead of the HIS-tag could solve this problem, as various *E. coli* proteins can bind to the nickel NTA used for HIS-tag purification [27]. The usage of other expression systems than *E. coli* could also help to increase purity and protein yields in future approaches [28, 29].

Recombinant expression of the taMyc and taMax protein will open new possibilities regarding experiments on the Myc/Max network in Placozoa. Protein binding studies will further broaden our knowledge on the function of these proteins at the base of the metazoan tree of life as e.g. target genes in *Trichoplax* can be identified by means of protein binding essays. Antibodies then can be synthesized to understand the role of protein interaction within the animal. Preliminary results of protein expression lay the foundation to successful unravel the biochemistry of the Myc/Max network in Placozoa.

Tamyc and tamax are highly expressed in the Placozoan multipotent stem cell area.

The expression pattern of *tamyc* and *tamax* apparently is very similar. Given that the proteins interact while transcriptional activation or repression of target genes [30], this is not surprising at first sight. However, a Myc independent role of Max is broadly known from other organisms and expression usually is ubiquitous even though at lower levels

(cf. [31]), which however cannot be discerned by our approach. Expression of *tamyc* and *tamax* thus likely differs at least temporally if not spatially what could not be shown in this study and has to be further validated by double *in situ* hybridization using both probes on one animal.

The pattern of *tamyc/tamax* expression clearly is dependent on the "growing-/ developmental stage" of the individual. As the placozoan life cycle still is unresolved, it is problematic to determine certain stages. Placozoan growth executes in an oscillating manner whereas proliferation mainly is restricted to the central or the marginal part of an individual respectively [32]. As a result the animal possesses excess, respectively too little central or marginal tissue at a certain time point of development. Former proliferation studies by means of BrdU incorporation confirmed this assumption (unpublished data). Individuals pictured in fig. 2.2.4 A and G (respectively D and K) do have a smooth margin and clearly pass through another growth stage than animals pictured in fig. 2.2.4 E and L which exhibit a wavy boundary. Both stages do show dissimilar patterns of Myc/Max expression in the marginal region (i) and throughout the whole animal (ii). Differences in *tamyc/tamax* expression associated to different morphological characteristics of the animal suggest the existence of different developmental stages that exhibit different levels and patterns of *tamyc/tamax* expression.

(i) Expression is strong in the stem cell region of individuals (fig. 2.2.4 A, D, G and K). Signal is found in small cells (arrows in fig. 3 B and H) as well as in large, bulky cells or rather cell clusters (asterisks in fig. 2.2.4 B and H). The outer margin of Placozoa is known to be the area of cell differentiation and the stem cells are located at the contact zone of upper and lower epithelia giving rise to different cell types [13]. Expression of *myc* often is associated with differentiation processes whereas the protein can either block or facilitate differentiation [33]. In *Hydra*, *myc* and *max* are both expressed in proliferating nematoblasts and *max* additionally throughout epithelial cells of the body column [8]. Signal of *tamyc* in the stem cell region of *Trichoplax adhaerens* likely is linked directly to differentiation events and the self-renewal of multipotent stem cells. Cell clusters then could be a result of the accumulation of proliferating stem cells that have not fully differentiated thus far. Signals in small cells then could be dedicated to stem cells that migrate towards their place of destination.

(ii) Signals found in fig. 2.2.4 E and L is restricted to small, interspersed cells evenly distributed over the whole individual with a ring of higher signal density close to the margin. This pattern likely is deducible to proliferation of epithelial cells as cell proliferation is under control of the Myc/Max network (for review see e.g. [3, 34]). The ring-shaped region of augmented signal strength (enclosed by arrowheads in fig. 2.2.4 E und L) then represents an area with higher proliferative activities. Co-staining of proliferating cells via BrdU and determination of protein abundance will help to further support the re-

sults of this study and will greatly extend knowledge on the Myc/Max network in Placozoa.

Gene knockdown and inhibition of taMyc/taMax interaction both lead to an increase of apoptosis and does affect cell proliferation.

The gene KD approach was performed with MO's that were designed to bind to the 5' end of the mRNA and thereby prevent translation of proteins (cf. [35]). Success of KD analyses thus merely can be verified by western blot analyses using a protein specific antibody, in our case anti *tamyc/tamax* or by quantitative analyses on expression levels of possible Myc/Max target genes [36]. As species-specific antibodies are not available to this point and target genes still remain to be identified, a second approach to simulate absence of *myc/max* expression was chosen to compare effects and thus assess specificity of MO approach. Myc/Max heterodimerization chemically was prevented by application of the inhibitor 10058-F4 [17]. Transfection of animals with MO's was successful, clearly visible in the fluorescence microscope (fig. 2.2.4). Inhibitor treatment furthermore gave results similar to the effects achieved by KD performance. The outcomes indicate that both approaches are affecting Myc and Max on the mRNA level (MO's) as well as on protein level (Inhibitor). However, results of the study have to be further validated by biochemical approaches.

Downregulation of the *myc* gene leads to defects that can have diverse manifestations in different model systems. In human cell lineages decrease of cMyc inhibits cell proliferation and can also induce apoptosis in certain cancer cells [37]. In the model system *D. melanogaster*, a downregulation of *myc* results in growth defects deducible to disorders in cellular growth, delay in development and female sterility [38]. The *Hydra myc* gene *hymyc1* has been shown to be important for maintenance of cellular homeostasis in the interstitial stem cell lineage [7]. Downregulation enhances proliferation of interstitial stem cells that lead to imbalances in cell differentiation. Myc's impact on the control of cell growth and -proliferation is expected being conserved throughout animal kingdom [3].

Gene KD analyses and inhibition of Myc/Max interaction in *Trichoplax adhaerens* both are lethal for the organism (fig. 2.2.5 and fig. 2.2.8, cf. also fig. A.2.2 and A.2.4). The amount of apoptotic cells furthermore was increased in both cases equally. Cell proliferation however was affected in both directions after MO treatment but not after inhibitor application. 24 h after initial gene KD the proliferation rate was decreased and 72 h of MO treatment resulted in an increase of cell division events. As the proliferation rate of both experimental KD approaches (after 24 h and 72 h) generally fluctuates, we cannot exclude external factors to be the explanation for this such as culturing conditions or seasonal variation in animal population and -size. Further experiments to increase sample size and to include additional time points for monitoring proliferation events will give us more information. Genetic and biochemical inhibition of taMax does have similar

2.2 The Myc/Max network at the base of the metazoan tree of life

effects as the inhibition of taMyc. It thus seems reasonable that the effects observed after inhibition of Max likely are assigned to the loss of Myc function. Max is required for all hitherto known Myc functions except for transcriptional activation by RNA polymerase III [39]. Discrete effects of *tamyc* or *tamax* downregulation could not be detected by experimental approaches and thus results of experiments are discussed mutually.

We assume that downregulation of *tamyc/tamax* does affect placozoan stem cell proliferation or rather differentiation processes, as *tamyc/ tamax* gene expression is prominent in the placozoan stem cell region and thus likely is involved in developmental processes. Additionally, a diminution of size and the reduction or rather loss of the ability to reproduce furthermore pleads for defects in developmental processes. Future experiments now have to focus on other methods to highlight developmental processes in Placozoa. The ParaHox gene of *Trichoplax*, *Trox-2* [13] can be used as a reference gene for double staining approaches and thereby possibly gives a more precise idea about the connection between the Myc/Max network in Placozoa and developmental processes.

Cell division is driven by Myc/Max target genes and thus, downregulation of Myc or Max likewise predominantly result in a reduction or rather complete inhibition of cell cycle events e.g. [37]. After genetic and chemical inhibition of Myc/Max function in Placozoa, BrdU signal as a result of cells entering the S-phase of the cell cycle is still strong. Apparent differences in nuclei sizes are deducible to different cell types on the one hand and distinct stages of the cell cycle that comes together with different levels of chromatin condensation. The BrdU staining is restricted to the chromatin and thus signal may appear brighter and nuclei bigger when chromatin is de-condensed. We assume that cell proliferation possibly is not under complete control of the *tamyc* gene. As placozoan reproduction principally consists of augmentation in size by massive proliferation and subsequent binary fission, it is conceivable that cell proliferation is not exclusively beyond the control of only one genetic network. Unknown feedback loops and rescue mechanism may play important roles in maintaining the proliferative activity of the individual, however this does not prevent defects in the long run as long-term inhibition of taMyc and taMax is lethal. The observed decrease of proliferation in dependence to chosen experimental time points has to be revised carefully and further experiments should be performed to validate present results. Myc is known to be involved into the control of apoptotic events, but the mechanism behind this control is not fully understood (cf. [40, 41]). In other organisms, *myc* downregulation is often associated with a reduction of apoptosis [42]. In our experiments we could however observe an increase in cell death due to Myc/Max inhibition and KD. Myc also was shown to prevent cells from undergoing apoptosis in certain cell lines [43] and thus downregulation of *myc* can also increase apoptosis under certain circumstances [44-46] Apoptosis generally is scarce in *Trichoplax adhaerens* (unpublished data) implying that the mechanism is tightly regulated in Placozoa. Placozoa mainly

2.2 The Myc/Max network at the base of the metazoan tree of life

reproduce by increasing size and subsequently divide, they do not possess organs and the organism has simple bauplan characteristics reducing the necessity of massive apoptosis due to developmental processes as known from other animals [47]. The increase of dying cells due to *tamyc/tamax* inhibition mainly is restricted to marginal regions of the animal and thus to the area, where the stem cell are presumed to lie. Assuming that *tamyc* plays a dominant role in placozan cell differentiation processes could explain both, the increase of apoptosis after *myc* downregulation and the unaffected high proliferation rate. Cells that fail to differentiate due to a lack of *tamyc* die via apoptosis and cell cycling is not exclusively under the control of the Myc/Max network.

Conclusion

The results of this study highlight the importance of basal animal model systems to address questions concerning highly complex mechanisms such as cell cycle control. With the evolution of multicellularity the requirement of molecular tools to control cellular homeostasis arose and thus investigations on these mechanisms in evolutionary older animals as e.g. Placozoa does give us information on primordial functions. The outcomes of performed experiments plead for a role of taMyc/taMax in animal development but do not clearly confirm its function in cell cycle control *per se*. Further studies on taMyc/taMax protein interaction and *whole mount* protein detection by means of specific antibodies will help to greatly enlarge our knowledge on the network at the base of the metazoan tree of life.

Acknowledgements

K. vdC. was funded by an Evangelische Studienwerk Villigst e.V. PhD fellowship, an "Otto Bütschli" scholarship from the Tierärztliche Hochschule Hannover and a travel grant from Boehringer Ingelheim Fonds.

References

1. Taub, R., Kirsch, I., Morton, C., Lenoir, G., Swan, D., Tronick, S., Aaronson, S., and Leder, P. (1982). *Translocation of the c-myc gene into the immunoglobulin heavy chain locus in human Burkitt lymphoma and murine plasmacytoma cells*. Proc Natl Acad Sci U S A 79, 7837-7841.
2. Meyer, N., and Penn, L.Z. (2008). *Reflecting on 25 years with MYC*. Nat Rev Cancer 8, 976-990.
3. Eilers, M., and Eisenman, R.N. (2008). *Myc's broad reach*. Genes Dev 22, 2755-2766.
4. Lüscher, B., and Vervoorts, J. (2012). *Regulation of gene transcription by the oncoprotein MYC*. Gene 494, 145-160.
5. Fernandez, P.C., Frank, S.R., Wang, L., Schroeder, M., Liu, S., Greene, J., Cocito, A., and Amati, B. (2003). *Genomic targets of the human c-Myc protein*. Genes Dev 17, 1115-1129.
6. Orian, A., van Steensel, B., Delrow, J., Bussemaker, H.J., Li, L., Sawado, T., Williams, E., Loo, L.W., Cowley, S.M., Yost, C., et al. (2003). *Genomic binding by the Drosophila Myc, Max, Mad/Mnt transcription factor network*. Genes Dev 17, 1101-1114.
7. Ambrosone, A., Marchesano, V., Tino, A., Hobmayer, B., and Tortiglione, C. (2012). *Hymyc1 downregulation promotes stem cell proliferation in Hydra vulgaris*. PLoS One 7, e30660.
8. Hartl, M., Mitterstiller, A.M., Valovka, T., Breuker, K., Hobmayer, B., and Bister, K. (2010). *Stem cell-specific activation of an ancestral myc protooncogene with conserved basic functions in the early metazoan Hydra*. Proc Natl Acad Sci U S A 107, 4051-4056.
9. Young, S.L., Diolaiti, D., Conacci-Sorrell, M., Ruiz-Trillo, I., Eisenman, R.N., and King, N. (2011). *Premetazoan ancestry of the Myc-Max network*. Mol Biol Evol 28, 2961-2971.
10. Schierwater, B. (2005). *My favorite animal, Trichoplax adhaerens*. Bioessays 27, 1294-1302.
11. Eitel, M., and Schierwater, B. (2010). *The phylogeography of the Placozoa suggests a taxon-rich phylum in tropical and subtropical waters*. Mol Ecol 19, 2315-2327.

2.2 The Myc/Max network at the base of the metazoan tree of life

12. Guidi, L., Eitel, M., Cesarini, E., Schierwater, B., and Balsamo, M. (2011). *Ultrastructural analyses support different morphological lineages in the phylum Placozoa*. Grell, 1971. J Morphol 272, 371-378.
13. Jakob, W., Sagasser, S., Dellaporta, S., Holland, P., Kuhn, K., and Schierwater, B. (2004). *The Trox-2 Hox/ParaHox gene of Trichoplax (Placozoa) marks an epithelial boundary*. Dev Genes Evol 214, 170-175.
14. Schierwater, B., de Jong, D., and Desalle, R. (2009). *Placozoa and the evolution of Metazoa and intrasomatic cell differentiation*. Int J Biochem Cell Biol 41, 370-379.
15. Schierwater, B., Eitel, M., Jakob, W., Osigus, H.J., Hadryś, H., Dellaporta, S.L., Kolokotronis, S.O., and DeSalle, R. (2009). *Concatenated Analysis Sheds Light on Early Metazoan Evolution and Fuels a Modern "Urmetazoon" Hypothesis*. Plos Biology 7, 36-44.
16. Ringrose, J.H., van den Toorn, H.W., Eitel, M., Post, H., Neerincx, P., Schierwater, B., Maarten Altelaar, A.F., and Heck, A.J. (2013). *Deep proteome profiling of Trichoplax adhaerens reveals remarkable features at the origin of metazoan multicellularity*. Nat Commun 4, 1408.
17. Huang, M.J., Cheng, Y.C., Liu, C.R., Lin, S., and Liu, H.E. (2006). *A small-molecule c-Myc inhibitor, 10058-F4, induces cell-cycle arrest, apoptosis, and myeloid differentiation of human acute myeloid leukemia*. Exp Hematol 34, 1480-1489.
18. Grell, K.G., and Benwitz, G. (1971). *Die Ultrastruktur von Trichoplax adhaerens F.E. Schulze*. Cytobiologie 4, 216-240.
19. Jakob, W., and Schierwater, B. (2007). *Changing hydrozoan bauplans by silencing Hox-like genes*. PLoS One 2, e694.
20. Srivastava, M., Begovic, E., Chapman, J., Putnam, N.H., Hellsten, U., Kawashima, T., Kuo, A., Mitros, T., Salamov, A., Carpenter, M.L., et al. (2008). *The Trichoplax genome and the nature of placozoans*. Nature 454, 955-960.
21. Blackwell, T.K., Kretzner, L., Blackwood, E.M., Eisenman, R.N., and Weintraub, H. (1990). *Sequence-specific DNA binding by the c-Myc protein*. Science 250, 1149-1151.
22. Ellenberger, T. (1994). *Getting a grip on DNA recognition: structures of the basic region leucine zipper, and the basic region helix-loop-helix DNA binding domains*. Current Opinion in Structural Biology 4, 12-21.
23. Cenik, C., Derti, A., Mellor, J.C., Berriz, G.F., and Roth, F.P. (2010). *Genome-wide functional analysis of human 5' untranslated region introns*. Genome Biol 11, R29.

2.2 The Myc/Max network at the base of the metazoan tree of life

24. Le Hir, H., Nott, A., and Moore, M.J. (2003). *How introns influence and enhance eukaryotic gene expression*. Trends Biochem Sci 28, 215-220.
25. Fieber, W., Schneider, M.L., Matt, T., Krautler, B., Konrat, R., and Bister, K. (2001). *Structure, function, and dynamics of the dimerization and DNA-binding domain of oncogenic transcription factor v-Myc*. J Mol Biol 307, 1395-1410.
26. Terpe, K. (2003). *Overview of tag protein fusions: from molecular and biochemical fundamentals to commercial systems*. Appl Microbiol Biotechnol 60, 523-533.
27. Hengen, P. (1995). *Purification of His-Tag fusion proteins from Escherichia coli*. Trends Biochem Sci 20, 285-286.
28. Terpe, K. (2006). *Overview of bacterial expression systems for heterologous protein production: from molecular and biochemical fundamentals to commercial systems*. Appl Microbiol Biotechnol 72, 211-222.
29. Geisse, S., Gram, H., Kleuser, B., and Kocher, H.P. (1996). *Eukaryotic expression systems: a comparison*. Protein Expr Purif 8, 271-282.
30. Blackwood, E.M., and Eisenman, R.N. (1991). *Max: a helix-loop-helix zipper protein that forms a sequence-specific DNA-binding complex with Myc*. Science 251, 1211-1217.
31. Hurlin, P.J., and Huang, J. (2006). *The MAX-interacting transcription factor network*. Semin Cancer Biol 16, 265-274.
32. Schwartz, V. (1984). *The radial polar pattern of differentiation in Trichoplax adhaerens F.E. Schulze (Placozoa)*. Z. Naturforsch. 39c, 818-832.
33. Conacci-Sorrell, M., and Eisenman, R.N. (2011). *Post-translational control of Myc function during differentiation*. Cell Cycle 10, 604-610.
34. Dang, C.V., O'Donnell, K.A., Zeller, K.I., Nguyen, T., Osthus, R.C., and Li, F. (2006). *The c-Myc target gene network*. Semin Cancer Biol 16, 253-264.
35. Bennett, C.F., and Swayze, E.E. (2010). *RNA targeting therapeutics: molecular mechanisms of antisense oligonucleotides as a therapeutic platform*. Annu Rev Pharmacol Toxicol 50, 259-293.
36. Grandori, C., and Eisenman, R.N. (1997). *Myc target genes*. Trends Biochem Sci 22, 177-181.
37. Vita, M., and Henriksson, M. (2006). *The Myc oncoprotein as a therapeutic target for human cancer*. Semin Cancer Biol 16, 318-330.

2.2 The Myc/Max network at the base of the metazoan tree of life

38. de la Cova, C., and Johnston, L.A. (2006). *Myc in model organisms: a view from the flyroom*. *Semin Cancer Biol* 16, 303-312.
39. Gallant, P., and Steiger, D. (2009). *Myc's secret life without Max*. *Cell Cycle* 8, 3848-3853.
40. Nesbit, C.E., Tersak, J.M., Grove, L.E., Drzal, A., Choi, H., and Prochownik, E.V. (2000). *Genetic dissection of c-myc apoptotic pathways*. *Oncogene* 19, 3200-3212.
41. Pelengaris, S., Khan, M., and Evan, G. (2002). *c-MYC: more than just a matter of life and death*. *Nat Rev Cancer* 2, 764-776.
42. Prendergast, G.C. (1999). *Mechanisms of apoptosis by c-Myc*. *Oncogene* 18, 2967-2987.
43. Gatti, G., Maresca, G., Natoli, M., Florenzano, F., Nicolini, A., Felsani, A., and D'Agnano, I. (2009). *MYC prevents apoptosis and enhances endoreduplication induced by paclitaxel*. *PLoS One* 4, e5442.
44. Adhikary, S., and Eilers, M. (2005). *Transcriptional regulation and transformation by Myc proteins*. *Nat Rev Mol Cell Biol* 6, 635-645.
45. D'Agnano, I., Valentini, A., Fornari, C., Bucci, B., Starace, G., Felsani, A., and Citro, G. (2001). *Myc down-regulation induces apoptosis in M14 melanoma cells by increasing p27(kip1) levels*. *Oncogene* 20, 2814-2825.
46. Zhang, P., Li, H., Wu, M.L., Chen, X.Y., Kong, Q.Y., Wang, X.W., Sun, Y., Wen, S., and Liu, J. (2006). *c-Myc downregulation: a critical molecular event in resveratrol-induced cell cycle arrest and apoptosis of human medulloblastoma cells*. *J Neurooncol* 80, 123-131.
47. Twomey, C., and McCarthy, J.V. (2005). *Pathways of apoptosis and importance in development*. *J Cell Mol Med* 9, 345-359.

2.3 Regeneration and self/non-self recognition in the phylum Placozoa

von der Chevallerie, K.¹

Kosubek, J.¹

Schleicherova, D.¹

Eitel, M.^{1,2}

Schierwater, B.^{1,3}

¹ Division of Ecology and Evolution, Stiftung Tierärztliche Hochschule Hannover, Hannover, Germany

² The Swire Institute of Marine Science, Faculty of Science, School of Biological Sciences, The University of Hong Kong, Hong Kong

³ Department of Molecular, Cellular and Developmental Biology, Yale University, New Haven, Connecticut, United States of America

Abstract

The ability to discriminate ‘self’ from ‘non-self’ tissue was one of the key inventions during metazoan evolution. Allorecognition is well studied in colonial marine invertebrates such as Sponges, Cnidaria and Tunicates where it is known to be responsible to maintain genetic integrity. We here describe evidence for tissue recognition mechanisms in the basal metazoan phylum Placozoa. By means of grafting experiments we observed chimeric fusion, rejection and transitory fusion of genetically distinct placozoan lineages. The results of our study suggest the existence of a primitive allorecognition machinery already within the Placozoa. The method could furthermore become a helpful tool to determine additional criteria for placozoan taxonomic classification and could highlight this animal group as a model system also for human transplantation research.

Keywords: Placozoan phylogeny, regeneration, allorecognition, *Trichoplax adhaerens*

Introduction

The exceptionally eclectic marine invertebrate *Trichoplax adhaerens* is the so far only described species in the phylum Placozoa (for review see e.g. [1,2]). Extensive sampling and phylogenetic analysis with different molecular markers revealed that the phylum Placozoa consists of at least 19 distinct genetic lineages (haplotypes H1-19) distributed worldwide [3]. Placozoan lineages cluster in different clades (I-VII) forming two main groups (A and B) with the subgroups A1 and A2 (c.f. [4]). The genetic diversity found thus far suggests the presence of different species, genera and families within the phylum [4,5]. However, description of new species is not trivial. Even though former studies revealed morphological differences [6], such characters are hard to assign to haplotypes because of ontogenetic plasticity and micro-environmental culture differences. The lack of the complete life cycle under laboratory conditions [7,8] is furthermore limiting experiments on taxonomic classification as no interbreeding experiments can be performed. Besides genetic and morphological analyses, observations on the ecology of different placozoan species do further confirm a high taxonomic diversity (unpublished data). The demands of haplotypes regarding their habitats are diverse and hard to simulate in the laboratory. That is why only a fraction of the known genetic lineages were successfully cultivated thus far (cf. [3-5,9,10]).

With the simplest known animal bauplan (e.g. [1]) and a basal position within the metazoan tree of life [11,12], Placozoa have drawn keen interest within the past years. Genome sequencing efforts revealed the existence of surprisingly complex genomic equip-

2.3 Regeneration and self/non-self recognition in Placozoa

ment [13,14]. As the organism is the best living surrogate for the “Urmetazoon” it is eligible to become a promising model system not only for evolutionary biology [12,15]. Placozoa possess a remarkable effective ability to regenerate - they are able to close wounds within minutes and to regenerate a whole individual out of a small proportion of tissue [16,17]. Regeneration is quite common in invertebrates [18-20] but the velocity and efficiency of regeneration in Placozoa is outstanding within animal kingdom.

In course of evolution, the capacity of distinguishing ‘self’ from ‘non-self’ became of immense importance whereas sessile colonial organisms had to avoid fusion with foreign tissue to sustain their own kind (cf. [21]). Marine colonial invertebrates undergo natural transplantation when different colonies grow into contact. Allorecognition is widely distributed within marine sessile invertebrate species such as sponges, cnidarians and tunicates and seems to be important in protection against germ line parasitism (e.g. [22-26]). The fusion of conspecifics to chimeric individuals thereby often is restricted to the early stages of development as animals exhibit an ontogenetic shift in the allorecognition response (e.g. [27,28]). Sponges are known to have a great regeneration capacity and grafting of genetically distinct conspecifics mostly comes along with rejection of foreign tissues. Investigations on the demosponge *Amphimedon queenslandica* even demonstrated that thorough mixture of cells of two individuals sort into territories two weeks after initiation of sponge metamorphosis [24]. However, natural chimerism of the demosponge *Scopalina lophyropoda* was reported [29] and the authors suggest a benefit in lower total individual mortality risks due to different fitness levels of cells. A recent publication of Pomponi et al. [30] furthermore shows that interspecific sponge hybridomas can be produced by fusion of non-dividing somatic cells with dividing cells of a different species. Colonial cnidarians such as e.g. the Hydrozoon *Hydractinia symbiolongicarpus* or the Anthozoon *Pocillopora damicornis* are capable to discriminate self and close kin from foreign tissues, but lack an allorecognition response in the first 2-8 months post settlement [28,31]. The fresh water cnidarian *Hydra vulgaris* on the opposite is not able to discriminate between self and conspecifics and thus the discrimination ability is either lost or reduced possibly due to its solitary lifestyle [32]. Studies on the anthozoan genus *Montipora* demonstrated that even when foreign tissue successfully was removed by allorecognition responses, motile cellular structures could be observed within the gastrovascular canals of *Montipora capitata* species after previous fusion and rejection of *Montipora flabellata* tissues [33]. The researchers hypothesize these cells to be a result from chimeric fusion of the two species during larval stage with a subsequent reabsorption of one partner. Fusion between linked colonies frequently was observed also in bryozoans. Frequency of intergrowth thereby positively correlated with the degree of relatedness of individuals and observations suggest an ontogenetic shift in the allorecognition response approximately two weeks after metamorphosis [34]. The urochordate *Botryllus schlosseri* is a well-studied

model for invertebrate allorecognition (for review see e.g. [35]). Contact of genetically distinct *Botryllus* individuals results in fusion or rejection of tissues. After fusion with allogeneic individuals, one competitor generally is resorbed but blood, soma and germ cells remain chimeric [36].

The genetic mechanism of invertebrate allorecognition so far exclusively has been elucidated in the cnidarian *Hydractinia symbiolongicarpus* and the tunicate *Botryllus schlosseri*. Active rejection of allogeneic tissue in both organisms can come along with tissue alterations at the contact zone through to destruction of the foreign cells: the colonies ‘fight’ for space in limited habitats [37]. Therefore, allorecognition also is a powerful factor driving selection. The molecular mechanism for tissue recognition in *Hydractinia* and *Botryllus* is known to lie in different gene loci encoding for polymorphic cell surface molecules. The allorecognition complexes (ARC) *Alr1/Alr2* in *Hydractinia* and *fuhc/fester* in *Botryllus*, could be identified by means of breeding experiments and positional cloning [38,39]. Closely related colonies share at least one allele of these loci resulting in fusion or tolerance of competitive colonies [40-43]. Although allodeterminants found so far do not show any homologies, the mechanism is deemed to represent the origin of the immune system also in higher animals with possible homologies in proteins of downstream signaling pathways [21,44]. Besides from evolutionary aspects, research on the allorecognition machinery in other lower animals can give some input into other fields, such as human transplantation research, by identifying general mechanisms in easy-to-culture and easy-to-quantify animal model systems.

In 1984, Schwartz reported on tissue-grafting experiments within individuals of *Trichoplax adhaerens* [17]. He transplanted marginal and central tissue into the center of a host individual and observed frequent acceptance of these autografts. Grafting of marginal cells thereby resulted in the formation of a new concentric margin as cells kept their marginal differentiation. We now extended his research by using different genetic placozoan lineages as donor and acceptor individuals. The outcome of this study further supports the hypothesis of placozoan taxonomic diversity and suggests the presence of an allorecognition system already in the basal metazoan phylum Placozoa.

Material and Methods

Tissue grafting

Animal material used in experiments was cultured as described in [1,8] and with algae-overgrown microscopic slides equally. Slides were used as additional food source to simulate natural environmental conditions and to increase fitness of diverse lineages. *Trichoplax adhaerens* (16S haplotype H1), H2, H7, H13, H15, H16 and H19 were used for grafting (cf. table 2.3.1). Grafting was performed with a sterile acupuncture needle (thickness 0.3 mm, length 13 mm, Suzhou Tianxie Acupuncture Instruments Co., Ltd.) and solely marginal

2.3 Regeneration and self/non-self recognition in Placozoa

tissue was grafted. As marginal cells are unable to dedifferentiate to cells of the central tissue, this method produces donut-shaped animals with a concentric second margin and thus successful transplants are easy to detect by eye (cf. fig. A.3.1 D, figure 2.3.1 A and C). Tissues were grafted exclusively into the center of individuals to increase chances for intergrowth. Animal movement is too fast particularly during the regenerative process and tissues, grafted into the marginal region, would simply move apart whereas likelihood of intergrowth is higher when acceptor tissues surround donor tissues. For exemplary visualization of graft intergrowth, donor tissue further was stained with Methylene blue (Carl Roth, Germany) or with the fluorescent DiI (Invitrogen). In each grafting experiment only two individuals were used, one serving as donor and the other as acceptor. We differentiate between three grafting types:

- Autograft: within a clonal lineage
- Intergraft: within a clade
- Xenograft: between two clades

These terms do not necessarily exactly reflect relatedness.

Haplotype	Name of clonal lineage	Clade	Origin, Country	Habitat	Reference
H1	'Grell'	I	Eilat, Israel	algae samples	[2]
H2	'CAR-PAN-4'	I	Bocas del Toro, Panama	mangroves	[4]
H2	'HKG-C1'	I	Hong Kong, China	flow-through seawater system	[3]
H2	'ROS'	I	Roscoff, France	flow-through seawater system	[10]
H7	'OJ-gamma'	III	unknown (aquarium sample)	unknown (aquarium sample)	Osigus et al., unpublished
H16	'KEN-A'	III	Mombasa, Kenya	coral reef	[4]
H19	'ADL-1'	IV	Adelaide, Australia	stony beach	[3]
H13	'M153E-2'	V	Hong Kong, China	mangroves	Eitel et al., unpublished
H15	'M2RS3-11'	V	Hong Kong, China	mangroves	Eitel et al., unpublished

Table 2.3.1: Haplotypes used in this study.

Worldwide isolates from nine haplotypes and four placozoan clades have been used for grafting experiments. To compare fusion success within H2, isolates from different locations and/or habitats were tested.

Microscopy

For visualization of DiI stained individuals, confocal microscopy has been performed using the Leica Confocal TCS-SP5 (Leica Microsystems, Heidelberg GmbH) and DiI coloration was detected with the 546 nm laser line of a helium-neon laser. Stereomicroscopy and light microscopy have been done with a Zeiss Stemi SV6 stereomicroscope and a Zeiss Axiovert 200M, respectively, each connected to digital cameras (Canon "Power Shot" G9, a Zeiss Axio Cam MRn for black and white pictures and a Zeiss Axio Cam ICc3 for color depiction). Pictures have been edited with Adobe Photoshop Elements 8.0 to improve contrast only.

Molecular analysis

In case of intergrowth between different lineages, transplanted animals have been cultivated at least for two weeks and were then checked for genetic chimeras by means of PCR analyses. The DNA of single animals was either isolated on FTA® Elute Cards (Whatman) depicted in [45] or DNA was isolated via phenol-chloroform extraction described in [46]. In both cases, isolated DNA of single individuals was resuspended in a final volume of 10 μ l distilled water (GIBCO, Invitrogen). After resuspension, 1 μ l of the solution was used as DNA template in a total volume of 25 μ l per PCR reaction. PCR conditions were: initial denaturation at 95 ° - 5min, 45 circles of 95 °C - 30 seconds, 55 °C - 30 seconds, 72 °C 1 minute, and a final elongation step at 72 °C for 4 minutes. A haplotype/clade-specific forward (fw) or reverse (rv) primer was combined with a respective fw or rv universal primer [45] to amplify a 16S-b fragment (see table A.3.1 for primer sequences). Sequence information to design the haplotype-specific primers was taken from [3-5,9]. Positive controls for used primer sets have been performed with genomic DNA from pools of multiple clonal individual for each haplotype. Success of DNA isolation was verified with the universal primer set.

Calculations and Statistics

Results for grafting experiments of certain acceptor/donor haplotypes and vice versa were combined (for raw data see table A.3.2) and percentages of intergrowth were calculated by dividing the number of intergrowths (i) by the number of experiments (n). For boxplot calculations, data were summed up to three taxonomic groups: autografts, intergrafts and xenografts (cf. table A.3.3). Calculations were made with Excel® (Excel® for Mac 2011)

Statistical analyses were performed with SPSS Statistics (IBM, version 21.0). To test influences of the donor/acceptor role allocation a Fisher's exact test has been done ([47], cf. table A.3.4). Significances of fusion frequencies in dependence on genetic distances have been calculated by means of the Jonckheere-Terpstra test for independent samples ([48,49], cf. table A.3.3).

Results

Self-compatibility and chimeras

All tested haplotypes were able to steadily accept autografts (fig. 2.3.1, table A.3.2). Intergrafting experiments showed that stable chimera could be generated between *Trichoplax adhaerens* and H2 ('PAN', 'ROS' and 'HKG-C1'). Long-term fusion was verified via PCR (table A.3.4) and stable *Trichoplax* /H2 chimeras have been cultured up to four months. Three H2 clones, derived from different locations, were used for intergrafting experiments (table 2.3.1). Fusion between individuals from different H2 clones was *cum grano salis*

2.3 Regeneration and self/non-self recognition in Placozoa

stable. Stability of chimera could only be observed microscopically as the H2 clones do not differ in their 16S sequence. To address this issue divergent genetic markers must be used, i.e. differing alleles of single copy genes or microsatellites of varying length. Under the microscope one could see, however, that transplanted tissue seamlessly integrated into the acceptor individual and donut shaped individuals were detected several days after experiment. This typical phenotype can be observed after successful intergrowth: the transplanted marginal tissue keeps its differentiation and produces a concentric hole in the acceptor animal that is bordered by marginal cells (cf. fig. A.3.1 D, fig. 2.3.2 A and C).

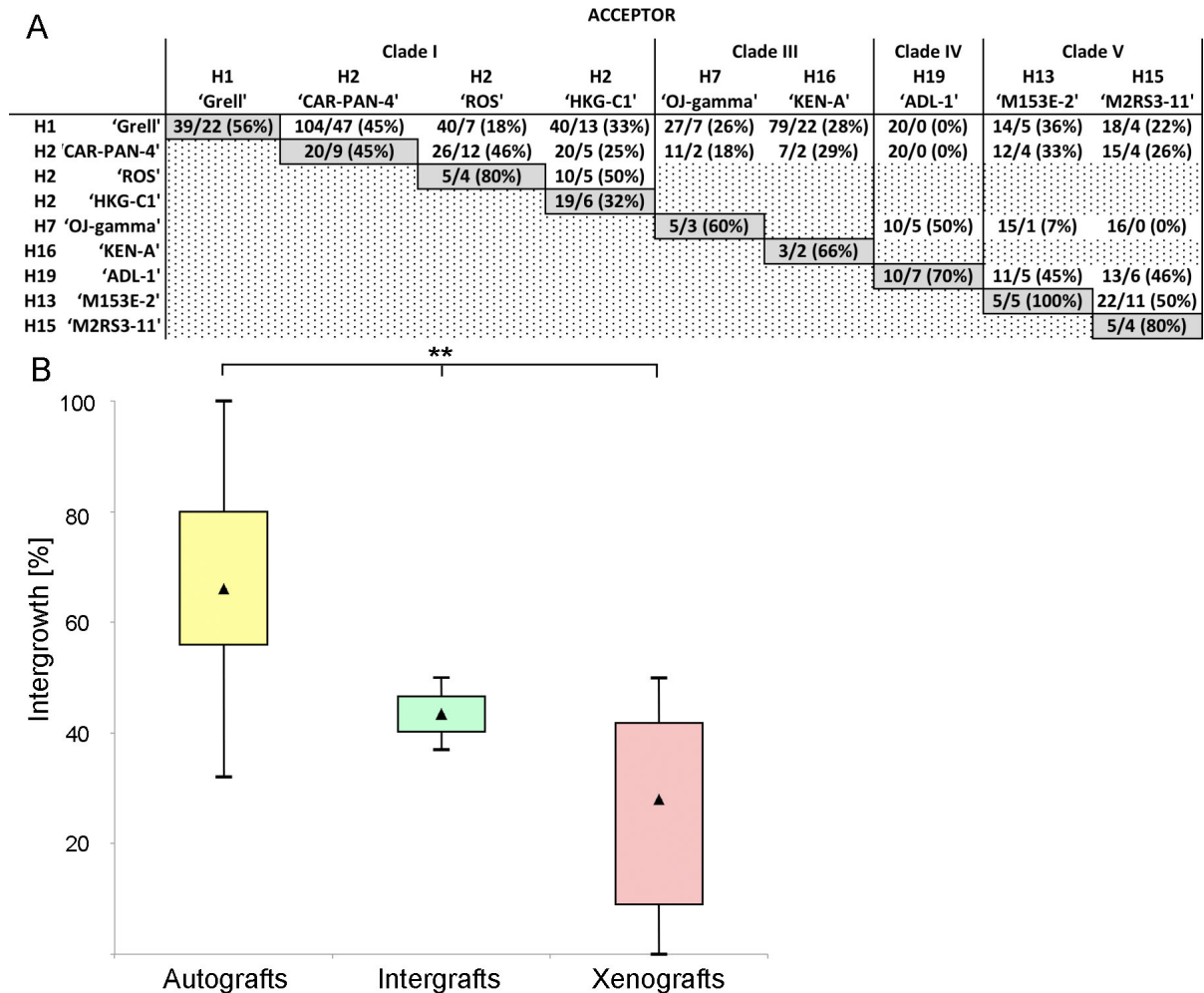


Figure 2.3.1: Frequencies of transient tissue intergrowth.

Frequencies of (transitory) graft intergrowth are shown in (A). Values for reciprocal transplantations were combined (for raw data see table A.3.2). Performed experiments / fusion of individuals are indicated, percentages of intergrowth success are enclosed in brackets. The reduction of fusion ability in inter- and xenografts becomes visible in (B). All tested haplotypes frequently accepted own tissue (autografts in yellow) whereas grafting of different clones of a single haplotype or haplotypes within a clade (intergraft in green) or even between clades (xenografts in red) was less successful. The fusion frequency decreases highly significant in accordance to greater genetic distances of grafted tissues ($p < 0.01$, Jonckheere-Terpstra test, indicated by asterisks). For data on boxplot analyses and statistics see table A.3.3.

2.3 Regeneration and self/non-self recognition in Placozoa

Transitory fusion in xenografts

Xenografting resulted in an initial intergrowth of donor and acceptor tissue, followed by repulsion of transplants after 18-48 hours. None of the host individuals did accept xenografts in the long run. Rejection after initial fusion was observed in grafts between *Trichoplax* and H7/H13/H15/H16, H2 ('PAN') and H7/H13/H15/H16, H13 and H7/H19, H15 and H19 as well as H7 and H19. No fusion occurred between H19 and H1/H2 ('PAN') as well as between H7 and H15. Fusion of H7 with H13 only was observed once and repulsion occurred shortly (~ 4 hours) after initial fusion. None of these lineages could be verified to form genetic chimeras (table A.3.4). The Fisher's exact test furthermore revealed that there was no notable difference between the two reciprocal transplantation

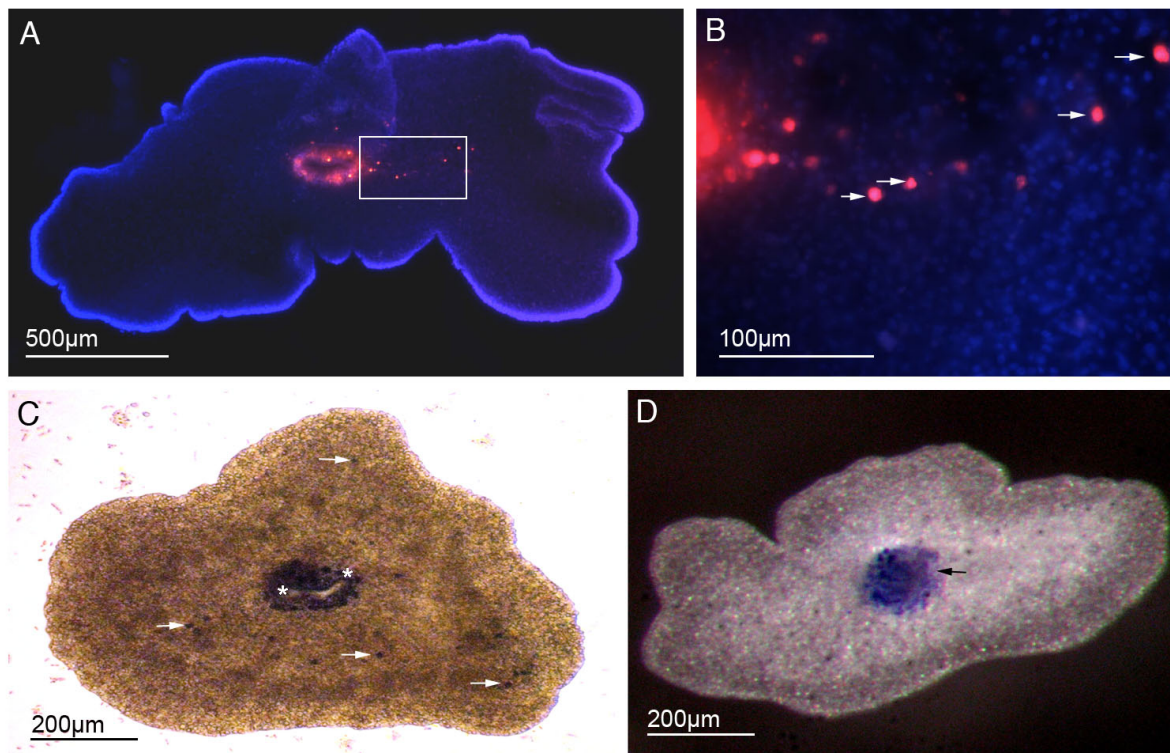


Figure 2.3.2: Exemplary intergrowth and cell migration 24 hours after transplantation.

Autograft between two H2 individuals of the 'PAN' clone are shown to illustrate intergrowth (A) and cell migration (B, higher magnification of the inlet in A). The donor animal was stained with DiI (red) before grafting. After fusion, the animal was fixed and subsequently nucleic acids were stained with DAPI (blue). Arrowheads mark cells migrating into the acceptor individual. An exemplary xenograft of a H2 ('PAN' clone) donor tissue in a H16 ('KEN-A') acceptor individual is shown under light and stereomicroscopy (C and D, respectively). In (C) a view on the lower epithelium is shown, while in (D) one looks on the upper epithelium. The donor H2 individual has been stained with Methylene blue. Cell migration events are detectable (arrowheads). The marginal cells of the donor tissue maintain their marginal differentiation, forming a hole in the middle of the chimera (marked by asterisks in C). In contrast to (C), the concentric margin of the donor tissue is not visible in (D). What one can see here, however, is an intergrowth of acceptor upper epithelium cells (arrowhead).

2.3 Regeneration and self/non-self recognition in Placozoa

experiments, i.e. it did not matter which individual served as acceptor and which as donor individual ($p > 0.05$, table A.3.4). Fusion ability in general declines in accordance to the increase of genetic divergence (fig. 2.3.1B). The Jonckheere-Terpstra test revealed a highly significant monotonic trend ($p < 0.01$) for fusion frequencies with regards to the genetic distances of donor and acceptor haplotypes (table A.3.3).

Cell migration, tissue alterations and active rejection of grafts during regeneration

Cell migration was observed in auto-, inter-, and xenografts (arrowheads in fig. 2.3.2 B and C). Migrating cells have a spherical appearance and a size of approximately $1 - 2 \mu\text{m}$ in diameter. In case of transitory fusion, active rejection of tissue was observed. The donor tissue often did not fuse with the acceptor tissue and, if occurring, intergrowth frequently was restricted to a small proportion of transplanted tissue (fig. 2.3.3 A). In the latter case, the transplant remained loosely connected for approximately 18-48 hours and was subsequently released. In other cases, the upper or lower epithelium of the host animal moved over the previously well-fused transplant and the donor tissue was repelled subsequently (arrowhead in fig. 2.3.2 D). Certain individuals even exposed tissue alterations in the area of transplantation, sometimes still visible also after tissue rejection (fig. 2.3.3 B and C). H7 acceptor individuals even died after H2 or H13 xenografts were rejected.

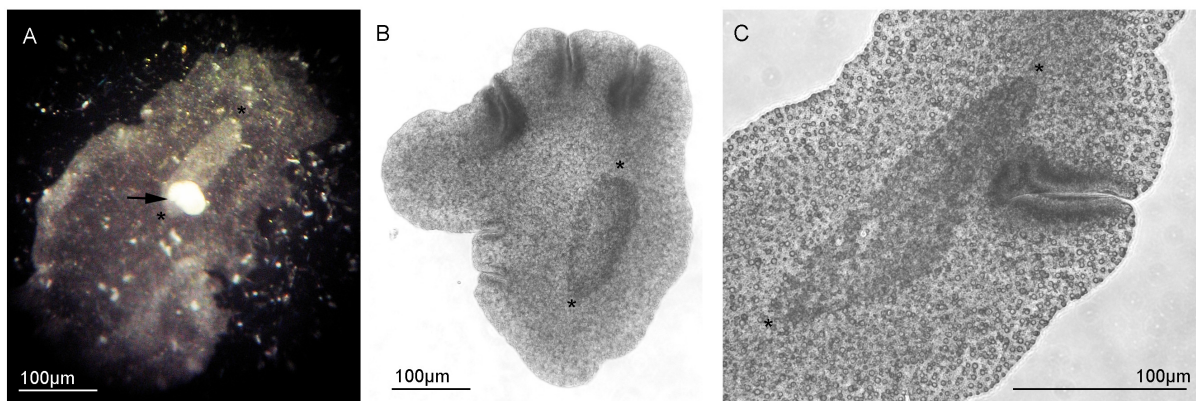


Figure 2.3.3: Xenografting can lead to morphological alterations in the acceptor tissue.

Shown are xenografts between *Trichoplax adhaerens* (H1, acceptor) and H13 (donor) before (A) and after (B, C) donor tissue rejection. 18 hours after grafting (A), the donor tissue (arrowhead) is almost completely repelled and the acceptor tissue around the donor material shows morphological alterations (framed by asterisks). This tissue variation persists even after the donor tissue was rejected (B and at higher magnification in C), strongly indicating allorecognition between the two individuals with different genetic background.

Discussion

Placozoa do possess a self/non-self recognition system

Our experiments have shown that all tested placozoan genetic lineages are able to discriminate between “self” and “non-self” tissue. Placozoa thus do likely possess a primitive self/non-self recognition system possibly similar to the allorecognition systems known e.g. from *Hydractinia* and *Botryllus* [21]. Unfortunately, not all of the identified placozoan lineages can be cultured routinely in the laboratory thus far, limiting our experimental possibilities to few genetic lineages. Additionally, the utilized H16 lineage became extinct in course of the experimental period what further limited the number of experiments. However the results of our studies clearly show that non-related placozoan lineages are able to repel foreign tissues and thereby sustain their own kind.

Placozoan lineages are self-compatible

All of the tested lineages were able to accept autografts as a consequence of the clonal propagation of the Placozoa [50]. Nevertheless, not all of the prepared autografts did fuse (cf. table A.3.3). This can be explained by extensive movement of individuals generally accompanies the regenerative process of Placozoa and the closing of wounds is happening fast [16,17]. Failure in fusion of autografts therefore was due to movement of both: donor and acceptor tissue whereas the acceptor- animal frequently closed the inflicted holes above the donor tissue and thus prevented intergrowth. In future studies, host and acceptor tissue should be prevented from moving to mirror more accurately the fusion rate.

Fusion ability declines with higher genetic divergence of donor and acceptor

Cell surface molecules are known to be responsible for invertebrate allorecognition (cf. [21]). This mechanism involves transmembrane receptor-proteins that allow the detection of foreign cells. Our data suggest that placozoan cells do possess such a recognition system. Auto- and intergraft fusion is more frequent than xenograft intergrowth whereas abundance of autograft fusion > intergraft fusion > xenograft fusion is highly significant (Jonckheere-Terpstra test, $p < 0.01$). *Trichoplax* and H2 (at least the ‘PAN’, ‘ROS’ and ‘HKG-C1’ clone) can form stable genetic chimeras, which pleads for close relatedness. Sequencing efforts on the H2 (‘PAN’ clone) nuclear genome revealed high genetic similarities between *Trichoplax* and H2 (unpublished data). Therefore proteins of the potential allorecognition machinery should be similar. Unfortunately H7 could not be tested for intergrowth with H16 but we would expect the results to be similar to the observations for *Trichoplax* with H2 as they belong to one clade and possess striking morphological characteristics namely frailty and density of cilia (own unpublished observations) that further support close relatedness. Chimera of H13 and H15 could not be verified by molecular approaches yet as conducted PCR analyses thus far failed to discriminate between the two haplotypes.

2.3 Regeneration and self/non-self recognition in Placozoa

Hence, long-term intergrowth between these lineages remains a speculation and has to be further investigated.

Allorecognition loci have been identified for the cnidarian *Hydractinia symbiolongicarpus* (*alr1* and *alr2* [42]) and the tunicate *Botryllus schlosseri* (*fuhc* and *fester* [38,41]). In these models, transitory fusion of tissue is possible when individuals share a single allele of one locus (*Botryllus*) or, respectively, at least one allele of both loci (*Hydractinia*). In our study, we observed throughout acceptance of grafts only in evolutionary closely related individuals. Transitory fusion and rejection of tissue happened when tissue was grafted between different placozoan lineages. In xenograft experiments we showed that fusion of tissue was only of transient nature and rejection occurred approximately 18-48 h post grafting. PCR analyses further revealed that donor tissue was not detectable in the acceptor individuals after rejection. Transitory fusion might be a result of the existence of a multi-loci allorecognition system in the Placozoa, which generally allows fusion in the first place due to genetic similarities. This multi-level system ensures, however, that foreign tissue will be removed later on, indicating the involvement of at least two, but most probably more membrane-bound allorecognition proteins. Accordingly, the degree of protein sequence similarity would determine the degree of intergrowth. Intergrowth, transitory fusion and rejection should thus directly reflect the evolutionary relationship of individuals, at least with regard to allorecognition proteins. Current placozoan nuclear genome sequencing projects will serve as the basis for future investigations in this field. Comparison of divergent whole genomes will possibly enable the identification of allorecognition genes in the Placozoa. Besides from giving new insights into the nature of allorecognition in lower metazoans, this would also shed additional light on the placozoan taxonomy.

Cell migration and tissue alterations

Tissue staining revealed cell migration in auto-, inter- and xenografts of *Trichoplax*, H2 and H16 individuals at least within the first 48 hours after grafting. Nevertheless, no cells are detectable by molecular approaches after rejection of grafted tissues in xenografts. This could be an indication for destruction of foreign cells in the host individual. Another explanation might be that migrating 'cells' belong to the so-called 'shiny spheres'. These structures are degenerated cells and do contain a greasy fluid (cf. [51,52]) which would also explain the strong signal after DiI coloration being a lipophilic dye. Due to their degeneracy they might have lost their ability to distinguish self from foreign cells and in turn also are not detectable as foreign in the host animal. Nevertheless, this is merely a hypothesis that has to be further investigated as the shiny spheres have been shown to be connected to the fiber cells [6] which would reduce their ability to migrate within the animal. Due to the animals' apparent plasticity, however, a certain mobility of cells within

2.3 Regeneration and self/non-self recognition in Placozoa

the individual cannot be excluded, including cells connected to shiny spheres. Possibly, shiny sphere are detached during grafting and are able to migrate into the acceptor's upper epithelium.

The occurrence of tissue alterations while rejection of foreign tissues gives hints to incompatibility reactions possibly associated with the release of certain signaling molecules and cytotoxic components. Tunnel assays on altered cells might reveal whether rejection is related to necrosis or apoptosis within tissues as it was observed e.g. in *Hydractinia* [53]. In cnidarians and tunicates, rejection of tissues is either passive or active with the latter coming along with recruitment of nematocytes (Cnidaria) or specializes 'morula' cells (Tunicate) to induce a cytotoxic reaction in the host individual (e.g. [21]). Alterations of host tissues after grafting might be an indication of an aggressive graft rejection.

Grafting experiments can help to unravel placozoan taxonomy

Beside molecular [3-5], morphological [6] and ecological data collected thus far, grafting experiments might help to unravel the relationships within the phylum Placozoa. Data collected in course of this study do support the current view of placozoan phylogeny given by molecular analyses. Close genetic relationship can result in the formation of genetic chimeras as it was observed in grafts between *Trichoplax* and H2 ('PAN', 'ROS' and 'HKG-C1'). Even though grafting experiments seem to be a good complement to morphological and molecular characters to help unravelling the placozoan systematics, one has to bear in mind that proteins of the allorecognition machinery may have been lost in course of evolution or are even more diverged than other genetic markers (see [54]). Genetic equipment and sequences of allorecognition genes thus might be highly diverse between in distantly related haplotypes and particularly in divergent clades. One has to wait for additional placozoan genomes to study the evolution of allorecognition genes and their usability as genetic markers in placozoan systematics.

Conclusions

The phylum Placozoa turned out to be much more diverse than initially thought [3-5]. 19 genetically different lineages have been found so far and despite all sampling efforts this is clearly not the end of the rope. Our study supports the assumption that placozoan taxonomy is diverse and genetic lineages likely even represent different species, genera and families. Results further show that Placozoa are able to discriminate 'self' from 'non-self' tissues and thus do possess a primitive allorecognition system. Future genome sequencing projects and grafting experiments will help to identify proteins involved in self/non-self recognition in Placozoa and will further shed light on phylogenetic relationship within the phylum. Therefore, recreation of the manifold ecological niches hosting the distinct lineages in the laboratory will be necessary which in turn requires a broader knowledge on

2.3 Regeneration and self/non-self recognition in Placozoa

the animals ecological needs. Ongoing research in this area will help to understand the biology of Placozoa facilitating further culturing efforts. Besides genetic, morphological and ecological data, grafting experiments will help to further unravel phylogenetic relationships among placozoan lineages and are yet another strong argument that the phylum Placozoa is highly diverse.

Acknowledgments

K. vdC. was funded by an Evangelische Studienwerk Villigst e.V. PhD fellowship, an "Otto Bütschli" scholarship from the Tierärztliche Hochschule Hannover and a travel grant from Boehringer Ingelheim Fonds.

References

1. Schierwater B (2005) *My favorite animal, Trichoplax adhaerens*. BioEssays 27: 1294-1302.
2. Grell KG, Benwitz G (1971) *Die Ultrastruktur von Trichoplax adhaerens F.E. Schulze*. Cytobiologie 4: 216-240.
3. Eitel M, Osigus HJ, Desalle R, Schierwater B (2013) *Global diversity of the placozoa*. PLoS One 8: e57131.
4. Eitel M, Schierwater B (2010) *The phylogeography of the Placozoa suggests a taxon-rich phylum in tropical and subtropical waters*. Mol Ecol 19: 2315-2327.
5. Voigt O, Collins AG, Pearse VB, Pearse JS, Ender A, et al. (2004) *Placozoa - no longer a phylum of one*. Curr Biol 14: R944-945.
6. Guidi L, Eitel M, Cesarini E, Schierwater B, Balsamo M (2011) *Ultrastructural analyses support different morphological lineages in the phylum Placozoa Grell, 1971*. J Morphol 272: 371-378.
7. Grell KG (1972) *Eibildung und Furchung von Trichoplax adhaerens F.E.Schulze (Placozoa)*. Z Morph Tiere 73: 297-314.
8. Eitel M, Guidi L, Hadrys H, Balsamo M, Schierwater B (2011) *New insights into placozoan sexual reproduction and development*. PLoS One 6: e19639.
9. Signorovitch AY, Dellaporta SL, Buss LW (2006) *Caribbean placozoan phylogeography*. Biol Bull 211: 149-156.
10. von der Chevallerie K, Eitel M, Schierwater B (2010) *Focus on an unexpected discovery in Roscoff - a warm water species of the phylum Placozoa*. Cah Biol Mar 212: 21.
11. Nosenko T, Schreiber F, Adamska M, Adamski M, Eitel M, et al. (2013) *Deep metazoan phylogeny: when different genes tell different stories*. Mol Phylogenet Evol 67: 223-233.
12. Schierwater B, Eitel M, Jakob W, Osigus HJ, Hadrys H, et al. (2009) *Concatenated Analysis Sheds Light on Early Metazoan Evolution and Fuels a Modern "Urmetazoon" Hypothesis*. Plos Biology 7: 36-44.
13. Srivastava M, Begovic E, Chapman J, Putnam NH, Hellsten U, et al. (2008) *The Trichoplax genome and the nature of placozoans*. Nature 454: 955-960.

2.3 Regeneration and self/non-self recognition in Placozoa

14. Ringrose JH, van den Toorn HW, Eitel M, Post H, Neerincx P, et al. (2013) *Deep proteome profiling of Trichoplax adhaerens reveals remarkable features at the origin of metazoan multicellularity*. Nat Commun 4: 1408.
15. Schierwater B, de Jong D, Desalle R (2009) *Placozoa and the evolution of Metazoa and intrasomatic cell differentiation*. Int J Biochem Cell Biol 41: 370-379.
16. Ruthmann A, Terwelp U (1979) *Disaggregation and reaggregation of cells of the primitive metazoan Trichoplax adhaerens*. Differentiation 13: 185-198.
17. Schwartz V (1984) *The radial polar pattern of differentiation in Trichoplax adhaerens F.E. Schulze (Placozoa)*. Z Naturforsch 39c: 818-832.
18. Holstein TW, Hobmayer E, Technau U (2003) *Cnidarians: an evolutionarily conserved model system for regeneration?* Dev Dyn 226: 257-267.
19. Bosch TC (2007) *Why polyps regenerate and we don't: towards a cellular and molecular framework for Hydra regeneration*. Dev Biol 303: 421-433.
20. Tanaka EM, Reddien PW (2011) *The cellular basis for animal regeneration*. Dev Cell 21: 172-185.
21. Rosengarten RD, Nicotra ML (2011) *Model systems of invertebrate allorecognition*. Curr Biol 21: R82-92.
22. Lakkis FG, Dellaporta SL, Buss LW (2008) *Allorecognition and chimerism in an invertebrate model organism*. Organogenesis 4: 236-240.
23. Puill-Stephan E, Willis BL, Abrego D, Raina J-B, van Oppen MJH (2012) *Allorecognition maturation in the broadcast-spawning coral Acropora millepora*. Coral Reefs 31: 1019-1028.
24. Gauthier M, Degnan BM (2008) *Partitioning of genetically distinct cell populations in chimeric juveniles of the sponge Amphimedon queenslandica*. Dev Comp Immunol 32: 1270-1280.
25. Muller WE, Muller IM (2003) *Origin of the metazoan immune system: identification of the molecules and their functions in sponges*. Integr Comp Biol 43: 281-292.
26. Hauenschild C (1954) *Genetische und entwicklungsphysiologische Untersuchungen über Intersexualität und Gewebeverträglichkeit bei Hydractinia echinata Flemm. (Hydroz. Bougainvill)*. Roux Arch Dev Biol 147: 1-41.

2.3 Regeneration and self/non-self recognition in Placozoa

27. McGhee KE (2005) *The importance of life-history stage and individual variation in the allorecognition system of a marine sponge*. Journal of Experimental Marine Biology and Ecology 333: 241-250.
28. Wilson ACC, Grosberg RK (2004) *Ontogenetic shifts in fusion-rejection thresholds in a colonial marine hydrozoan, Hydractinia symbiolongicarpus*. Behav Ecol Sociobiol 57: 40-49.
29. Blanquer A, Uriz MJ (2011) *"Living together apart": the hidden genetic diversity of sponge populations*. Mol Biol Evol 28: 2435-2438.
30. Pomponi SA, Jevitt A, Patel J, Diaz MC (2013) *Sponge Hybridomas: Applications and Implications*. Integr Comp Biol.
31. Hidaka M, Yurugi K, Sunagawa S, Kinzie RA (1997) *Contact reactions between young colonies of the coral Pocillopora damicornis*. Coral Reefs 16: 13-20.
32. Kuznetsov SG, Bosch TC (2003) *Self/nonsel self recognition in Cnidaria: contact to allogeneic tissue does not result in elimination of nonself cells in Hydra vulgaris*. Zoology (Jena) 106: 109-116.
33. Work TM, Forsman ZH, Szabo Z, Lewis TD, Aeby GS, et al. (2011) *Inter-specific coral chimerism: genetically distinct multicellular structures associated with tissue loss in Montipora capitata*. PLoS One 6: e22869.
34. Hughes RN, Manriquez PH, Morley S, Craig SF, Bishop JD (2004) *Kin or self-recognition? Colonial fusibility of the bryozoan Celleporella hyalina*. Evol Dev 6: 431-437.
35. Rinkevich B (2005) *Natural chimerism in colonial urochordates*. Journal of Experimental Marine Biology and Ecology 322: 93-109.
36. Raftos DA (1991) *Cellular restriction of histocompatibility responses in the solitary urochordate, Styela plicata*. Dev Comp Immunol 15: 93-98.
37. Oren M, Paz G, Douek J, Rosner A, Amar KO, et al. (2013) *Marine invertebrates cross phyla comparisons reveal highly conserved immune machinery*. Immunobiology 218: 484-495.
38. De Tomaso AW, Saito Y, Ishizuka KJ, Palmeri KJ, Weissman IL (1998) *Mapping the genome of a model protochordate. I. A low resolution genetic map encompassing the fusion/histocompatibility (Fu/HC) locus of Botryllus schlosseri*. Genetics 149: 277-287.

2.3 Regeneration and self/non-self recognition in Placozoa

39. Mokady O, Buss LW (1996) *Transmission genetics of allorecognition in Hydractinia symbiolongicarpus (Cnidaria:Hydrozoa)*. Genetics 143: 823-827.
40. Scofield VL, Schlumpberger JM, West LA, Weissman IL (1982) Protochordate allorecognition is controlled by a MHC-like gene system. Nature 295: 499-502.
41. Nyholm SV, Passegue E, Ludington WB, Voskoboynik A, Mitchel K, et al. (2006) *fester, A candidate allorecognition receptor from a primitive chordate*. Immunity 25: 163-173.
42. Cadavid LF, Powell AE, Nicotra ML, Moreno M, Buss LW (2004) *An invertebrate histocompatibility complex*. Genetics 167: 357-365.
43. Nicotra ML, Powell AE, Rosengarten RD, Moreno M, Grimwood J, et al. (2009) *A hypervariable invertebrate allodeterminant*. Curr Biol 19: 583-589.
44. Dishaw LJ, Litman GW (2009) *Invertebrate allorecognition: the origins of histocompatibility*. Curr Biol 19: R286-288.
45. Signorovitch AY, Dellaporta SL, Buss LW (2005) *Molecular signatures for sex in the Placozoa*. Proc Natl Acad Sci U S A 102: 15518-15522.
46. Ender A, Schierwater B (2003) *Placozoa are not derived cnidarians: evidence from molecular morphology*. Mol Biol Evol 20: 130-134.
47. Fisher R (1922) *On the Interpretation of χ^2 from Contingency Tables, and the Calculation of P*. Journal of the Royal Statistical Society 85: 87-94.
48. Jonkheere A (1954) *A distribution-free k-sample test against ordered alternatives*. Biometrika 41: 133-145.
49. Terpstra T (1952) *The asymptotic normality and consistency of Kendall's test against trend, when ties are present in one ranking*. Indagationes Mathematicae 14: 327-333.
50. Grell KG (1984) *Reproduction of Placozoa*. In: Engels W, editor. Advances in Invertebrate Reproduction: Elsevier. pp. 541-546.
51. Grell KG, Ruthmann A (1991) *Placozoa*. In: Harrison FW, Westfall, J.A., editor. Microscopic Anatomy of Invertebrates, Placozoa, Porifera, Cnidaria, and Ctenophora. New York: Wiley-Liss. pp. 13-28.
52. Syed T, Schierwater B (2002) *Trichoplax adhaerens: discovered as a missing link, forgotten as a hydrozoan, re-discovered as a key to metazoan evolution*. Vie Milieu 52: 177-187.

2.3 Regeneration and self/non-self recognition in Placozoa

53. Buss LW, Anderson C, Westerman E, Kritzberger C, Poudyal M, et al. (2012) *Allorecognition triggers autophagy and subsequent necrosis in the cnidarian Hydractinia symbiolongicarpus*. PLoS One 7: e48914.
54. Miller DJ, Hemmrich G, Ball EE, Hayward DC, Khalturin K, et al. (2007) *The innate immune repertoire in cnidaria - ancestral complexity and stochastic gene loss*. Genome Biol 8: R59.

3 General Discussion

"Nature was not designed to
make life easy for biologists."

(Colin Tudge, 2007)

3.1 General Discussion

Cell cycle control at the base of the metazoan tree of life

The sequencing of the genome of *Trichoplax adhaerens* in 2008 revealed the presence of more than 11,000 protein-coding genes, a much higher genomic complexity than expected from such a simple animal [1]. Most identified genes are homologous to higher metazoan genes involved in various mechanisms from cell signaling to stimuli perception. With the evolution of Metazoa from a unicellular ancestor came the requirement to control maintenance of cellular homeostasis within a tissue [2]. As Placozoa possess the highest similarities to the hypothetical "Urmetazoon" [3, 4] its genetic repertoire is suspected to hold a primitive or even basal version of genetic networks responsible e.g. for cell cycle control [5]. In this thesis two networks that are of crucial importance regarding cell cycle and apoptosis control in other animals have been investigated in *Trichoplax adhaerens*: (i) the basic helix-loop-helix leucine zipper Myc and Max and (ii) the tumor suppressor p53 with its ubiquitin ligase Mdm2.

(i) First experimental approaches on the Myc/Max network of transcription factors in *Trichoplax adhaerens* were performed. Deregulations of *myc* gene expression have been known to be responsible for a large number of human malignancies [6]. By means of gene expression analyses and inhibition studies in combination with the detection of apoptosis (TUNEL) and cell proliferation (BrdU), Myc/Max homologous have been investigated in *Trichoplax adhaerens* (taMyc and taMax). Both genes are expressed in a similar pattern that varies dependent on the developmental stage of the individual. Artificial downregulation of taMyc and taMax (by means of morpholino oligonucleotides or via inhibitor application) both result in an increase of apoptotic events lethal to the animals. Cell proliferation was monitored after inhibition of taMyc and taMax what however gave controversial results and thus should be reinvestigated under different conditions. Overall the findings of this study suggest that downregulation of taMyc and taMax on mRNA and protein level does affect placozoan stem cell proliferation or rather differentiation processes. Both genes are strongly expressed in the placozoan marginal region where the placozoan stem cells are known to be located and thus taMyc and taMax are most probably also involved in differentiation processes.

Further experiments in this field should confirm and extend recent findings. Particularly experiments on protein binding capability have to be performed to validate interaction of the *Trichoplax* Myc and Max proteins. Recombinant expression of both proteins will furthermore allow the production of antibodies that can be used to unravel protein interaction *in situ* which would essentially enrich our knowledge on *tamyc* and *tamax* mRNA distribution. To further clarify the involvement of the *Trichoplax* Myc/Max network of transcription factors in the development of individuals, double staining with antibodies

against the *Trichoplax Trox-2* protein, which is known to be crucial for the animals' development, will help to detect functional coherences. Previous difficulties in recombinant protein expression occurred in connection with poor solubility of the full-length *Trichoplax* Myc protein. Future approaches thus should focus on shorter transcripts of the protein that contain corresponding domains of interest as e.g. the C-terminal part of the protein that contain DNA and Max binding sites [7].

(ii) Investigations on interactions of the tumor suppressor p53 and its ubiquitin ligase Mdm2 in Placozoa were done by application of known inhibitors of p53/Mdm2 interaction: the purine roscovitine and the cis-imidazoline Nutlin-3 [8, 9]. Both inhibitors turned out to be lethal for the organism and significantly increased the amount of cell death via apoptosis monitored with the TUNEL assay. Application of roscovitine furthermore decreased cell proliferation events detected by means of BrdU incorporation. This however likely is deducible to its function as cyclin-dependent kinase inhibitor [10]. Phenotypic abnormalities could be observed after usage of inhibitors characterized by an imbalance of central-marginal tissue ratios. Overall the study suggests that p53 and Mdm2 are involved in the control of apoptosis and also in developmental processes. Former transcriptome analyses furthermore revealed the existence of different splicing variants of the *Trichoplax* p53 gene (unpublished data) suggesting the interaction to be more complex as initially thought. Additional research including gene expression and protein- interaction studies will help to further shed light on the role of these genes in Placozoa.

Allorecognition in Placozoa

The enigmatic phylum Placozoa possesses the ability to regenerate in an unchallenged manner. Described in detail by Schwartz in 1984 [11] grafting experiments performed in course of this thesis included the usage of different placozoan lineages. Results demonstrate that placozoans do possess the ability to distinguish self from non-self tissue. The regeneration capability further yields the potential to become a valid tool for placozoan taxonomic classification.

Trichoplax adhaerens has been thought to be the only representative of the phylum Placozoa, but the discovery of genetically distinct individuals suggests that variety of species is much more diverse than initially thought [12]. The classification of placozoan genetic lineages into different species, genera and families is a main focus of current research [13]. Molecular markers thus far defined 19 different lineages grouping into seven clades, which in turn cluster into two main groups (A and B) with the subgroups A1 and A2 [14]. Besides genetic criteria, morphological traits and ecological needs are taken into account ([15], Schierwater *et al.* unpublished data). As Placozoa mainly reproduce vegetatively under laboratory conditions, interbreeding experiments cannot be easily [16]. The remarkable regeneration efficiency of different placozoan lineages however

allows grafting experiments in which two genetically distinct individuals are mixed and investigated for intergrowth. Seven of the 19 different haplotypes described thus far have been used for grafting experiments in which marginal tissue was grafted between two genetically distinct placozoan lineages.

Grafting experiments resulted in three distinct reactions after bringing together non-self tissues: (i) fusion, (ii) transitory fusion and (iii) rejection of grafted tissues. (i) Fusion of tissues resulted in the formation of genetic chimeras and was observed in autografts (i.e. between identical haplotypes) as well as intergrafts of H1 and H2. (ii) Transitory fusion is characterized by initial fusion and rejection of tissue after 12-48 hours. The rejection reaction then can come along with tissue alterations at the contact zone. (iii) Immediate rejection does not come along with any intergrowth. Foreign tissues simply move apart after grafting. The outcomes of performed experiments do suggest the existence of a multi-loci self/non-self recognition system in the Placozoa whereas congruities in gene loci result in (transitory) fusion of tissues. Thus, the degree of lineage relatedness, at least regarding the coding region of the recognition system, is mirrored by the degree of intergrowth. The results of our study reflect, in essence, the taxonomy created by former molecular analyses at least regarding the relation of different clades. Likelihood for successful intergrowth generally declines with increased genetic distances. To make a more detailed statement about relationships of lineages within a clade we first and foremost have to increase sample size and include experiments on different individuals of one clade. Not all discovered placozoan lineages can be cultured in the laboratory yet what drastically limits our experimental possibilities. Tissue grafting between placozoan species H1 and H2 demonstrated a close relatedness of these two lineages, as individuals were able to merge to genetic chimeras. The overall results of experiments conducted in course of this thesis further support the hypothesis that Placozoan taxonomy is much more diverse as previously expected and also highlights *Trichoplax* as a model for research on invertebrate allorecognition systems. The identification of the underlying genetic mechanism controlling acceptance or repulsion of tissue in this simple organism could help to understand the evolution of histocompatibility also in higher animals.

The potential of Placozoa as a model system for applied research

With its flat, translucent appearance *Trichoplax* can be designated a "crawling epithelia culture". The cultivation of animals is straightforward and their way of reproduction facilitates the maintenance of clonal lineages [17]. As the placozoan genome is sequenced, information on the genetic equipment is accessible [1]. Standard cell biology and developmental genetic methods (e.g. BrdU staining or the TUNEL assay, gene expression and gene knock downs [18-20]) are applicable to the individuals. Its regenerative capacity enables conduction of experiments that open a wide range of experimental possibilities:

3.1 General Discussion

Experimentally treated tissues could for instance merge into untreated individuals as a control experiment and one could also test influences of different chemicals or drugs in one and the same individual (and thus identical conditions) by simply cutting one individual into two or more.

To further qualify the Placozoa as a serious model system on an equal level as well-known models such as *Hydra* [21], *Caenorhabditis* [22] or *Drosophila* [23], the creation of transgenic *Trichoplax* individuals is one of the most important tasks to fulfill. Even though cultivation of animals is straightforward using artificial seawater and a mixture of algae and soil extract, methods have to become more standardized at least for transgenic organisms to avoid the occurrence of threatening contaminations. Epitopes of most commercially available antibodies do not fit *Trichoplax* proteins. As the genome is sequenced, recombinant protein synthesis for antibody manufacture is straightforward. A set of standard antibodies (e.g. cell cycle markers) will help to determine developmental stages of investigated individuals and thus facilitate comparability of e.g. gene expression studies.

In order to get valid information on gene expression pattern within the organisms, e.g. during different developmental stages, microarray technology could be used to test several genes in one approach [19]. Again, the sequenced genome gives us an advantage, as it facilitates also the design of microarrays.

Placozoa do possess a great potential to serve as a model system for many areas of biological research. As the animal is the best living surrogate for the first metazoan, its genetic equipment can be seen as a "basic toolkit" for multicellular organisms. Thus, complicated mechanisms such as signaling pathways and cell cycle control might be rather simple in this frugal organism. Ongoing research in this area will soon further emphasize the importance of Placozoa as a model system not only for evolutionary biology.

References

1. Srivastava, M., Begovic, E., Chapman, J., Putnam, N.H., Hellsten, U., Kawashima, T., Kuo, A., Mitros, T., Salamov, A., Carpenter, M.L., et al. (2008). *The Trichoplax genome and the nature of placozoans*. *Nature* 454, 955-960.
2. Grosberg, R.K., and Strathmann, R.R. (2007). *The Evolution of Multicellularity: A Minor Major Transition?* *Annu. Rev. Ecol. Evol. Syst.* 38, 621-654.
3. Schierwater, B., Eitel, M., Jakob, W., Osigus, H.J., Hadryś, H., Dellaporta, S.L., Kolokotronis, S.O., and DeSalle, R. (2009). *Concatenated Analysis Sheds Light on Early Metazoan Evolution and Fuels a Modern "Urmetazoon" Hypothesis*. *Plos Biology* 7, 36-44.
4. Schierwater, B., Desalle, R., Jakob, W., Schroth, W., Hadryś, H., and Dellaporta, S. (2006). *Total evidence analysis identifies Placozoa as basal to extant Metazoa*. *Integrative and Comparative Biology* 46, E126-E126.
5. Schierwater, B., de Jong, D., and Desalle, R. (2009). *Placozoa and the evolution of Metazoa and intrasomatic cell differentiation*. *Int J Biochem Cell Biol* 41, 370-379.
6. Lüscher, B., and Vervoorts, J. (2012). *Regulation of gene transcription by the oncoprotein MYC*. *Gene* 494, 145-160.
7. Fieber, W., Schneider, M.L., Matt, T., Krautler, B., Konrat, R., and Bister, K. (2001). *Structure, function, and dynamics of the dimerization and DNA-binding domain of oncogenic transcription factor v-Myc*. *J Mol Biol* 307, 1395-1410.
8. Lu, W., Chen, L., Peng, Y., and Chen, J. (2001). *Activation of p53 by roscovitine-mediated suppression of MDM2 expression*. *Oncogene* 20, 3206-3216.
9. Vassilev, L.T., Vu, B.T., Graves, B., Carvajal, D., Podlaski, F., Filipovic, Z., Kong, N., Kammlott, U., Lukacs, C., Klein, C., et al. (2004). *In vivo activation of the p53 pathway by small-molecule antagonists of MDM2*. *Science* 303, 844-848.
10. Meijer, L., Borgne, A., Mulner, O., Chong, J.P., Blow, J.J., Inagaki, N., Inagaki, M., Delcros, J.G., and Moulinoux, J.P. (1997). *Biochemical and cellular effects of roscovitine, a potent and selective inhibitor of the cyclin-dependent kinases cdc2, cdk2 and cdk5*. *Eur J Biochem* 243, 527-536.
11. Schwartz, V. (1984). *The radial polar pattern of differentiation in Trichoplax adhaerens F.E. Schulze (Placozoa)*. *Z. Naturforsch.* 39c, 818-832.

3.1 General Discussion

12. Voigt, O., Collins, A.G., Pearse, V.B., Pearse, J.S., Ender, A., Hadrys, H., and Schierwater, B. (2004). *Placozoa - no longer a phylum of one*. *Curr Biol* 14, R944-945.
13. Eitel, M., and Schierwater, B. (2010). *The phylogeography of the Placozoa suggests a taxon-rich phylum in tropical and subtropical waters*. *Mol Ecol* 19, 2315-2327.
14. Eitel, M., Osigus, H.-J., DeSalle, R., and Schierwater, B. (2013). *Global diversity of the Placozoa*. *PLoS One* 8: e57131.
15. Guidi, L., Eitel, M., Cesarini, E., Schierwater, B., and Balsamo, M. (2011). *Ultrastructural analyses support different morphological lineages in the phylum Placozoa Grell, 1971*. *J Morphol* 272, 371-378.
16. Grell, K.G., and Ruthmann, A. (1991). *Placozoa*. In *Microscopic Anatomy of Invertebrates, Placozoa, Porifera, Cnidaria, and Ctenophora*, Volume Vol. 2, F.W. Harrison, Westfall, J.A., ed. (New York: Wiley-Liss), pp. 13-28.
17. Schierwater, B. (2005). *My favorite animal, Trichoplax adhaerens*. *Bioessays* 27, 1294-1302.
18. Gavrieli, Y., Sherman, Y., and Ben-Sasson, S.A. (1992). *Identification of programmed cell death in situ via specific labeling of nuclear DNA fragmentation*. *J Cell Biol* 119, 493-501.
19. Schena, M., Shalon, D., Davis, R.W., and Brown, P.O. (1995). *Quantitative monitoring of gene expression patterns with a complementary DNA microarray*. *Science* 270, 467-470.
20. Jakob, W., Sagasser, S., Dellaporta, S., Holland, P., Kuhn, K., and Schierwater, B. (2004). *The *Trox-2* Hox/ParaHox gene of Trichoplax (Placozoa) marks an epithelial boundary*. *Dev Genes Evol* 214, 170-175.
21. Galliot, B. (2012). *Hydra, a fruitful model system for 270 years*. *Int J Dev Biol* 56, 411-423.
22. Brenner, S. (2009). *In the beginning was the worm*. *Genetics* 182, 413-415.
23. Beckingham, K.M., Armstrong, J.D., Texada, M.J., Munjaal, R., and Baker, D.A. (2005). *Drosophila melanogaster—the model organism of choice for the complex biology of multi-cellular organisms*. *Gravit Space Biol Bull* 18, 17-29.

A Appendix

A.1 Inhibitors of the p53-Mdm2 interaction in the placozoon *Trichoplax adhaerens*

A

Day No	Nutlin-3 10 μ M						Roscovitine 20 μ M					
	Experiment No1	Experiment No2	Experiment No3	Experiment No4	Average	Standard Deviation	Experiment No1	Experiment No2	Experiment No3	Experiment No4	Average	Standard Deviation
1	22	20	20	20	20.5	0.8660254	25	23	21	20	22.25	1.92028644
2	14	20	22	21	19.25	3.1124749	27	23	25	21	24	2.23606798
3	17	25	22	18	20.5	3.20156212	29	6	22	22	19.75	8.43726852
4	14	23	20	22	19.75	3.49106001	26	4	9	17	14	8.3366666
5	14	18	12	13	14.25	2.27760839	21	0	8	16	11.25	7.98044485
6	13	1	0	10	6	5.61248608	17	0	6	10	8.25	6.17960355
7	11	0	0	4	3.75	4.49305019	20	6	6	3	9.66666667	7.40870359
8	3	0	0	3	2	1.41421356	15	6	0	0	7	6.164414
9	1	0	0	3	1.33333333	1.24721913	7	1	0	0	2.66666667	3.09120617
10	1	0	0	0	0.33333333	0.47140452	5	0	0	0	1.66666667	2.3570226

Day No	ASW						0.1% DMSO					
	Experiment No1	Experiment No2	Experiment No3	Experiment No4	Average	Standard Deviation	Experiment No1	Experiment No2	Experiment No3	Experiment No4	Average	Standard Deviation
1	25	24	21	20	22.5	2.06155281	24	26	22	20	23	2.23606798
2	24	24	24	23	23.75	0.4330127	25	26	23	23	24.25	1.29903811
3	27	27	25	24	25.75	1.29903811	26	28	24	24	25.5	1.6583124
4	29	27	26	31	28.25	1.92028644	28	28	23	26	26.25	2.04633819
5	28	28	29	31	29	1.22474487	32	31	27	26	29	2.54950976
6	26	28	30	30	28.5	1.6583124	32	31	28	28	29.75	1.78535711
7	28	29	29	35	30.6666667	3.09120617	33	29	29	24	28.6666667	3.68178701
8	31	30	37	32	32.6666667	3.09120617	34	29	27	30	2.94392029	
9	31	29	33	31	1.63299316		29	30	25	28	2.1602469	
10	32	31	40	34	34.3333333	4.02768199	31	30	25	28.6666667	2.62466929	

B

Day	ASW/ 10 μ M Nutlin-	DMSO/ 10 μ M Nutlin-	ASW+DMSO/ 10 μ M Nutlin-3	ASW/ 20 μ M Roscovitine	DMSO/ 20 μ M Roscovitine	ASW+DMSO/ 20 μ M Roscovitine
1	0.17231	0.12098	0.09785	0.88289	0.67484	0.72837
2	0.04779*	0.04246*	0.00495**	0.85549	0.875252	1
3	0.03896*	0.05316	0.00623**	0.26917	0.29078	0.11176
4	0.01015*	0.03191*	0.00207**	0.02787*	0.04834*	0.00327**
5	6.207E-05***	0.0003***	1.026E-06***	0.00889**	0.01046*	0.0003***
6	0.00055***	0.00043***	2.184E-06***	0.00154***	0.00116**	1.123E-05***
7	0.00273**	0.00462**	0.0001***	0.02084*	0.03144*	0.0019**
8	0.00022***	0.00027***	3.719E-06***	0.00624**	0.0089**	0.00025***
9	0.00038***	0.00011***	2.2308E-05***	0.00091***	0.00069***	5.461E-05***
10	0.00029***	0.00011***	1.344E-05***	0.00058***	0.00041***	2.782E-05***

Table A.1.1: Raw data on animal population size after inhibitor treatment.

Animals were treated with Nutlin-3 (10 μ M) and Roscovitine (20 μ M) in four independent experiments and were counted daily (A). Statistical analyses (B) were performed with a two-tailed T-test. P-values are indicated and significances are highlighted with asterisks: p < 0.05 *, p < 0.01 **, p < 0.001 ***.

A.1 Inhibitors of the p53-Mdm2 interaction in the placozoon *Trichoplax adhaerens*

A

A

	Day1				Day2			
	0.1% DMSO	ASW	Nutlin-3 10µM	Roscovetine 20µM	0.1% DMSO	ASW	Nutlin-3 10µM	Roscovetine 20µM
No. samples	81	98	72	84	91	90	75	56
Average	16.3231728	13.7761429	12.06779167	9.568	14.6341319	12.0524348	10.14993333	5.761089286
Standard deviation	8.15255916	7.4704374	5.948545922	4.914228378	6.91200371	7.46855523	5.27872515	3.639351783
Minimum	2.933	0.213	0.19	0.494	0.628	0.948	2.643	0.166
Median	15.518	12.695	10.9105	8.6435	14.792	11.35	8.307	5.6925
Maximum	45.844	39.57	33.573	24.908	37.676	48.561	26.874	16.846
lower Quartile	10.641	8.09075	8.04875	6.02475	8.9505	7.0025	6.481	2.418
upper Quartile	21.617	18.57425	15.12875	12.493	18.8835	14.92675	13.277	8.15875
	Day3				Day4			
	0.1% DMSO	ASW	Nutlin-3 10µM	Roscovetine 20µM	0.1% DMSO	ASW	Nutlin-3 10µM	Roscovetine 20µM
No. samples	96	80	73	51	93	90	46	44
Average	12.0277188	9.5746375	6.551013699	4.400431373	9.33095745	8.19874725	4.317553191	3.945688889
Standard deviation	6.4992532	5.13002725	2.807819622	2.756764097	4.78004903	5.81595977	2.11697346	2.560011891
Minimum	0.488	0.334	0.007	0.387	0.404	0.256	0.377	0
Median	11.738	8.601	6.28	3.893	8.962	7.417	4.167	4.017
Maximum	33.438	25.495	16.235	10.702	29.138	34.888	9.42	8.991
lower Quartile	7.15475	6.2335	4.631	2.584	6.33975	5.1565	2.723	1.856
upper Quartile	15.98825	12.65625	8.02	5.9805	11.7985	9.643	5.6515	5.235
	Day5				Day6			
	0.1% DMSO	ASW	Nutlin-3 10µM	Roscovetine 20µM	0.1% DMSO	ASW	Nutlin-3 10µM	Roscovetine 20µM
No. samples	108	96	15	39	65	66	15	24
Average	7.41075229	7.62501042	3.907	3.114525	7.49198462	7.76989394	3.531058824	2.016625
Standard deviation	4.54853908	6.40020231	2.421557671	2.180252187	4.80115835	5.39581514	1.814386996	1.543898281
Minimum	0.156	0.281	0	0	0.572	0.189	0	0.185
Median	7.259	6.5825	3.429	2.837	7.042	6.975	3.003	1.744
Maximum	22.058	43.341	8.507	7.729	25.17	31.329	6.936	5.809
lower Quartile	4.36	4.1705	2.85625	1.24125	4.722	4.098	2.719	0.57675
upper Quartile	10.294	8.34725	5.30925	4.6855	9.991	10.0145	4.654	3.001
	Day7				Day8			
	0.1% DMSO	ASW	Nutlin-3 10µM	Roscovetine 20µM	0.1% DMSO	ASW	Nutlin-3 10µM	Roscovetine 20µM
No. samples	59	57	9	23	58	59	7	14
Average	7.72226667	8.34837097	3.0332	1.924	7.19842857	8.2246	1.918571429	1.870133333
Standard deviation	4.12965629	6.09125725	1.79001714	1.271002754	4.6059325	6.34178848	1.062105168	1.034304395
Minimum	0.289	0.517	0	0	0.935	0.481	0	0
Median	7.379	6.7785	2.805	1.9785	5.938	6.738	1.706	2.135
Maximum	18.114	33.754	7.42	4.561	22.502	34.516	3.634	4.271
lower Quartile	4.67875	4.72575	2.23025	0.89775	4.29	4.5965	1.551	1.3145
upper Quartile	10.279	10.6845	3.58175	2.82625	9.846	10.07475	2.494	2.3405
	Day9				Day10			
	0.1% DMSO	ASW	Nutlin-3 10µM	Roscovetine 20µM	0.1% DMSO	ASW	Nutlin-3 10µM	Roscovetine 20µM
No. samples	22	36	1	8	18	21	1	5
Average	6.83636364	6.24330556	0.962	1.239666667	8.58210526	5.29486364	1.821	0.7828
Standard deviation	3.22902019	3.50347845	0.962	0.530476725	3.42996263	2.09572544	0	0.496386704
Minimum	0.488	0.395	0	0	2.295	1.486	1.821	0.256
Median	6.907	5.866	0.962	1.401	8.764	5.3355	1.821	0.58
Maximum	11.674	16.974	1.924	1.877	12.978	9.74	1.821	1.502
lower Quartile	4.629	3.93275	0.481	1.006	6.0125	3.8295	1.821	0.343
upper Quartile	9.623	8.07325	1.443	1.42	11.6605	6.48425	1.821	1.233

A.1 Inhibitors of the p53-Mdm2 interaction in the placozoon *Trichoplax adhaerens*

A

B

Day	ASW/ 10 μ M Nutlin-3	DMSO/ 10 μ M Nutlin-3	ASW+DMSO/ 10 μ M Nutlin-3	ASW/ 20 μ M Roscovitine	DMSO/ 20 μ M Roscovitine	ASW+DMSO/ 20 μ M Roscovitine
1	0.11298	0.00039***	0.00612**	1.969E-05***	1.332E-09***	3.127E-08***
2	0.06632	8.802E-06***	0.00075***	3.07E-08***	3.345E-15***	1.81E-12***
3	1.775E-05***	3.092E-10***	1.284E-08***	1.133E-09***	4.743E-13***	2.067E-12***
4	6.695E-08***	2.661E-10***	3.128E-07***	8.644E-11***	7.807E-06***	6.607E-08***
5	0.01755*	0.00192**	0.00651**	3.003E-05***	6.399E-08***	1.301E-06***
6	0.00226**	0.00145**	0.00139**	2.013E-06***	5.225E-07***	3.918E-07***
7	0.00864**	0.00087***	0.00333**	2.394E-06***	2.768E-09***	7.974E-08***
8	0.02732*	0.01253*	0.01902*	0.00063***	0.00011***	0.00024***
9	0.23855	0.16082	0.19604	0.00043***	0.0001***	0.0001***
10	0.12816	0.07783	0.1401	0.0001***	7.494E-05***	0.00019***

Table A.1.2: Raw data of animal sizes after inhibitor treatment.

After treatment with Nutlin-3 (10 μ M) and Roscovitine (20 μ M) as well as 0.1 % DMSO and ASW only (negative controls) the body sizes of animals were measured daily (indicated in mm², A). A two-tailed T-test was performed and p-values are stated in (B). Significances are highlighted with asterisks: p < 0.05 *, p < 0.01 **, p < 0.001 ***.

A.1 Inhibitors of the p53-Mdm2 interaction in the placozoon *Trichoplax adhaerens*

A

A

Day of experiment	Experiment I				Experiment II			
	10µM Nutlin-3		20µM Roscovitine		10µM Nutlin-3		20µM Roscovitine	
	No. animals monitored	No. abnormal phenotypes	No. animals monitored	No. abnormal phenotypes	No. animals monitored	No. abnormal phenotypes	No. animals monitored	No. abnormal phenotypes
1	21	0	30	9	22	3	25	0
2	29	1	7	0	23	5	21	10
3	26	7	5	0	20	6	13	8
4	18	2			12	0	9	7
5							7	5
6							7	2
Day of experiment	Experiment III				Experiment IV			
	10µM Nutlin-3		20µM Roscovitine		10µM Nutlin-3		20µM Roscovitine	
	No. animals monitored	No. abnormal phenotypes	No. animals monitored	No. abnormal phenotypes	No. animals monitored	No. abnormal phenotypes	No. animals monitored	No. abnormal phenotypes
1	20	0	16	0		0	20	0
2	16	2	14	2	8	0	19	0
3	14	2	16	1	10	0	17	0
4	10	1	16	0	7	0	19	0
5	5	0	10	1	13	0	15	0
6	4	0	6	0	13	0	11	0
7	2	0			7	0	14	0
8	3	0			3	0	13	0
9					1	0	8	0
10					1	0	5	0

B

Day	Nutlin 10µM	Roscovitine 20µM
1	0.57339	0.55026
2	0.38187	0.48107
3	0.52287	0.61148
4	0.60167	0.71799
5	0.85997	0.75337
6	1	1
7	1	1
8	1	1
9	1	1

Table A.1.3: Data on presence of abnormal *Trichoplax* phenotypes after inhibitor treatment.

Data indicate the number of monitored individuals and the amount of *Trichoplax* individuals with divergent phenotypic characteristics in four independent experiments (A). Statistical revision of data with a two-tailed T-test however did not reveal any significances (B, $p > 0.05$).

A.1 Inhibitors of the p53-Mdm2 interaction in the placozoon *Trichoplax adhaerens*

A

A

0,1% DMSO in ASW (48h)					10µM Nutlin-3 in ASW (48h)					20µM Roscovitine in ASW (48h)				
Name	Nuclei	TUNEL Signal	Quotient	Percentage	Name	Nuclei	TUNEL Signal	Quotient	Percentage	Name	Nuclei	TUNEL Sinal	Quotient	Percentage
Tier1a	291	3	0.01030928	1	Tier1a	329	16	0.04863222	4.9	Tier1a	286	4	0.01398601	1.4
Tier1b	677	5	0.00738552	0.7	Tier1b	313	9	0.02875399	2.9	Tier1b	302	6	0.01986755	2
Tier1c	626	2	0.00319489	0.3	Tier1c	472	5	0.01059322	1.1	Tier2a	289	20	0.06920415	6.9
Tier2a	647	2	0.00309119	0.3	Tier2a	432	20	0.0462963	4.6	Tier2b	377	11	0.02917772	2.9
Tier2b	716	6	0.00837989	0.8	Tier2b	368	38	0.10326087	10	Tier2c	357	11	0.03081232	3.1
Tier2c	793	3	0.0037831	0.3	Tier2c	463	15	0.03239741	3.2	Tier3a	497	9	0.01810865	1.8
Tier3b	659	3	0.00455235	0.4	Tier3a	468	15	0.03205128	3.2	Tier3b	438	8	0.01826484	1.8
Tier3c	471	2	0.00424628	0.4	Tier3b	400	18	0.045	4.5	Tier3c	410	7	0.01707317	1.7
Tier4a	487	6	0.01232033	0.1	Tier3c	264	20	0.07575758	7.6	Tier4a	521	7	0.0134357	1.3
Tier4b	654	4	0.00611621	0.6	Tier4a	336	14	0.04166667	4.2	Tier4b	343	7	0.02040816	2
Tier5a	653	1	0.00153139	0.2	Tier4b	307	18	0.05863192	5.9	Tier6a	231	3	0.01298701	1.3
Tier5b	357	2	0.00560224	0.6	Tier4c	443	14	0.03160271	3.1	Tier6b	233	4	0.01716738	1.7
Tier5c	440	2	0.00454545	0.5	Tier5a	415	3	0.00722892	0.7					
Tier6a	301	1	0.00332226	0.3	Tier5b	282	9	0.03191489	3.2					
Tier6b	574	5	0.0087108	0.9	Tier5c	402	18	0.04477612	4.5					
Tier7a	625	1	0.0016	0.2	Tier6a	553	16	0.02893309	2.9					
Tier7b	916	1	0.0010917	0.1	Tier6b	348	13	0.03735632	3.7					
					Tier6c	138	9	0.06521739	6.3					
Average	581.588235	2.882352941	0.00528135	0.452941176	Average	374.055556	15	0.04278172	4.25	Average	357	8.083333333	0.02337439	2.325
Stdev	165.041905	1.67621257	0.00310561	0.265944813	Stdev	93.7843106	7.325753659	0.02203605	2.14715574	Stdev	91.471307	4.348531042	0.01482495	1.48218589
Minimum	291	1	0.0010917	0.1	Minimum	138	3	0.00722892	0.7	Minimum	231	3	0.01298701	1.3
Median	626	2	0.00454545	0.4	Median	384	15	0.03951149	3.95	Median	350	7	0.01818675	1.8
Maximum	916	6	0.01232033	1	Maximum	553	38	0.10326087	10	Maximum	521	20	0.06920415	6.9
upper Quartile	659	4	0.00738552	0.6	upper Quartile	440.25	18	0.04804824	4.825	upper Quartile	417	9.5	0.02260055	2.225
lower Quartile	471	2	0.00319489	0.3	lower Quartile	317	10	0.03168076	3.125	lower Quartile	288.25	5.5	0.01630138	1.625

B

0,1% DMSO in ASW (48h)					10µM Nutlin-3 in ASW (48h)					20µM Roscovitine in ASW (48h)				
Name	Nuclei	BrdU signal	Quotient	Percentage	Name	Nuclei	BrdU signal	Quotient	Percentage	Name	Nuclei	BrdU signal	Quotient	Percentage
Tier1a	815	64	0.07852761	8	Tier1a	396	8	0.02020202	2	Tier2a	903	115	0.12735327	13
Tier1b	685	316	0.46131387	46	Tier1b	612	45	0.07352941	7	Tier2b	604	151	0.25	25
Tier2a	764	212	0.27748691	28	Tier2a	405	125	0.30864198	31	Tier2c	815	205	0.25153374	25
Tier2b	799	286	0.35794743	36	Tier2b	542	148	0.27306273	27	Tier1a	625	67	0.1072	11
Tier3a	672	120	0.17857143	18	Tier3a	427	51	0.11943794	12	Tier1b	815	97	0.1190184	12
Tier3b	814	53	0.06511057	7	Tier3b	280	8	0.02857143	3	Tier1c	647	50	0.07727975	8
Tier4a	952	181	0.19012605	19	Tier4a	555	37	0.06666667	6	Tier3a	405	18	0.04444444	4
Tier4b	949	209	0.22023182	22	Tier4b	607	27	0.04448105	5	Tier3b	629	4	0.0063593	1
Tier5a	879	337	0.38339022	38	Tier5a	765	306	0.4	40	Tier4a	682	157	0.23020528	23
Tier5b	827	288	0.34824667	35	Tier5b	701	302	0.43081312	43	Tier4b	721	118	0.16366158	16
Tier6a	694	100	0.14409222	14	Tier6a	741	57	0.07692308	8	Tier5a	360	50	0.13888889	14
Tier6b	650	170	0.26153846	26	Tier7a	815	13	0.01595092	2	Tier6a	582	109	0.18728522	19
Tier7a	732	103	0.14071038	14	Tier7b	473	17	0.0359408	4					
Average	787.0769231	187.615385	0.23902259	23.92307692	Average	563	88	0.14570932	14.6153846	Average	649	95.08333333	0.14193582	14.25
Stdev	95.99315804	93.13806	0.11747154	11.68471413	Stdev	156.749678	100.86396	0.14523196	14.4463914	Stdev	151.781641	57.1933247	0.0752935	7.47356452
Minimum	650	53	0.06511057	7	Minimum	280	8	0.01595092	2	Minimum	360	4	0.0063593	1
Median	799	181	0.22023182	22	Median	555	45	0.07352941	7	Median	638	103	0.13312108	13.5
Maximum	952	337	0.46131387	46	Maximum	815	306	0.43081312	43	Maximum	903	205	0.25153374	25
upper Quartile	827	286	0.34824667	35	upper Quartile	701	125	0.27306273	27	upper Quartile	744.5	126.25	0.19801524	20
lower Quartile	694	103	0.14409222	14	lower Quartile	427	17	0.0359408	4	lower Quartile	598.5	50	0.09971994	10.25

C

Method	Nutlin 10µM / DMSO	Roscovitine 20µM DMSO
BrdU (48h)	0.09551	0.02811*
TUNEL (48h)	4.834E-08***	3.837E-05***

Table A.1.4: Raw data on BrdU and TUNEL staining after inhibitor treatment.

After 48 h of treatment with Nutlin-3 (10µM) and Roscovitine (20µM), animals were monitored for apoptosis (A, TUNEL) and cell proliferation (B, BrdU). Statistical analyses were performed with a two-tailed T-test and significances are indicated with asterisks (p < 0.05 *, p < 0.001 ***).

A.2 The Myc/Max network at the base of the metazoan tree of life

A

<p>1 <i>taMyc</i> CDS (NCBI accession number XM_002113921) + 5' end 5'- GAAAAATACTGTGAGAATTAATAATAGCAGCTGCAGCTATAAAAGCAGCGCATTATTTACGTCITTCATTGG AATAAAATCCTGAGCAACGAACTTTCA(ATG)CTGAAATCGCCTTCAAATCGATCTATCAAG (ATG) GCA GTT CAT GCG GAA GCC TTT TCA AAT AAG TTA GAT TTT GAG CCT TAC GGC TCT TAC TAC ATG GGT GAA GAT AGT GAA GAT GAT AAC ATA TGG AGT TGT CTT GAC ATC ATG CCA ACT CCA CCA TTG TCA CCG GCT CGC CAG CAA TAC ATA ACT GAT ACT TCA TCA AAT TAT CTC GCT GAC AAA TTG TTG CAA GTA ACC GAA AAT TTA GAT TTC GAC AAT GCC TTG ATT GAC ATG GTA GGG GAT ACC AAT AGT ATT TTC AAT GGT GGT TCG AAA CTT CGA <u>TCC/T</u> AGC <u>TCTA</u> ATC CAG GAT TGC ATG TGG AAT GCT GGC ATT TGT GAA ACC GAC AAG AAG AAT TTG GTT AAC ACG AAC GTT AGT GCT TTT GAT ACG CCT TGT GCA ACG CCA CCG CGA GCA GAA GAG TTT ATT TCG ACT AGT GAC TGT GTC GAT CCC ATC GCT GTA TTT CCT TAC ACT CTT AGC GAT CAA GGA <u>CAA/G</u> CAA CAA TTT GTA GAA GCT CAG TCC GAT TCA GAA GAG GAA ATT GAT GTA GTA ACA GTA GAA AAA CCG AAT AAA CGA AAG CTA AGT TCC ATT GAA TTA CCT CAG CAG CAC AAA GTG ACC GAA GAT TTA CAA AGC CCT ACG AAA CGT GCG AAA TCT CCG CAA ATA AGT ACC AAA GGC AAA GAA GCT TGT AGC CCG AAG GGA GGG TTA TCC GTA AAG CCG GAT ATT GAT AAT GAT GTT AAA CGT GCA ACT CAT AAT GTT TTA GAG AGG AAG AGA CGC AAT GAT CTG AGG TAT AGT TTC CAG ACG CTC CGT GAT CAA ATA CCG GAC TTG GAA GAT AAC GAA CGT GCA CCG AAA GTT AAC ATT TTA AAG AAG TCA ACA GAG TAC ATC AAG TTC TTG AAA GAG GAG GAG AGT AAG CTA ATC TCG ATG AAA GAA ACG GAA AGA GAA AGA AGG AAA GCT CTC TTG GCC AAA ATC GAC ATT TTA AAG AGC AAA AGA AAT (TAG)- 3'</p> <p>2 <i>taMyc</i> Protein (NCBI accession number XP_002113957) MAVHAEAFSNKLDPEFYGSYYMGEDSEDDNIW\$CLDIMPTPLSPARQQYITDTSNNYLADKLLQVTENLDFDNA LIDMVGDTNSIFNGGSKLR\$SLIQDCMWNAGICETDKKNLVNTNVS\$AFDTPCATPPRAEEFISTSDCV\$PIAVFPYT LSDQGGQQVFVEAQSDSEEEIDVVVEKPNKRKLS\$IELPQHKVTELDQ\$PTKRAKSPQISTK\$GKEACSPKGGLSV KPDIDNDVKRATHNVLERKRRN\$DLRY\$FQTLRDQIPDLEDNERAPKVNILKSTHEYIKFLKEESKLSMKETERE RRKALLAKIDILKSKRN*</p>
<p>3 <i>taMax</i> CDS (NCBI accession number XM_002107825) + 5'end 5'- GAAAAATCGTGGGACTAGCTGAACGCTGAGTATTATAATTCTTCCCTTCCCGGATAGAAAGCTCGAAAATA AAAACGTTTTAGTCTACGCTGTGATTAGTGAACCACTGTGCTGGAGATTGGACAAGTTAACAATTTGGCCTTC ATAC (ATG) AGT GAC GAA GAT AAG TAC TTG GAC GTC GAT ATT GAC AGT GAT GAC AAT GGA GAT ACT GAT AAG TCA ACA TCC GGT CTA ACT CAA GCG GAT AAA AGA GCC CAT CAT AAC GCT TTG GAG CGT AAG AGG <u>CGT/C</u> GAT CAC ATT AAA GAT TGT TTC TTT GGC TTA CGC GAT TCA GTT CCT ACC TTA CAA GGA GAA AAG GCT TCA CGT GCT CAA ATA CTG AAT AAG GCA ACT GAT TAC ATT CAG TTT ATG AAA CAA AAA AAT CAG AAT CAT CAG TCA GAT ATA GAA GAT ATC AGG AAA GAG AAT TAT CAG TTA GAA TTA CAA TTG AAA ACC TTA GAG AGG ACG CGC AAT AAT TTA ACT GGT ACG GCG ACA TCT GAG AAT ATC GAT AGT TCA ACT ACG ACT ACT ACC AAT AGT GGT AGA ACA ACA AGG AAT AAA GCC AAA CGA GAA TTG CAA TCG GAC GGT AAC GAT GAA CAA AAG ACA GAT ACT AAA AAG GTC AAA GCA GAG (TAG)-3'</p> <p>4 <i>ta Max</i> Protein (NCBI accession number XP_002107861) MSDEDKYLDV\$DSD\$DNGD\$TDK\$T\$SGLTQADKRAHHNALERKRRDHKDCFFGLRDSVPTLQGEKASRAQILNK ATDYIQFMKQKNQNHQSDIEDIRKENYQLELQLKTLERTRNNLTGATSENIDSSTTTTTNSGRITRNRKAKRELQS DGND\$QKTDTKKVKAE*</p>

B

	JGI scaffold numbers(http://genome.jgi-psf.org/Triad1/Triad1.home.html)	
	<i>taMyc</i>	<i>taMax</i>
sequenced (5' End)	scaffold 7: 1.295.083-1.300.412	scaffold 1: 4.863.546-4.866.680
predicted (JGI)	scaffold 7: 1.299.399-1.300.412	scaffold 1: 4.864.128-4.866.680
transcriptome (unpublished data)	scaffold 7: 1.298.394-1.201.082	scaffold 1: 4.863.508-4.867.705

Table A.2.1: *taMyc*, *taMax* sequence information.

(A) Information on the *tamyc* (A1, 2) and *tamax* (A3, 4) cDNA- and protein sequences were taken from NCBI¹. The sequenced 5' end is written in red, fragments used for RNA *in situ* probes in green. Sequences used for morpholino oligonucleotide manufacture are printed in bold. Start and stop codons of cDNA were put into brackets. Alternative nucleotide compositions are underlined. Asterisks indicate stop codons of the protein sequences.

(B) Localization of *tamyc* and *tamax* genomic scaffolds. The 5' end sequenced in this study, the predicted open reading frame (taken from JGI² and NCBI) and unpublished transcriptome data of the whole fragments.

¹<http://www.ncbi.nlm.nih.gov>, ²<http://genome.jgi-psf.org/Triad1/Triad1.home.html>

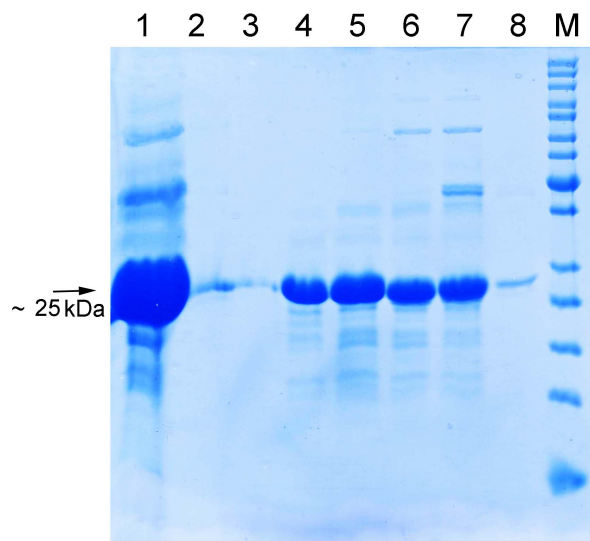


Figure A.2.1: Gel filtration of the taMax-containing ÄKTA- fraction.

Before gel filtration (1), fraction A7 (2), A11 (3), A15 (4), B15 (5), B14 (6), B13 (7), B11 (8), marker (M). The taMax protein can be found at a size of 25 kDa. Impurities of the protein are still visible after gel purification.

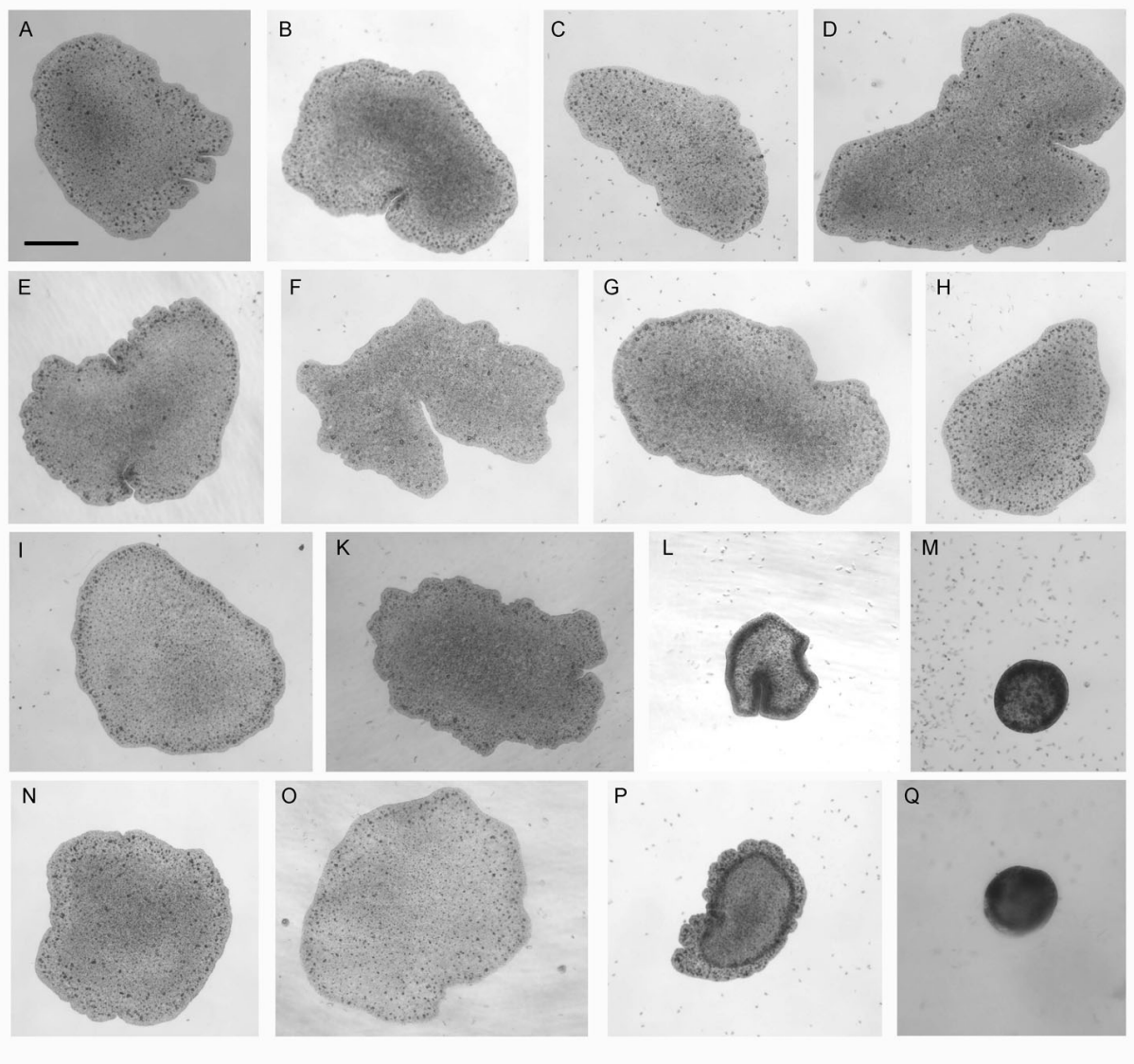


Figure A.2.2: Light microscopy of knockdown individuals.

ASW control (A - D), *Cnox-2* control (E - H), *tamyc* KD (I - M) and *tamax* KD (N - Q) Pictures were taken after one day (A, E, I, N), three days (B, F, K, O), five days (C, G, L, P) and seven days (D, H, M, Q). The size bar in (A) marks 100 μm and is representative for every picture.

Day	taMyc				taMax			
	Experiment No1	Experiment No2	Experiment No3	Standard Deviation	Experiment No1	Experiment No2	Experiment No3	Standard Deviation
0	25	25	25	0	25	25	25	0
1	24	17	25	3.559026084	23	22	25	1.247219129
2	26	17	20	3.741657387	23	22	19	1.699673171
3	28	22	16	4.898979486	25	25	18	3.299831646
4	23	23	18	20.5	27	25	23	2
5	1	19	18	12.6666667	13	23	20	4.18993503
6	1	19	17	12.3333333	1	21	19	8.993825042
7	0	17	21	12.6666667	0	8	17	6.944222219
8	0	16	19	17.5	0	0	16	8
9	0	14	16	15	0	0	11	5.5
10	0	1	7	4	0	0	4	2
11	0	0	0	0	0	0	0	0

Day	ASW				Crox-2			
	Experiment No1	Experiment No2	Experiment No3	Standard Deviation	Experiment No1	Experiment No2	Experiment No3	Standard Deviation
0	25	25	25	0	25	25	25	0
1	24	23	25	0.816496581	25	25	25	0
2	22	21	20	0.816496581	26	23	33	4.18993503
3	25	22	20	2.054804668	31	23	34	4.642796092
4	28	24	25	26.5	29	25	34	31.5
5	28	24	26	1.632993162	27	23	32	2.943920289
6	26	22	27	2.160246899	34	23	33	4.966554809
7		23	26	1.5		24	32	28
8		22	25	23.5		21	35	28
9		27	26	26.5		24	33	28.5
10		30	20	5		25	29	2
11		27	18	22.5		24	28	2

A.2 The Myc/Max network at the base of the metazoan tree of life

A

B

Day No	<i>taMyc</i> /ASW	<i>taMyc</i> /Cnox-2	<i>taMyc</i> /Cnox-2+ASW	<i>taMax</i> /ASW	<i>taMax</i> /Cnox-2	<i>taMax</i> /Cnox-2+ASW
1	0.48182	0.29912	0.18979	0.56144	0.13178	0.17047
2	1	0.189	0.3776	0.8149	0.14428	0.37757
3	0.93356	0.30694	0.44904	0.062396	0.1338	0.25485
4	0.07766	0.05797	0.03784*	0.74152	0.23806	0.3607
5	0.08866	0.06873	0.01101*	0.08237	0.06148	0.01427*
6	0.09821	0.05757	0.01567*	0.15816	0.08781	0.03075*
7	0.15881	0.18182	0.09035	0.12354	0.12713	0.02827*
8	0.04216*	0.20738	0.09034	0.19717	0.20064	0.06077
9	0.00932**	0.0995	0.01358*	0.03553*	0.26675	0.03178*
10	0.06919	0.0237*	0.00474**	0.24901	0.09517	0.02274*
11	0.03775*	0.00587**	0.00199**	0.03775*	0.00587**	0.00199**

Table A.2.2: Raw data of animal population sizes after "knockdown".

Given are numbers of individuals counted up to 11 days after initial knockdown experiment in three independent experiments (A). Averages and standard deviations were used for graphical representation. Statistical analyses have been performed with a two-tailed t-test (B). Significances are indicated with asterisks: $p < 0.05$ *, $p < 0.01$ **.

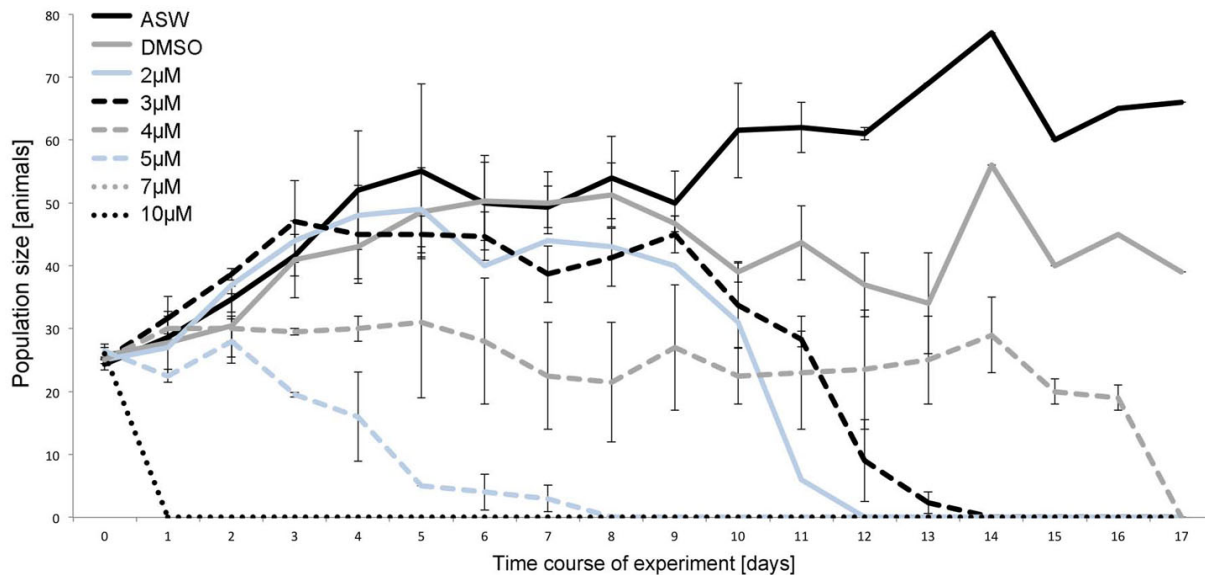


Figure A.2.3: Animal population size after treatment with the 10058-F4 inhibitor.

Shown is the time course of animal population after treatment with different concentrations of the 10058-F4 inhibitor.

A.2 The Myc/Max network at the base of the metazoan tree of life

A

A

	Day1				Day2			
	Myc	Max	Cnox	ASW	Myc	Max	Cnox	ASW
Number of Values	43	48	44	58	41	42	55	49
Average	12.9471163	14.8664583	12.8356818	12.3298966	14.1549268	11.216	11.3899455	12.7541837
Standard Deviation	5.56390223	7.17011353	6.12819308	5.02612966	8.34008814	7.20842514	6.84748594	7.37944966
Standard Error	5.50031269	7.09657196	6.0597195	4.98335331	8.24020324	7.12411318	6.78607227	7.30528245
Median	11.755	12.107	11.2875	10.9	15.376	10.957	10.632	10.907
Minimum	5.24	6.019	1.881	2.802	0.189	0.267	2.104	0.743
Maximum	28.049	37.283	25.829	30.351	33.388	27.317	33.171	35.025
lower Quartile	9.368	9.99925	8.30875	9.35075	7.794	4.83225	6.7355	8.451
upper Quartile	13.81	18.60875	16.464	15.0865	19.094	15.77725	14.646	15.124
	Day3				Day4			
	Myc	Max	Cnox	ASW	Myc	Max	Cnox	ASW
Number of Values	52	43	61	44	35	34	47	40
Average	10.0159057	7.22154545	10.6433548	11.4222667	8.11405556	5.39054286	8.72289583	11.8286585
Standard Deviation	6.91256475	5.28812562	5.19615809	6.0687954	5.13261773	2.97949242	4.4757188	6.56694691
Standard Error	6.84826042	5.22903856	5.15475378	6.00246778	5.06278294	2.93781915	4.42981278	6.488298
Median	10.845	7.2105	9.944	10.329	7.818	4.716	8.008	10.642
Minimum	0.303	0.191	1.743	0.207	0.285	0.186	1.675	0.562
Maximum	24.87	18.679	27.032	29.38	22.181	11.182	22.035	30.359
lower Quartile	3.046	1.9595	6.70375	8.545	4.53775	3.077	5.35325	7.543
upper Quartile	13.421	11.88875	14.49325	15.024	12.05875	8.137	11.6635	15.477
	Day5				Day6			
	Myc	Max	Cnox	ASW	Myc	Max	Cnox	ASW
Number of Values	53	41	66	62	34	31	61	58
Average	7.12454717	2.94234146	9.03322727	9.56404918	6.25482353	1.89493548	7.29334426	9.17827586
Standard Deviation	6.70280694	1.75560426	3.99693365	4.63937699	4.8382983	0.92213686	4.224631	6.16370385
Standard Error	6.6404539	1.7345783	3.96699365	4.60240925	4.76867887	0.90761411	4.19042289	6.11124584
Median	4.551	2.578	8.743	8.0815	5.2935	1.752	7.141	7.912
Minimum	0.457	0.427	1.249	2.782	0.852	0.385	0.586	0.183
Maximum	28.441	9.07	18.247	20.126	23.9	4.847	18.476	33.033
lower Quartile	1.797	2.08	6.423	6.169	3.2965	1.2935	4.45	4.892
upper Quartile	10.966	3.349	11.801	12.83575	6.76325	2.394	8.913	12.20025
	Day7				Day8			
	Myc	Max	Cnox	ASW	Myc	Max	Cnox	ASW
Number of Values	34	13	66	49	24	13	39	19
Average	5.19574286	1.99	7.17770149	9.63737255	4.86856	0.91692857	6.70685	5.5622381
Standard Deviation	4.37105819	1.29035062	4.8923606	5.74334024	5.17099081	0.4331223	4.07483979	3.30816966
Standard Error	4.3099215	1.24659713	4.85625412	5.68784772	5.07057367	0.41843589	4.02483986	3.23210961
Median	4.39	1.5425	6.367	8.019	2.675	0.922	5.727	4.337
Minimum	0.319	0	0.336	2.595	0.867	0	1.172	0.817
Maximum	18.353	4.576	28.445	27.881	19.32	1.719	18.525	12.644
lower Quartile	2.0155	1.10925	3.9395	5.004	1.067	0.71425	3.5555	3.796
upper Quartile	6.552	2.90375	10.1095	13.2435	4.93	1.1455	9.083	8.469
	Day9				Day10			
	Myc	Max	Cnox	ASW	Myc	Max	Cnox	ASW
Number of Values	19	7	38	31	2	1	14	19
Average	4.5293	0.760625	6.36061538	6.16309375	1.7055	0	8.24006667	9.46385
Standard Deviation	3.69837162	0.35624007	3.97190031	3.54911986	1.2895	0	4.66946175	3.3494642
Standard Error	3.60924113	0.33586635	3.92193731	3.49493164	1.05287234	0	4.52118689	3.26874236
Median	3.1705	0.772	6.118	5.818	1.7055	0	8.029	8.633
Minimum	0.633	0	0.964	0.86	0.416	0	2.13	3.94
Maximum	11.7	1.23	20.868	12.7	2.995	0	15.76	15.994
lower Quartile	1.285	0.62075	3.797	3.16775	1.06075	0	3.946	7.27675
upper Quartile	7.14425	1.007	8.1805	7.9475	2.35025	0	11.5685	12.36725

A.2 The Myc/Max network at the base of the metazoan tree of life

A

B

Day No	<i>taMyc/Cnox-2</i>	<i>taMyc/ASW</i>	<i>taMyc/Cnox-2+ASW</i>	<i>taMax/Cnox-2</i>	<i>taMax/ASW</i>	<i>taMax/Cnox-2+ASW</i>
1	0.93031	0.56518	0.69477	0.15388	0.03691*	0.03279*
2	0.40565	0.08114	0.12955	0.90481	0.32445	0.5363
3	0.5836	0.29627	0.35274	0.00139**	0.0009***	0.00023***
4	0.56876	0.00851**	0.0688	0.0003***	1.255E-06***	9.486E-06***
5	0.05862	0.02772*	0.01195*	5.358E-06***	1.138E-13***	3.195E-06***
6	0.28386	0.02125*	0.05805	5.503E-10***	5.644E-09***	1.080E-09***
7	0.04893*	0.00025***	0.00292**	0.00021**	7.813E-06**	3.724E-05***
8	0.12196	0.6066	0.16458	3.327E-06***	1.489E-05***	2.181E-06***
9	0.09722	0.12552	0.0743	0.00032***	0.00016***	0.00012***
11	0.08417	0.00564**	0.0185*	0.12105	0.01457*	0.03761*
12	0.17554	0.03486*	0.07902	0.17554	0.03486*	0.07902

Table A.2.3: Raw data on animal sizes after "knockdown".

Size of individuals was measured daily. Values stem from three independent experiments and the animal sizes are indicated in mm^2 (A). Minimum, maximum, median, upper and lower quartile was used for boxplot depiction. Significances are indicated with asterisks: $p < 0.05$ *, $p < 0.01$ ** (B).

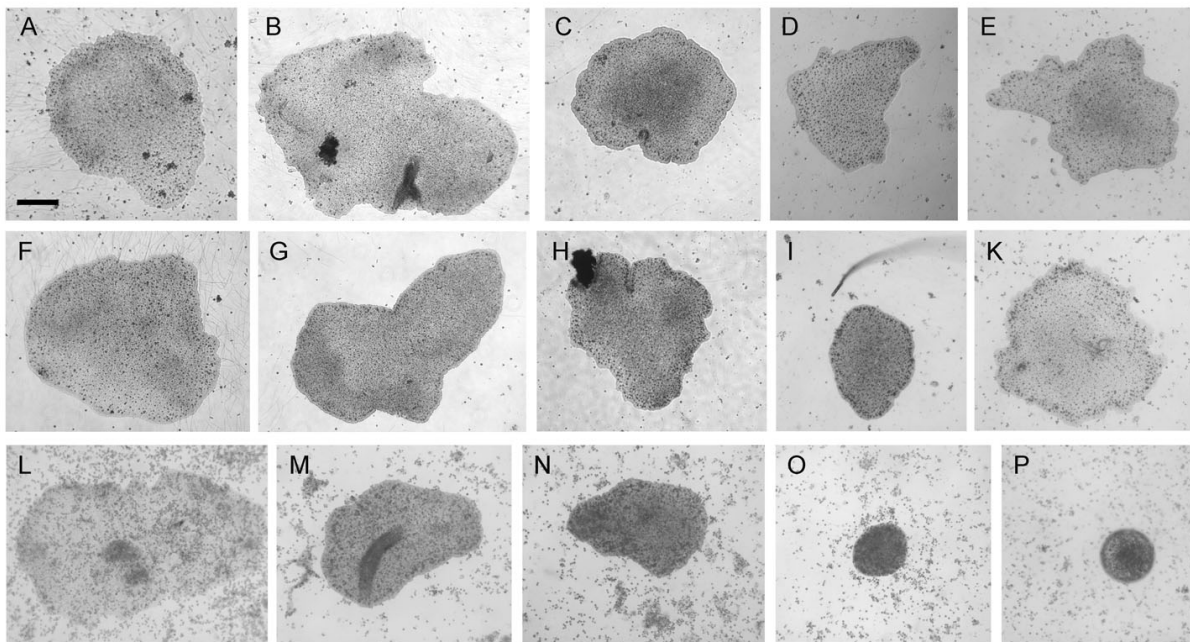


Figure A.2.4: Light microscopy of *Trichoplax* individuals after treatment with 10058-F4 inhibitor ($5 \mu\text{M}$). ASW control (A-E), 0.1 % DMSO (F-K) and $5 \mu\text{M}$ inhibitor 10058-F4 (L-P). Day 0 (A,F,L), day 2 (B,G,M), day 4 (C,H,N), day 6 (D,I,K) and day 7 (E,K,P). The bar marks $100 \mu\text{m}$ for all pictures.

A.2 The Myc/Max network at the base of the metazoan tree of life

A

A

Knock Down (ASW)					Knock Down (<i>Cnox-2</i>)				
Name	Nuclei	BrdU signal	Quotient	Percentage	Name	Nuclei	BrdU signal	Quotient	Percentage
Tier1a	663	184	0.2775264	28	Tier1a	346	263	0.76011561	76
Tier1c	407	192	0.47174447	47	Tier1b	194	86	0.44329897	44
Tier2b	678	317	0.46755162	47	Tier2a	390	259	0.66410256	66
Tier2c	680	455	0.66911765	67	Tier2b	830	303	0.36506024	37
Tier3a	613	369	0.60195759	60	Tier3a	657	227	0.34550989	35
Tier3b	506	223	0.44071146	44	Tier3b	878	216	0.24601367	25
Tier3c	460	219	0.47608696	48	Tier4a	895	192	0.21452514	21
Tier4a	575	172	0.29913043	30	Tier5a	614	221	0.35993485	36
Tier4b	801	286	0.35705368	36	Tier5b	539	113	0.2096475	21
Tier5a	746	166	0.22252011	22	Tier6a	559	132	0.23613596	24
Tier6b	566	239	0.42226148	42	Tier6b	492	363	0.73780488	74
Tier7a	693	266	0.38383838	38	Tier8a	730	172	0.23561644	24
Tier7b	553	165	0.29837251	30	Tier8b	555	156	0.28108108	28
Tier8a	553	181	0.32730561	33	Tier8c	502	370	0.73705179	74
Tier8b	601	203	0.33777038	34					
Tier9a	533	179	0.3358349	34					
Average	601.75	238.5	0.39929898	40	Average	584.357143	219.5	0.4168499	41.7857143
Stdev	101.030008	79.8506418	0.11544411	11.5108644	Stdev	195.717583	83.4965782	0.20584433	20.5432595
Minimum	407	165	0.22252011	22	Minimum	194	86	0.2096475	21
Median	801	455	0.66911765	67	Median	895	370	0.76011561	76
Max	588	211	0.37044603	37	Max	557	218.5	0.35272237	35.5
upper Quartile	678.5	271	0.46859983	47	upper Quartile	711.75	262	0.60890167	60.5
lower Quartile	548	180.5	0.32026181	32.25	lower Quartile	494.5	160	0.23860538	24.25
Knock Down (<i>taMyc</i>)					Knock Down (<i>taMax</i>)				
Name	Nuclei	BrdU signal	Quotient	Percentage	Name	Nuclei	BrdU signal	Quotient	Percentage
Tier1a	830	187	0.2253012	23	Tier1a	776	361	0.46520619	47
Tier1b	938	123	0.13113006	13	Tier1b	670	465	0.69402985	70
Tier2a	820	170	0.20731707	21	Tier1c	687	265	0.38573508	39
Tier2b	848	96	0.11320755	22	Tier2a	635	136	0.21417323	21
Tier3a	801	442	0.55181024	55	Tier2b	517	138	0.26692456	27
Tier3b	723	374	0.51728907	52	Tier2c	550	168	0.30545455	31
Tier5a	558	108	0.19354839	19	Tier3a	742	239	0.32210243	32
Tier5b	834	167	0.20023981	20	Tier3b	335	38	0.11343284	11
Tier6a	539	188	0.34879406	35	Tier4a	269	34	0.12639405	13
Tier6b	758	238	0.31398417	31	Tier4b	272	50	0.18382353	18
Tier7a	763	179	0.23460026	23	Tier4c	553	145	0.26220615	26
Tier7b	738	174	0.23577236	24	Tier5a	549	86	0.15664845	16
					Tier6a	501	229	0.45708583	46
					Tier7a	735	90	0.12244898	12
					Tier8a	491	205	0.41751527	42
Average	762.5	203.833333	0.27274952	28.1666667	Average	552.133333	176.6	0.2995454	30.0666667
Stdev	110.499246	99.4717995	0.13277586	12.5288556	Stdev	157.467824	117.736882	0.15690974	15.905834
Minimum	539	96	0.11320755	13	Minimum	269	34	0.11343284	11
Median	938	442	0.55181024	55	Median	776	465	0.69402985	70
Max	782	176.5	0.22995073	23	Max	550	145	0.26692456	27
upper Quartile	831	200.5	0.32268664	32	upper Quartile	678.5	234	0.40162518	40.5
lower Quartile	734.25	156	0.19856695	20.75	lower Quartile	496	88	0.17023599	17

A.2 The Myc/Max network at the base of the metazoan tree of life

A

B

Knock Down (ASW)					Knock Down (<i>Cnox-2</i>)				
Name	Nuclei	BrdU signal	Quotient	Percentage	Name	Nuclei	BrdU signal	Quotient	Percentage
Tier1a	676	42	0.06213018	6	Tier1a	375	47	0.12533333	13
Tier1b	229	27	0.11790393	12	Tier1b	599	55	0.0918197	9
Tier1c	600	61	0.10166667	10	Tier2a	772	218	0.28238342	28
Tier2a	339	48	0.14159292	14	Tier2b	778	334	0.42930591	43
Tier2b	382	40	0.10471204	10	Tier2c	419	109	0.2601432	26
Tier3a	654	210	0.32110092	32	Tier3a	393	74	0.18829517	19
Tier3b	794	193	0.24307305	24	Tier3b	825	311	0.3769697	38
Tier3c	734	192	0.26158038	26	Tier4a	671	196	0.29210134	29
Tier4a	454	66	0.14537445	15	Tier4b	747	82	0.10977242	11
Tier4b	519	64	0.12331407	12	Tier5a	488	50	0.10245902	10
Tier4c	387	49	0.12661499	13	Tier5b	695	62	0.08920863	9
Tier5a	532	64	0.12030075	12	Tier6a	538	38	0.07063197	7
Tier5b	485	87	0.17938144	18	Tier6b	533	55	0.10318949	10
Tier6a	634	63	0.09936909	10	Tier7a	623	167	0.26805778	27
Tier6b	620	50	0.08064516	8	Tier7b	578	130	0.22491349	22
Tier7a	661	61	0.09228442	9					
Tier8a	673	133	0.19762259	20					
Tier8b	434	49	0.11290323	11					
Average	544.833333	83.2777778	0.14619835	14.5555556	Average	602.266667	128.533333	0.20097231	20.0666667
Stdev	147.58171	55.9243592	0.06696254	6.71004407	Stdev	140.384456	93.5669932	0.10999338	11.0421415
Minimum	229	27	0.06213018	6	Minimum	375	38	0.07063197	7
Median	794	210	0.32110092	32	Median	825	334	0.42930591	43
Max	566	62	0.12180741	12	Max	599	82	0.18829517	19
upper Quartile	659.25	81.75	0.17087969	17.25	upper Quartile	721	181.5	0.2752206	27.5
lower Quartile	439	49	0.10242801	10	lower Quartile	510.5	55	0.10282425	10
Knock Down (<i>taMyc</i>)					Knock Down (<i>taMax</i>)				
Name	Nuclei	BrdU signal	Quotient	Percentage	Name	Nuclei	signal	Quotient	Percentage
Tier1a	317	117	0.36908517	37	Image1b	570	147	0.25789474	26
Tier1b	850	454	0.53411765	53	Image1_c	330	55	0.16666667	17
Tier1c	752	185	0.24601064	25	Image1	793	106	0.13366961	13
Tier2a	970	336	0.34639175	35	Tier2a	870	146	0.16781609	17
Tier2b	643	313	0.48678072	49	Tier3a	770	137	0.17792208	18
Tier2c	726	276	0.38016529	38	Tier3b	732	131	0.17896175	18
Tier3a	362	38	0.10497238	10	Tier3c	967	196	0.20268873	20
Tier3b	800	79	0.09875	10	Tier4a	840	250	0.29761905	30
Tier3c	797	99	0.12421581	12	Tier4b	639	190	0.29733959	30
Tier4a	825	180	0.21818182	22	Tier4c	665	190	0.28571429	29
Tier4b	633	112	0.17693523	18	Tier5a	1141	174	0.15249781	15
Tier4c	817	192	0.23500612	24	Tier5b	852	166	0.19483568	19
Tier5a	455	71	0.15604396	16	Tier5c	768	161	0.20963542	21
Tier5b	693	71	0.1024531	10	Tier6a	466	158	0.33905579	34
Tier5c	591	64	0.10829103	11	Tier6b	348	86	0.24712644	25
Tier6a	548	104	0.18978102	19	Tier6c	298	153	0.51342282	51
Tier6b	522	103	0.19731801	20	Tier7a	584	171	0.29280822	29
Tier7a	451	105	0.23281596	23	Tier7b	882	198	0.2244898	22
Tier7b	577	75	0.12998267	13					
Average	648.894737	156.526316	0.23354202	23.4210526	Average	695.277778	156.388889	0.24112025	24.1111111
Stdev	173.269457	109.330194	0.12776632	12.8034362	Stdev	223.82528	43.438512	0.08760128	8.76158845
Minimum	317	38	0.09875	10	Minimum	298	55	0.13366961	13
Median	970	454	0.53411765	53	Median	1141	250	0.51342282	51
Max	643	105	0.19731801	20	Max	750	159.5	0.21706261	21.5
upper Quartile	798.5	188.5	0.2962012	30	upper Quartile	849	186	0.29103474	29
lower Quartile	535	77	0.12709924	12.5	lower Quartile	573.5	139.25	0.178182	18

Table A.2.4: Raw data on BrdU signal after gene "knockdown".

Data on cell proliferation were collected 24 h (A) and 72 h (B) after initial KD. Values for minimum, median, maximum, upper and lower quartile were used for boxplot analyses.

A.2 The Myc/Max network at the base of the metazoan tree of life

A

Knock Down (ASW)					Knock Down (Cnox-2)				
Name	Nuclei	TUNEL signal	Quotient	Percentage	Name	Nuclei	TUNEL signal	Quotient	Percentage
Tier1	837	4	0.00477897	0.5	Tier1b	233	2	0.00858369	0.9
Tier1_b	592	4	0.00675676	0.7	Tier2	223	2	0.00896861	0.9
Tier2	572	4	0.00699301	0.7	Tier2b	493	2	0.0040568	0.4
Tier2b	591	5	0.00846024	0.8	Tier3b	512	4	0.0078125	0.8
Tier2c	750	3	0.004	0.4	Tier4	763	2	0.00262123	0.3
Tier3	772	3	0.00388601	0.4					
Tier3c	586	3	0.00511945	0.5					
Average	671.428571	3.714285714	0.00571349	0.571428571	Average	444.8	2.4	0.00640857	0.66
Stdev	102.583565	0.699854212	0.00159338	0.148461498	Stdev	201.06954	0.8	0.00257413	0.25768197
Minimum	572	3	0.00388601	0.4	Minimum	223	2	0.00262123	0.3
Median	837	5	0.00846024	0.8	Median	763	4	0.00896861	0.9
Max	592	4	0.00511945	0.5	Max	493	2	0.0078125	0.8
upper Quartile	761	4	0.00687488	0.7	upper Quartile	512	2	0.00858369	0.9
lower Quartile	588.5	3	0.00438949	0.45	lower Quartile	233	2	0.0040568	0.4
Knock Down (taMyc)					Knock Down (taMax)				
Name	Nuclei	TUNEL signal	Quotient	Percentage	Name	Nuclei	TUNEL signal	Quotient	Percentage
Tier1	524	13	0.02480916	2.5	Tier1	485	11	0.02268041	2.2
Tier1b	390	14	0.03589744	2.3	Tier1c	519	13	0.02504817	2.5
Tier1c	528	2	0.00378788	0.4	Tier2b	584	11	0.01883562	1.9
Tier2	306	4	0.0130719	1.3	Tier2c	520	6	0.01153846	1.1
Tier2b	719	9	0.01251739	1.3	Tier3	611	9	0.01472995	1.5
Tier3	441	15	0.03401361	3.4	Tier3b	915	8	0.00874317	0.8
Tier3b	346	7	0.02023121	2	Tier3c	709	9	0.01269394	1.3
Tier3c	835	4	0.00479042	0.5	Tier4	442	7	0.0158371	1.6
Tier4	499	4	0.00801603	0.8	Tier4b	628	10	0.01592357	1.6
Tier4b	283	5	0.01766784	1.7	Tier4c	517	14	0.0270793	2.7
Tier5	359	3	0.00835655	0.8	Tier5	545	10	0.01834862	1.8
Tier5b	424	5	0.01179245	1.1	Tier5b	475	12	0.02526316	2.5
Tier5c	752	5	0.00664894	0.6	Tier5c	375	12	0.032	3.2
Tier6	425	9	0.02117647	2.1	Tier6	440	10	0.02272727	2.2
Tier6b	503	5	0.00994036	0.9	Tier6b	466	2	0.00429185	0.5
Tier6c	596	8	0.01342282	1.3					
Tier7b	573	3	0.0052356	0.5					
Tier7c	353	13	0.0368272	3.7					
Average	492	7.111111111	0.01601129	1.511111111	Average	548.733333	9.6	0.01838271	1.82666667
Stdev	151.907501	4.039924214	0.01043841	0.95387449	Stdev	127.465795	2.916619047	0.00724307	0.71504468
Minimum	283	2	0.00378788	0.4	Minimum	375	2	0.00429185	0.5
Median	835	15	0.0368272	3.7	Median	915	14	0.032	3.2
Max	470	5	0.01279464	1.3	Max	519	10	0.01834862	1.8
upper Quartile	561.75	9	0.02094016	2.075	upper Quartile	597.5	11.5	0.02388772	2.35
lower Quartile	366.75	4	0.00810116	0.8	lower Quartile	470.5	8.5	0.01371194	1.4

Table A.2.5: Raw data on TUNEL staining 24h after initial *tamyc/tamax* gene "knockdown".

Amount of TUNEL signal was estimated 24 h after KD. Values for minimum, median, maximum upper and lower quartile were used for boxplot depiction.

Method	<i>taMyc/Cnox-2</i>	<i>taMyc/ASW</i>	<i>taMyc/Cnox-2+ASW</i>	<i>taMax/Cnox-2</i>	<i>taMax/ASW</i>	<i>taMax/Cnox-2+ASW</i>
BrdU (24h)	0.06665	0.01918*	0.02363*	0.10778	0.0627	0.04637*
BrdU (72h)	0.44033	0.01548*	0.04922*	0.26435	0.00109*	0.01301*
TUNEL (24h)	0.073	0.02052*	0.00417**	0.00327**	0.00029***	1.028E-05***

Table A.2.6: Statistical analyses on BrdU and TUNEL staining.

Statistical analyses of data in table A.2.4 and A.2.5 have been performed with a two-tailed t-test. Significances are indicated with asterisks $p < 0.05$ *, $p < 0.01$ **, $p < 0.001$ ***.

A.2 The Myc/Max network at the base of the metazoan tree of life

A

Day No	ASW				DMSO				2µM				
	Experiment No1	Experiment No3	Experiment No4	Standard Deviation	Experiment No1	Experiment No2	Experiment No3	Experiment No4	Average	Standard Deviation	Experiment No1	Average	Standard Deviation
0	25	25	23	24.33333333	0.942809042	25	25	25	25.75	1.299038106	25	-	-
1	29	28	29	28.66666667	0.471404521	25	33	21	27.75	4.968651729	27	-	-
2	32	37	35	34.66666667	2.054804668	29	38	31	30.5	5.024937811	37	-	-
3	38	41	46	41.66666667	3.299831646	39	48	48	45	6.123724357	44	-	-
4	39	61	56	52	9.416297928	39	49	47	47	5.099019514	48	-	-
5	38	72	55	55	13.88044188	39	47	49	48.5	7.123903424	49	-	-
6	40	52	58	50	7.483314774	53	53	41	50.25	6.219927652	40	-	-
7	45	50	53	49.33333333	3.299831646	47	44	52	50	4.949747468	44	-	-
8	46	62	54	54	6.531972647	48	54	45	51.25	5.068283733	43	-	-
9	45	55	55	50	5	45	47	48	46.66666667	1.247219129	40	-	-
10	54	69	69	61.5	7.5	41	37	39	39	1.632993162	31	-	-
11	58	66	66	62	4	39	52	40	43.66666667	5.906681716	6	-	-
12	62	60	60	61	1	42	39	30	37	5.099019514	0	-	-
13	69	69	69	69	0	26	26	42	34	8	0	-	-
14	77	77	77	77	0	56	56	56	56	0	0	-	-
15	60	60	60	60	0	40	40	40	45	0	0	-	-
16	65	65	65	65	0	45	45	45	39	0	0	-	-
17	66	66	66	66	0	39	39	39	0	0	0	-	-
Day No	3µM				4µM				5µM				
	Experiment No2	Experiment No3	Experiment No4	Standard Deviation	Experiment No1	Experiment No2	Experiment No3	Experiment No4	Average	Standard Deviation	Experiment No1	Average	Standard Deviation
0	25	25	25	25	25	25	25	25	25	0	25	26.5	1.06066017
1	35	33	27	31.66666667	3.399346342	28	32	30	24	2	24	22.5	1.06066017
2	38	40	38	38.66666667	0.942809042	28	32	30	23	33	28	3.5353391	
3	56	44	41	47	6.480740698	30	29	29.5	20	19	19.5	0.3535339	
4	44	55	36	45	7.788880964	28	32	30	6	26	16	7.07106781	
5	49	42	44	45	2.943920289	19	43	31	5	5	5	0	
6	50	41	43	44.66666667	3.858612301	18	38	28	10	8	4	2.82842712	
7	45	36	35	38.66666667	4.496912521	14	31	22.5	0	6	3	2.12132034	
8	46	35	43	41.33333333	4.642796092	12	31	21.5	0	0	0	0	
9	48	41	46	45	2.943920289	17	37	27	10	0	0	0	
10	43	27	31	33.66666667	6.798692685	18	27	22.5	4.5	0	0	0	
11	27	30	28	28.33333333	1.247219129	14	32	23	9	0	0	0	
12	12	0	15	9	6.480740698	14	33	23.5	9.5	0	0	0	
13	3	0	4	2.333333333	1.699673171	18	32	25	7	0	0	0	
14	0	0	0	0	0	23	35	29	6	2	2	2	2
15	0	0	0	0	0	22	18	20	2	2	2	2	2
16	0	0	0	0	0	21	17	19	2	2	2	2	2
17	0	0	0	0	0	0	0	0	0	0	0	0	0
Day No	7µM				10µM								
	Experiment No4	Average	Standard Deviation	Experiment No1	Average	Standard Deviation	Experiment No1	Standard Deviation					
0	26	-	-	36	-	-	-	-					
1	0	-	-	0	-	-	-	-					

A.2 The Myc/Max network at the base of the metazoan tree of life

A

B

Day	10058-F4 2μM/ASW	10058-F4 2μM/DMSO	10058-F4 2μM/ ASW+DMSO	10058-F4 3μM/ASW	10058-F4 3μM/DMSO	10058-F4 3μM/ ASW+DMSO	10058-F4 4μM/ASW	10058-F4 4μM/DMSO	10058-F4 4μM /ASW+DMSO
1	0.12961	0.93333	0.91422	0.284	0.27964	0.19464	0.32946	0.37916	0.3607
2	0.50626	0.51039	0.42553	0.06661	0.09951	0.05476	0.06574	0.41897	0.14832
3	0.66667	0.6859	0.61657	0.35826	0.32329	0.20899	0.00663**	0.09357	0.01455*
4	0.79224	0.48346	0.9189	0.46333	0.64212	0.80161	0.03121*	0.03989*	0.02767*
5	0.78875	0.57992	0.94393	0.37533	1	0.53197	0.11642	0.13816	0.06649
6	0.44444	0.39072	0.30042	0.42098	0.53801	0.39459	0.04836*	0.04382*	0.00795**
7	0.37146	0.51434	0.3146	0.05384	0.08461	0.01455*	0.00783	0.0098**	0.00029***
8	0.35591	0.37446	0.27632	0.08909	0.14316	0.05452	0.01056*	0.01069*	0.00074***
9	0.45437	0.06341	0.15122	0.35611	0.5019	0.33935	0.07015	0.02811*	0.00508**
10	0.25633	0.07418	0.3141	0.04464	0.34142	0.15358	0.00935**	0.00439**	0.02152*
11	0.07836	0.04583*	0.02411	0.00182**	0.02292*	0.0173*	0.01302*	0.02292*	0.01215*
12	0.01807*	0.03595*	0.03752*	0.00317**	0.00864**	0.00562**	0.01334*	0.10885	0.04581*
13	-	-	-	0.0031**	0.01427*	0.02635*	0.03213*	0.33853	0.19201
14	-	-	-	-	-	-	0.20592	0.23391	0.04442*
15	-	-	-	-	-	-	0.055	0.10918	0.09874
16	-	-	-	-	-	-	0.04785*	0.08432	0.07172
17	-	-	-	-	-	-	-	-	0.06021

Day	10058-F4 5μM/ASW	10058-F4 5μM/DMSO	10058-F4 5μM /ASW+DMSO	10058-F4 7μM/ASW	10058-F4 7μM/DMSO	10058-F4 7μM /ASW+DMSO	10058-F4 10μM/ASW	10058-F4 10μM/DMSO	10058-F4 10μM /ASW+DMSO
1	0.01421*	0.47356	0.16094	0.00054***	0.06488	0.00156**	0.00054***	0.06488	0.00156**
2	0.1081	0.30522	0.8668	-	-	-	-	-	-
3	0.00071***	0.01219*	0.00048***	-	-	-	-	-	-
4	0.01504*	0.02013*	0.00342**	-	-	-	-	-	-
5	0.00701**	0.0002***	0.00054***	-	-	-	-	-	-
6	0.042*	0.02121*	0.0014**	-	-	-	-	-	-
7	-	-	-	-	-	-	-	-	-
8	-	-	-	-	-	-	-	-	-
9	-	-	-	-	-	-	-	-	-
10	-	-	-	-	-	-	-	-	-
11	-	-	-	-	-	-	-	-	-
12	-	-	-	-	-	-	-	-	-
13	-	-	-	-	-	-	-	-	-
14	-	-	-	-	-	-	-	-	-
15	-	-	-	-	-	-	-	-	-
16	-	-	-	-	-	-	-	-	-
17	-	-	-	-	-	-	-	-	-

Table A.2.7: Raw data on population sizes after treatment with the 10058-F4 inhibitor.

Animals were counted daily after initial treatment with the 10058-F4 inhibitor. Shown is the animal population size at different time points of the experiment (A). The average value (with standard deviation) was used for graph depiction. Significances are indicated with asterisks $p < 0.05$ *, $p < 0.01$ **, $p < 0.001$ *** (B).

A.2 The Myc/Max network at the base of the metazoan tree of life

A

A

	Day0								
	ASW	DMSO	2μM	3μM	4μM	5μM	7μM	10μM	
Number of Values	87	71	16	73	35	34	25	30	
Average	16.632931	17.3919737	22.529625	13.8299855	17.0960625	18.9226563	16.9332727	19.2103667	
Standard Deviation	10.4270716	9.03170553	8.39941206	5.3832254	7.75360623	9.65553911	10.0913202	9.0670467	
Median	15.077	15.861	21.3125	13.073	15.741	19.5315	14.9815	18.116	
Minimum	1.324	2.075	11.515	2.362	6.716	2.529	0.927	2.48	
Maximum	56.781	41.468	40.743	27.949	33.9	45.764	44.685	38.99	
upper Quartile	23.503	23.1855	27.631	16.968	21.47075	22.8195	23.23125	24.2565	
lower Quartile	8.4965	11.53125	15.184	9.984	10.46275	14.05975	9.663	12.166	
	Day1								
	ASW	DMSO	2μM	3μM	4μM	5μM	7μM	10μM	
Number of Values	99	92	24	85	35	32	0	0	
Average	14.84588	13.1727097	13.55108	10.5078519	10.8134688	5.5283871	0	0	
Standard Deviation	9.42702012	7.83156967	7.4467789	5.20598791	7.19576345	3.03644189	0	0	
Median	13.6035	11.535	13.319	10.202	8.6225	5.235	0	0	
Minimum	1.162	1.289	1.962	0.898	2.866	0.835	0	0	
Maximum	43.635	38.036	35.454	22.271	28.354	12.073	0	0	
upper Quartile	20.75775	17.432	18.882	14.414	13.1455	7.5005	0	0	
lower Quartile	7.2545	7.51	6.698	7.023	5.53675	2.815	0	0	
	Day2								
	ASW	DMSO	2μM	3μM	4μM	5μM	7μM	10μM	
Number of Values	71	105	30	103	41	31	0	0	
Average	10.8607941	13.3438933	7.74309677	7.01640594	10.9738205	3.94596667	0	0	
Standard Deviation	7.62084044	7.90519543	5.51597162	4.84259066	6.1660734	2.99473443	0	0	
Median	8.6395	12.202	6.75	6.014	10.364	3.473	0	0	
Minimum	1.777	0	1.508	0.269	2.619	0.729	0	0	
Maximum	36.51	32.619	23.8	27.269	26.135	13.502	0	0	
upper Quartile	16.067	19.371	9.963	8.82	14.4015	4.48375	0	0	
lower Quartile	5.132	6.694	3.2415	3.272	5.5965	1.78225	0	0	
	Day3								
	ASW	DMSO	2μM	3μM	4μM	5μM	7μM	10μM	
Number of Values	95	115	39	98	51	21	0	0	
Average	10.6080349	11.4245243	5.68882927	8.05092708	8.23768627	3.80518182	0	0	
Standard Deviation	7.14966217	7.26055507	3.63335751	5.41025265	4.9642708	3.15679391	0	0	
Median	9.555	9.014	5.454	7.2065	7.393	3.2275	0	0	
Minimum	1.758	1.033	0	0.883	1.139	0.519	0	0	
Maximum	31.758	42.599	16.155	22.506	22.926	11.699	0	0	
upper Quartile	14.1075	15.30525	8.174	11.026	10.887	5.35575	0	0	
lower Quartile	4.2175	5.54325	2.411	3.87925	3.9735	1.051	0	0	
	Day4								
	ASW	DMSO	2μM	3μM	4μM	5μM	7μM	10μM	
Number of Values	119	128	41	118	44	15	0	0	
Average	7.72159259	9.8727913	4.48142424	6.19853846	7.69616667	3.862125	0	0	
Standard Deviation	5.84195159	6.5429913	2.45706384	4.07993858	4.39985406	2.13323138	0	0	
Median	5.868	8.087	4.154	5.256	6.6095	3.7855	0	0	
Minimum	0.787	0.796	0.64	0	2.129	0.636	0	0	
Maximum	27.283	34.253	10.886	21.423	17.919	7.777	0	0	
upper Quartile	11.2935	12.734	5.412	7.919	10.7585	5.642	0	0	
lower Quartile	3.1775	4.524	2.674	3.421	4.24075	1.98575	0	0	
	Day5								
	ASW	DMSO	2μM	3μM	4μM	5μM	7μM	10μM	
Number of Values	155	167	35	111	57	12	0	0	
Average	8.02905455	9.7161194	4.20955556	7.146	3.58653381	1.32107692	0	0	
Standard Deviation	6.64193246	6.01101638	2.30310759	4.55402361	6.1725	0.81011684	0	0	
Median	5.4185	8.4525	3.6625	5.92	1.696	0.855	0	0	
Minimum	0.899	1.362	0.99	1.072	17.256	0.546	0	0	
Maximum	52.524	30.001	10.742	27.994	9.21775	3.395	0	0	
upper Quartile	11.0435	12.44875	5.362	9.697	4.1285	1.553	0	0	
lower Quartile	3.3215	4.3555	2.608	3.763	0.713	0	0	0	

A.2 The Myc/Max network at the base of the metazoan tree of life

A

	Day6							
	ASW	DMSO	2μM	3μM	4μM	5μM	7μM	10μM
Number of Values	114	122	31	98	47	6	0	0
Average	8.07558879	8.98201639	5.2719375	6.00439583	6.58068889	1.03228571	0	0
Standard Deviation	6.36613433	6.01816715	2.53945763	3.66272016	4.91946549	0.49552936	0	0
Median	5.369	7.8815	5.211	5.5035	4.545	1.079	0	0
Minimum	0.938	0.858	1.198	0.723	1.693	0	0	0
Maximum	29.27	31.794	12.501	18.363	26.639	1.674	0	0
upper Quartile	11.53025	11.263	7.17725	7.91525	9.55	1.3195	0	0
lower Quartile	3.504	4.122	3.23675	3.00075	3.253	0.917	0	0
	Day7							
	ASW	DMSO	2μM	3μM	4μM	5μM	7μM	10μM
Number of Values	112	138	29	99	38	2	0	0
Average	6.75354082	8.17142857	5.78643333	5.602	6.57044444	1.125	0	0
Standard Deviation	4.88040368	5.96775412	3.13354544	3.72806855	4.02454035	0.79549607	0	0
Median	5.406	6.241	5.374	5.278	5.8485	1.686	0	0
Minimum	1.019	0.979	0.86	0.705	1.434	0	0	0
Maximum	24.323	32.969	12.844	18.167	21.392	1.689	0	0
upper Quartile	9.645	10.69725	7.763	7.07475	8.6805	1.6875	0	0
lower Quartile	2.768	3.63675	3.47175	2.6035	3.74975	0.843	0	0
	Day8							
	ASW	DMSO	2μM	3μM	4μM	5μM	7μM	10μM
Number of Values	63	102	29	102	38	0	0	0
Average	7.89914286	7.82974757	3.93016667	5.62448515	4.91297222	0	0	0
Standard Deviation	5.68126371	5.95270673	2.09004306	3.353584	3.35067767	0	0	0
Median	6.307	6.103	3.491	5.081	4.423	0	0	0
Minimum	1.034	1.158	0.658	0.918	0.681	0	0	0
Maximum	34.357	34.227	8.754	17.894	14.64	0	0	0
upper Quartile	10.074	9.858	5.23825	7.645	5.9885	0	0	0
lower Quartile	3.9455	4.012	2.6115	2.983	2.686	0	0	0
	Day9							
	ASW	DMSO	2μM	3μM	4μM	5μM	7μM	10μM
Number of Values	73	83	17	89	49	0	0	0
Average	6.78482192	6.67480952	3.69394444	4.53748276	4.97176596	0	0	0
Standard Deviation	4.75110337	5.62727274	2.2700426	3.26450149	3.29419945	0	0	0
Median	5.081	4.939	3.2705	3.731	4.718	0	0	0
Minimum	1.079	1.575	0.459	0.439	0.381	0	0	0
Maximum	26.429	28.354	9.337	18.316	15.267	0	0	0
upper Quartile	9.113	7.83575	4.126	5.2135	6.514	0	0	0
lower Quartile	3.298	3.16525	2.24875	2.254	2.5925	0	0	0
	Day10							
	ASW	DMSO	2μM	3μM	4μM	5μM	7μM	10μM
Number of Values	81	98	9	84	45	0	0	0
Average	7.56181481	9.85868687	2.23044444	3.78959036	5.73286047	0	0	0
Standard Deviation	5.62964172	7.07800445	1.54284363	3.03900284	3.83750679	0	0	0
Median	6.88	7.89	1.385	2.767	4.702	0	0	0
Minimum	0.556	1.369	0.656	0.662	1.199	0	0	0
Maximum	39.721	33.088	5.037	15.548	18.97	0	0	0
upper Quartile	9.069	13.604	3.044	4.7775	7.672	0	0	0
lower Quartile	4.104	4.551	0.966	1.883	2.777	0	0	0
	Day11							
	ASW	DMSO	2μM	3μM	4μM	5μM	7μM	10μM
Number of Values	56	74	0	46	36	0	0	0
Average	8.72601786	8.59304054	0	3.36004444	7.546	0	0	0
Standard Deviation	5.64590333	5.44936734	0	2.22285111	5.60874218	0	0	0
Median	6.7665	7.029	0	2.698	6.089	0	0	0
Minimum	1.702	1.72	0	0.617	1.506	0	0	0
Maximum	26.936	29.166	0	11.033	23.212	0	0	0
upper Quartile	11.94025	12.479	0	4.005	9.454	0	0	0
lower Quartile	4.70775	4.66725	0	1.922	3.4595	0	0	0

A.2 The Myc/Max network at the base of the metazoan tree of life

	Day12							
	ASW	DMSO	2μM	3μM	4μM	5μM	7μM	10μM
Number of Values	42	53	0	34	43	0	0	0
Average	5.66685366	5.04130189	0	3.33724242	7.80297674	0	0	0
Standard Deviation	3.6170615	6.03384249	0	2.96340011	5.46267096	0	0	0
Median	4.914	3.234	0	2.478	6.29	0	0	0
Minimum	0.785	0.644	0	0.536	1.443	0	0	0
Maximum	17.841	34.279	0	17.37	32.948	0	0	0
upper Quartile	7.352	5.29	0	3.51	10.635	0	0	0
lower Quartile	3.026	2.217	0	1.862	3.774	0	0	0
	Day13							
	ASW	DMSO	2μM	3μM	4μM	5μM	7μM	10μM
Number of Values	48	55	0	6	32	0	0	0
Average	7.3870625	5.37808929	0	2.06466667	8.085	0	0	0
Standard Deviation	5.26315158	5.97991983	0	1.1323771	3.18782398	0	0	0
Median	6.032	2.7135	0	1.5545	8.072	0	0	0
Minimum	0.827	0.483	0	1.069	2.171	0	0	0
Maximum	30.173	23.4	0	4.276	15.751	0	0	0
upper Quartile	9.11125	5.86225	0	2.49425	10.447	0	0	0
lower Quartile	3.95325	1.59425	0	1.2335	6.0045	0	0	0
	Day14							
	ASW	DMSO	2μM	3μM	4μM	5μM	7μM	10μM
Number of Values	49	27	0	0	43	0	0	0
Average	6.18464	7.21467857	0	0	8.41411628	0	0	0
Standard Deviation	4.44826708	5.16291924	0	0	4.75639918	0	0	0
Median	4.9285	6.1125	0	0	7.249	0	0	0
Minimum	0.85	0.754	0	0	1.198	0	0	0
Maximum	24.106	23.916	0	0	18.355	0	0	0
upper Quartile	8.654	10.0495	0	0	11.281	0	0	0
lower Quartile	2.87275	3.01125	0	0	4.2395	0	0	0
	Day15							
	ASW	DMSO	2μM	3μM	4μM	5μM	7μM	10μM
Number of Values	34	27	0	0	45	0	0	0
Average	5.13014286	6.26775	0	0	1.75408889	0	0	0
Standard Deviation	3.0877939	3.77824968	0	0	0.94745722	0	0	0
Median	3.985	5.7595	0	0	1.389	0	0	0
Minimum	1.027	1.002	0	0	0.581	0	0	0
Maximum	13.504	16.062	0	0	4.058	0	0	0
upper Quartile	7.3795	7.394	0	0	2.45	0	0	0
lower Quartile	2.568	3.76325	0	0	0.996	0	0	0
	Day16							
	ASW	DMSO	2μM	3μM	4μM	5μM	7μM	10μM
Number of Values	35	26	0	0	39	0	0	0
Average	4.82502778	5.65144444	0	0	1.97476923	0	0	0
Standard Deviation	2.98059142	3.25379702	0	0	0.84916675	0	0	0
Median	4.262	5.093	0	0	1.76	0	0	0
Minimum	0.983	0.481	0	0	0.675	0	0	0
Maximum	13.076	14.32	0	0	4.354	0	0	0
upper Quartile	6.2185	7.6305	0	0	2.5925	0	0	0
lower Quartile	2.405	3.0585	0	0	1.3725	0	0	0
	Day17							
	ASW	DMSO	2μM	3μM	4μM	5μM	7μM	10μM
Number of Values	32	21	0	0	0	0	0	0
Average	3.57475758	3.87040909	0	0	0	0	0	0
Standard Deviation	1.75255858	1.96587574	0	0	0	0	0	0
Median	3.226	3.207	0	0	0	0	0	0
Minimum	1.009	0.924	0	0	0	0	0	0
Maximum	6.898	8.88	0	0	0	0	0	0
upper Quartile	5.169	5.16	0	0	0	0	0	0
lower Quartile	2.041	2.48725	0	0	0	0	0	0

A.2 The Myc/Max network at the base of the metazoan tree of life

A

B

Day	10058-F4 2μM/ASW	10058-F4 2μM/DMSO	10058-F4 2μM/ASW+DMSO	10058-F4 3μM/ASW	10058-F4 3μM/DMSO	10058-F4 3μM/ ASW+DMSO	10058-F4 4μM/ASW	10058-F4 4μM/DMSO	10058-F4 4μM /ASW+DMSO
0	0.0367*	0.08679	0.03479*	0.04557*	0.06965	0.0363*	0.82074	0.94788	0.84005
1	0.52752	0.83028	0.7904	0.0003***	0.0105*	0.00082***	0.02924*	0.1393	0.04984*
2	0.00435**	0.01263*	0.00474**	1.597E-07***	1.323E-06***	2.815E-08***	0.30274	0.74826	0.471
3	0.00038***	2.891E-05***	5.501E-05***	0.01992*	0.00116**	0.00187**	0.08307	0.01442*	0.02524*
4	0.00279**	3.872E-05***	0.0003**	0.03291*	1.166E-05***	0.00038***	0.97843	0.11495	0.40262
5	0.00183**	1.406E-06***	5.695E-05***	0.39289	0.00188**	0.03312*	0.33372	0.00537**	0.05481
6	0.028*	0.00134**	0.00667**	0.01363*	3.808E-05***	0.00045***	0.23679	0.01974	0.06332
7	0.42785	0.04195*	0.12145	0.1281	0.00036***	0.00378**	0.974	0.15021	0.39034
8	0.00064***	0.00064***	0.00046***	0.0029**	0.00142**	0.00076***	0.0077**	0.00639**	0.00483**
9	0.01208	0.03104*	0.01852*	0.00098***	0.00281**	0.00067***	0.034*	0.06154	0.03655*
10	0.00749**	0.00184**	0.00343**	6.404E-07***	1.331E-11***	2.798E-10***	0.0755	0.00048***	0.00406**
11	0.14589	0.1241	0.12826	1.070E-07***	1.500E-08***	6.804E-09***	0.40664	0.36003	0.332
12	-	-	-	0.84517	0.13865	0.03981*	0.4089	0.02356*	0.0115*
13	-	-	-	0.0188*	0.1877	0.07649	0.51416	0.02298*	0.10388
12	-	-	-	0.17917	0.18875	0.17645	0.02324*	0.32586	0.04305*
15	-	-	-	-	-	-	1.585E-09***	1.231E-10***	6.530E-11***
16	-	-	-	-	-	-	2.930E-07***	8.246E-09***	1.300E-08***
17	-	-	-	-	-	-	0.05649	0.07388	0.0547

Day	10058-F4 5μM/ASW	10058-F4 5μM/DMSO	10058-F4 5μM /ASW+DMSO	10058-F4 7μM/ASW	10058-F4 7μM/DMSO	10058-F4 7μM /ASW+DMSO	10058-F4 10μM/ASW	10058-F4 10μM/DMSO	10058-F4 10μM /ASW+DMSO
0	0.28505	0.47678	0.2826	0.90442	0.40706	0.92156	0.23437	0.35769	0.23205
1	3.464E-07***	6.230E-07***	2.193E-07***	0.12215	0.09951	0.11147	0.12215	0.09951	0.11147
2	3.709E-07***	3.933E-07***	1.071E-07***	-	-	-	-	-	-
3	3.958E-05***	1.212E-05***	1.832E-05***	-	-	-	-	-	-
4	0.01144*	0.00103**	0.00339**	-	-	-	-	-	-
5	0.00065***	4.182E-06***	5.333E-05***	-	-	-	-	-	-
6	0.01281*	0.00218**	0.00508**	-	-	-	-	-	-
7	0.1676	0.13368	0.14961	-	-	-	-	-	-
8	0.1857	0.19564	0.18749	-	-	-	-	-	-
9	-	-	-	-	-	-	-	-	-
10	-	-	-	-	-	-	-	-	-
11	-	-	-	-	-	-	-	-	-
12	-	-	-	-	-	-	-	-	-
13	-	-	-	-	-	-	-	-	-
12	-	-	-	-	-	-	-	-	-
15	-	-	-	-	-	-	-	-	-
16	-	-	-	-	-	-	-	-	-
17	-	-	-	-	-	-	-	-	-

Table A.2.8: Raw data on animal sizes after treatment with the 10058-F4 inhibitor.

Animal size was measured daily in mm² and data were taken from four different experiments (A). Minimum, median, maximum, upper and lower quartile was used for boxplot depiction. Significances are indicated with asterisks p < 0.05 *, p < 0.01 **, p < 0.001 *** (B).

A.2 The Myc/Max network at the base of the metazoan tree of life

A

A

0,1% DMSO in ASW					5µM 10058-F4 in ASW (72h)				
Name	Nuclei	BrdU signal	Quotient	Percentage	Name	Nuclei	BrdU signal	Quotient	Percentage
Tier1a	650	56	0.08615385	8.6	Tier1a	636	303	0.47641509	48
Tier1b	282	64	0.22695035	22.7	Tier1b	726	22	0.03030303	30
Tier2a	661	245	0.37065053	37	Tier2a	777	59	0.07593308	7.6
Tier3a	611	62	0.101473	10	Tier2b	762	206	0.27034121	27
Tier3b	338	108	0.31952663	32	Tier2c	746	138	0.1849866	18
Tier4a	651	171	0.26267281	26	Tier3a	422	233	0.5521327	55
Tier5a	641	335	0.5226209	52	Tier3b	642	266	0.41433022	41
Tier5b	775	297	0.38322581	38	Tier4a	379	209	0.55145119	55
Tier5c	325	143	0.44	44	Tier4b	589	142	0.24108659	24
Tier6a	811	320	0.3945746	39	Tier5a	611	279	0.45662848	46
Tier6b	795	166	0.20880503	21	Tier5b	762	191	0.25065617	25
Tier7a	732	364	0.49726776	50	Tier6a	776	178	0.22938144	23
Tier7b	621	352	0.5668277	56	Tier6b	581	42	0.07228916	7.2
Tier8a	981	180	0.18348624	18	Tier7a	772	82	0.10621762	11
Tier8b	877	190	0.21664766	22	Tier7b	606	210	0.34653465	35
					Tier8a	597	28	0.04690117	4.7
					Tier8b	534	131	0.24531835	25
					Tier9a	572	187	0.32692308	33
					Tier9b	572	242	0.42307692	42
Average	650.066667	203.533333	0.31872552	31.7533333	Average	634.842105	165.684211	0.27899509	29.3421053
Stdev	195.165389	105.311517	0.14513625	14.4317643	Stdev	114.400158	84.1809158	0.16376745	15.2720355
Minimum	282	56	0.08615385	8.6	Minimum	379	22	0.03030303	4.7
Median	651	180	0.31952663	32	Median	611	187	0.25065617	27
Max	981	364	0.5668277	56	Max	777	303	0.5521327	55
upper Quartile	785	308.5	0.4172873	41.5	upper Quartile	754	221.5	0.41870357	41.5
lower Quartile	616	125.5	0.21272635	21.5	lower Quartile	576.5	106.5	0.14560211	20.5

B

0,1% DMSO in ASW					5µM 10058-F4 in ASW (24h)				
Name	Nuclei	BrdU signal	Quotient	Percentage	Name	Nuclei	BrdU signal	Quotient	Percentage
1	625	105	0.168	17	A	863	119	0.13789108	14
12	762	174	0.22834646	23	B	557	129	0.23159785	23
13	553	114	0.20614828	21	C	546	94	0.17216117	17
14	936	205	0.21901709	22	D	567	53	0.09347443	9
17	554	60	0.10830325	11	E	595	141	0.23697479	24
18	815	118	0.14478528	14	F	401	93	0.2319202	23
3	535	114	0.21308411	21	G	546	94	0.17216117	17
15	899	244	0.27141268	27	H	496	71	0.14314516	14
					I	613	66	0.10766721	11
					J	733	215	0.29331514	30
					K	759	229	0.30171278	30
					L	918	79	0.08605664	9
					M	1040	318	0.30576923	31
					N	1056	295	0.27935606	28
					O	809	51	0.06304079	6
Average	709.875	141.75	0.19488714	19.5	Average	699.933333	136.466667	0.19041625	19.0666667
Stdev	153.036301	56.605543	0.04840683	4.84767986	Stdev	194.604031	83.8728138	0.08115762	8.22570497
Minimum	535	60	0.10830325	11	Minimum	401	51	0.06304079	6
Median	936	244	0.27141268	27	Median	1056	318	0.30576923	31
Max	693.5	116	0.2096162	21	Max	613	94	0.17216117	17
upper Quartile	836	181.75	0.22134943	22.25	upper Quartile	836	178	0.25816543	26
lower Quartile	553.75	111.75	0.16219632	16.25	lower Quartile	551.5	75	0.12277914	12.5

Table A.2.9: Raw data on BrdU signal after treatment with the 10058-F4 inhibitor (5µM).

Data on cell proliferation were collected 24 h (A) and 72 h (B) after initial inhibitor treatment with the small molecule inhibitor. Values for minimum, median, maximum, upper and lower quartile were used for boxplot analyses.

A.2 The Myc/Max network at the base of the metazoan tree of life

A

0,1% DMSO in ASW					5µM 10058-F4 in ASW (24h)				
Name	Nuclei	TUNEL signal	Quotient	Percentage	Name	Nuclei	TUNEL signal	Quotient	Percentage
Tier1_a	483	12	0.02484472	2.5	Tier1_a	555	18	0.03243243	3.2
Tier1_b	787	5	0.00635324	0.6	Tier1_b	439	34	0.07744875	7.7
Tier1_c	512	8	0.015625	0.15	Tier1_c	765	30	0.03921569	3.9
Tier2_b	484	10	0.02066116	2	Tier2_a	538	17	0.03159851	3.1
Tier2_c	569	10	0.01757469	1.8	Tier2_b	462	19	0.04112554	4.1
Tier3_a	409	5	0.01222494	1.2	Tier2_c	492	29	0.05894309	5.8
Tier3_b	474	5	0.01054852	0.1	Tier3_a	392	17	0.04336735	4.3
Tier3_c	374	9	0.02406417	0.24	Tier3_b	457	13	0.02844639	2.8
Tier4_a	298	9	0.03020134	3	Tier3_c	495	17	0.03434343	3.4
Tier4_c	568	2	0.00352113	0.3	Tier4_a	504	22	0.04365079	4.3
Tier5_a	437	8	0.01830664	1.8	Tier4_b	516	17	0.03294574	3.3
Tier5_b	741	7	0.00944669	1	Tier4_c	504	14	0.02777778	2.7
Tier5_c	836	4	0.00478469	0.5	Tier5_a	423	15	0.03546099	3.5
Tier6_a	665	3	0.00451128	0.5	Tier5_b	430	31	0.07209302	7.2
Tier6_c	869	6	0.00690449	0.7	Tier6_a	391	9	0.0230179	2.3
Tier7_a	693	3	0.004329	0.4	Tier7_a	325	17	0.05230769	5.2
Tier7_b	446	8	0.01793722	1.8	Tier7_b	261	8	0.03065134	3
Tier7_c	580	4	0.00689655	0.7	Tier7_c	352	1	0.00284091	0.3
Average	568.055556	6.55555556	0.01326308	1.07166667	Average	461.166667	18.22222222	0.03931485	3.89444444
Stdev	159.793086	2.773329772	0.00795407	0.84714062	Stdev	105.136023	8.270130696	0.01704644	1.69753816
Minimum	298	2	0.00352113	0.1	Minimum	261	1	0.00284091	0.3
Median	869	12	0.03020134	3	Median	765	34	0.07744875	7.7
Max	540	6.5	0.01138673	0.7	Max	459.5	17	0.03490221	3.45
upper Quartile	686	8.75	0.01821428	1.8	upper Quartile	504	21.25	0.04357993	4.3
lower Quartile	453	4.25	0.00648907	0.425	lower Quartile	399.75	14.25	0.03088813	3.025

0,1% DMSO (ASW)					5µM 10058-F4 in ASW (72h)				
Name	Nuclei	Signal	Quotient	Percentage	Name	Nuclei	Signal	Quotient	Percentage
Tier1a	400	5	0.0125	1.3	Tier1a	484	14	0.02892562	2.9
Tier1b	516	5	0.00968992	1	Tier1b	342	19	0.05555556	5.5
Tier2a	521	7	0.0134357	1.3	Tier1c	546	12	0.02197802	2.2
Tier2b	469	8	0.01705757	1.7	Tier2a	576	15	0.02604167	2.6
Tier3a	577	1	0.0017331	0.2	Tier2b	506	9	0.01778656	1.7
					Tier3a	476	5	0.0105042	1
					Tier3b	606	13	0.02145215	2.1
					Tier3c	334	6	0.01796407	1.7
					Tier4a	357	7	0.01960784	1.9
					Tier4b	329	3	0.00911854	6.5
					Tier5a	244	16	0.06557377	3.7
					Tier5b	325	12	0.03692308	3.7
					Tier6a	471	10	0.02123142	2.1
					Tier6b	656	3	0.00457317	0.5
Average	496.6	5.2	0.01088326	1.1	Average	446.571429	10.28571429	0.02551683	2.72142857
Stdev	59.2101343	2.4	0.00514588	0.50199602	Stdev	120.587677	4.802210375	0.01643369	1.596057
Minimum	516	5	0.0125	1.3	Minimum	473.5	11	0.02134178	2.15
Median	400	1	0.0017331	0.2	Median	244	3	0.00457317	0.5
Max	577	8	0.01705757	1.7	Max	656	19	0.06557377	6.5
upper Quartile	521	7	0.0134357	1.3	upper Quartile	536	13.75	0.02820463	3.5
lower Quartile	469	5	0.00968992	1	lower Quartile	336	6.25	0.01783094	1.75

Table A.2.10: Raw data on TUNEL signal after treatment with 5µM 10058-F4 inhibitor (5µM).

Data on apoptosis were collected 24 h (A) and 72 h (B) after initial treatment with the small molecule inhibitor. Values for minimum, median, maximum upper and lower quartile were used for boxplot depiction.

Method	Inhibitor/DMSO
BrdU (24h)	0.89719
BrdU (72h)	0.65267
TUNEL (24h)	5.761E-07***
TUNEL (72h)	0.04981*

Table A.2.11: Statistical analyses on BrdU and TUNEL staining..

Statistical analyses of data in table A.2.9 and A.2.10. Significances are indicated with asterisks $p < 0.05$ *, $p < 0.001$ ***.

A.3 Regeneration and self/ non-self recognition in the phylum Placozoa

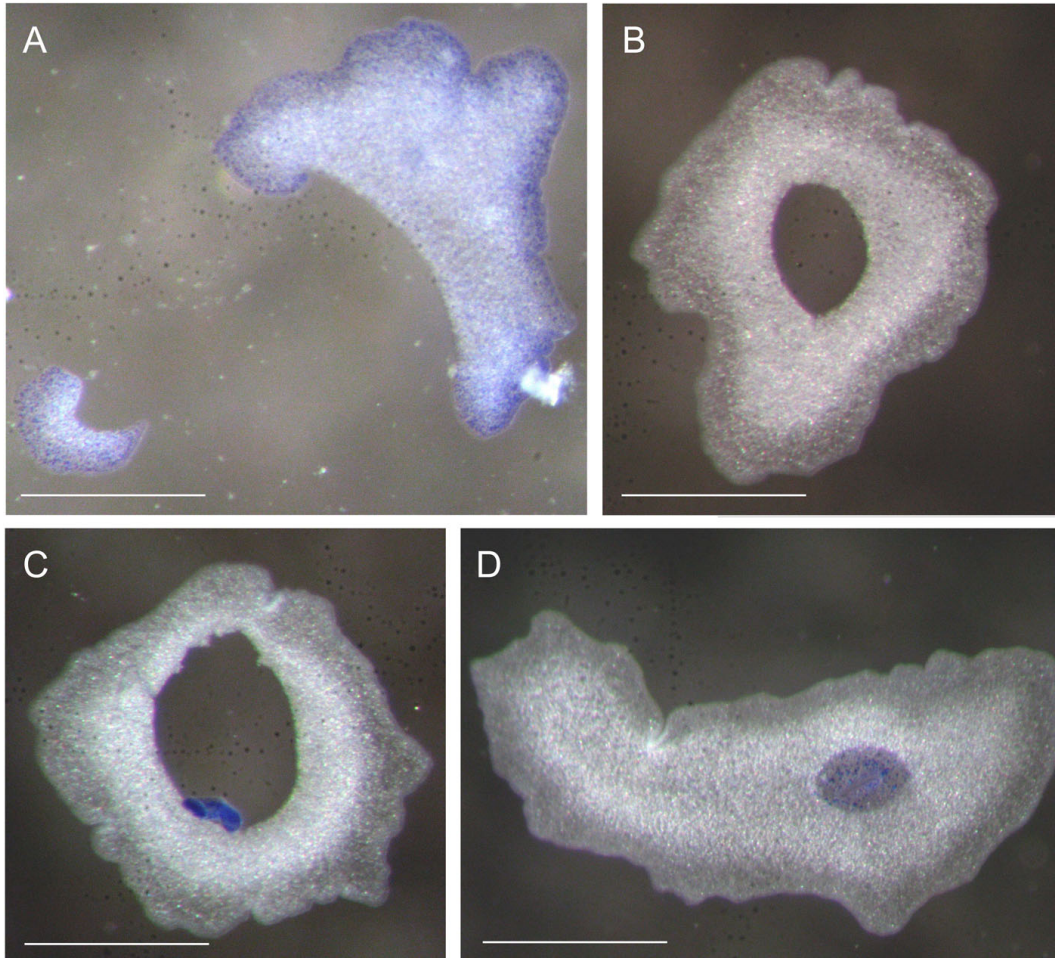


Figure A.3.1: Grafting procedure exemplified by a *Trichoplax adhaerens* autograft.

To visualize the donor tissue, the animal was stained with methylene blue and after this live coloration, a piece of margin was cut off with a sterile acupuncture needle (A). The acceptor individual was prepared for the transplantation by cutting a small hole in the animals' center (B). The blue stained donor tissue was then placed into the hole for tissue intergrowth (C). After 18 hours, the donor tissue completely merged into the acceptor individual (D) forming a central hole surrounded by cells of the donor tissue that keep their marginal fate. Scale bar marks 100 μm in A-D.

A.3 Regeneration and self/ non-self recognition in the phylum Placozoa

No.	PRIMER NAME	SEQUENCE	FITS FOR HAPLOTYPE
1	H1_spez_rv	5'-ACCGGGCCCCAACCTA-3'	H1, H17
2	H2_spez_rv	5'-CCCAGGGATCCTAACGATC-3'	H2
3	CladeV_spez_rv	5'-CGGATCCTTCTCCTGATT-3'	H4, H9, H13, H14, H15
4	CladeIII_spez_fw	5'-TCCAACGGATCCCTTAGGTACC-3'	H7, H8, H16
5	placo_uni_fw	5'-CGAGAAGACCCATTGAGCTTTACTA-3'	all known haplotypes
6	placo_uni_rv	5'-TACGCTGTTATCCCCATGGTAACTTT-3'	all known haplotypes

Table A.3.1: Primers used for genetic haplotype and clade identification.

Haplotype/clade-specific primers (no. 1-4) were combined with the respective universal forward (fw) or reverse (rv) primer (no. 5/6) to specifically amplify parts of the placozoan 16S-b fragment.

		ACCEPTOR									
		Clade I				Clade III		Clade IV	Clade V		
		H1	H2	H2	H2	H7	H16	H19	H13	H15	
		'Grell'	'CAR-Pan-4'	'ROS'	'HKG-C1'	'OJ-gamma'	'KEN-A'	'ADL-1'	'M153E-2'	'M2RS3-11'	
DONOR	H1	'Grell'	39/22	63/24	20/1	20/7	17/4	34/11	10/0	6/2	7/2
	H2	'CAR-Pan-4'	41/23	20/9	16/7	10/1	5/0	7/2	10/0	5/2	7/1
	H2	'ROS'	20/6	10/5	5/4	5/2					
	H2	'HKG-C1'	20/6	10/4	5/3	19/6					
	H7	'OJ-gamma'	10/3	6/2			5/3		5/3	10/1	5/0
	H16	'KEN-A'	45/11					3/2			
	H19	'ADL-1'	10/0	10/0			5/2		10/7	5/2	8/2
	H13	'M153E-2'	8/3	7/2			5/0		6/3	5/5	12/5
	H15	'M2RS3-11'	11/2	8/3			11/0		5/4	10/6	5/4

Table A.3.2: Cross classification - Raw data of grafting experiments.

The numbers indicate experiments/successful (transitory) fusion of tissues. In case of grafting of different haplotypes, individuals were used as both: donor and acceptor respectively. Autografts are highlighted in yellow, intergrafts in green and xenografts in red.

A.3 Regeneration and self/ non-self recognition in the phylum Placozoa

	experiment	fusions	fus/exp [%]	taxonomic group
within H1	39	22	56	1
within H2 ('PAN')	20	9	45	1
within H2 ('ROS')	5	4	80	1
within H2 ('HKG')	19	6	32	1
within H7	5	3	60	1
within H16	3	2	66	1
within H19	10	7	70	1
within H13	5	5	100	1
within H15	5	4	80	1
within clade I	240	89	37	2
within clade V	22	11	50	2
clade I / cladeIII	124	33	27	3
clade I / clade IV	40	0	0	3
clade I / clade V	59	17	29	3
clade III / clade IV	10	5	50	3
clade III / clade V	31	1	3	3
Clade IV /clade V	24	11	46	3

	Group 1	Group 2	Group 3
Median	66.00	43.50	28.00
Minimum	32.00	37.00	0.00
Maximum	100.00	50.00	50.00
Upper Quartile	80	46.75	41.75
Lower Quartile	56	40.25	9

Jonckheere-Terpstra-Test	
	Fusion Frequencies
Number of Levels in taxonomic group	3
N	15
Observed J-T-Statistic	5.5
Median J-T-Statistic	34
Std. Deviation of J-T-Statistic	9.138
Std J-T-Statistic	-3.119
Asymptotic significance (2-tailed)	0.002
a Grouping Variable: taxonomic group	

Table A.3.3: Data used for boxplot analyses.

Intergrowth frequencies were pooled into different taxonomic groups depending on the phylogenetic relatedness of grafted tissues: autografts (group 1) intergrafts (group 2) and xenografts (group 3). For graphical representation via boxplot (figure 2.3.1 B) the median, minimum, maximum, lower and upper quartile values were calculated with Excel® (Microsoft® Excel® for Mac 2011, version 14.2.5). Statistical analyses were performed with the Jonckheere-Terpstra test in SPSS® Statistics (IBM® SPSS® Statistics, version 21.0).

A.3 Regeneration and self/ non-self recognition in the phylum Placozoa

		Clade I			Clade III		Clade IV	Clade V	
		H2 'CAR-PAN-4'	H2 'ROS'	H2 'HKG-C1'	H7 'OJ-gamma'	H16 'KEN-A'	H19 'ADL-1'	H13 'M153E-2'	H15 'M2RS3-11'
H1	'Grell'	0.11	0.09	1.00	1.00	0.46	1.00	1.00	1.00
H2	'CAR-PAN-4'		1.00	0.30	0.45	-	1.00	1.00	0.57
H2	'ROS'			1.00					
H2	'HKG-C1'								
H7	'OJ-gamma'						1.00	1.00	1.00
H16	'KEN-A'								
H19	'ADL-1'							1.00	0.10
H13	'M153E-2'								0.67

Table A.3.4: Statistical analyses on donor/acceptor roles.

Utilized haplotype combinations were investigated for possible effects on donor/acceptor role allocation. Indicated numbers are the 'p' values of the two-tailed Fisher's exact test. None of the tested haplotype combinations shows significances concerning which haplotype is donor and which acceptor ($p > 0.05$), thus the arrangement of donor/acceptor individuals does not influence intergrowth success. Analyses were made with in in SPSS® Statistics (IBM® SPSS® Statistics, version 21.0).

		Clade I			Clade III		Clade IV	Clade V	
		H2 'CAR-PAN-4'	H2 'ROS'	H2 'HKG-C1'	H7 'OJ-gamma'	H16 'KEN-A'	H19 'ADL-1'	H13 'M153E-2'	H15 'M2RS3-11'
H1	'Grell'	143/70	23/5	23/1	transplants died	36/0	no intergrowth	7/0	8/0
H2	'CAR-PAN-4'				9/0	extinct	no intergrowth	13/0	4/0
H2	'ROS'								
H2	'HKG-C1'								
H7	'OJ-gamma'						2/0	transplants died	12/0
H16	'KEN-A'								
H19	'ADL-1'							4/0	2/0
H13	'M153E-2'								-

Table A.3.5: Results of PCR analyses.

Data are summed up independent of the genetic background of the donor/acceptor tissue. The first number indicates performed experiments while the second states the number of identified chimeras. Only intergrafts of *Trichoplax adhaerens* (H1) and H2 (here the 'PAN' 'ROS' and 'HKG-C1' clone) tissue produced long-term chimeras. Transplants of H1 and H13 with H7 died before being tested. Some intergraft and xenograft experiments with H16 could not be performed as this lineage died off. Haplotype combinations tested were used as donor and acceptor equally (data not shown). Intergrowth of H13 and H15 could not be tested (-) as their 16S sequences are separated by only 1 base pair and PCR-based specific haplotype detection was not successful yet.

Curriculum Vitae

Dipl. Biol. Karolin von der Chevallerie

Lutherstrasse 34, 30171 Hannover, born 22.12.1981 in Großburgwedel

Education

- Sept. 2008 - Dez 2013** PhD Student, Leibniz Universität Hannover title of PhD thesis: "Experimental studies on the tumor suppressor *p53*, the *myc* proto-oncogene and tissue compatibility in the basal metazoan phylum Placozoa"
- Oct. 2005 - Aug 2008** M. Sc. (Diplom) Biology Leibniz Universität Hannover examination subjects: zoology, genetics, microbiology; title of diploma thesis: "First Experimental Approaches to Vision, Proliferation and Apoptosis in *Trichoplax adhaerens*", grade: *very good*
- Oct. 2002 - Oct 2005** B. Sc. (Vordiplom) Biology Leibniz Universität Hannover
- June 2002** General qualification for university entrance (Abitur) Gymnasium Mellendorf, Wedemark

Research Experiences

- Nov. 2009** Cold Spring Harbor Course "Immunocytochemistry, *In Situ* Hybridization & Live Cell Imaging", Cold Spring Harbor Laboratories, New York, USA.
- Sept. 2008 - Dez 2013** PhD thesis: ITZ, Ecology & Evolution, Stiftung Tierärztliche Hochschule Hannover, Prof. Dr. Bernd Schierwater.
- Feb. 2008 - May 2008** Diploma thesis: Cellular Competition, Centro National Investigation Oncológicas (CNIO) Madrid, Spain, Dr. Eduardo Moreno.
- Nov. 2007 - Aug. 2008** Diploma thesis: ITZ, Ecology & Evolution, Stiftung Tierärztliche Hochschule Hannover, Prof. Dr. Bernd Schierwater.
- Mar. 2007 - Apr. 2007** Research projects: Department of Molecular, Cellular and Developmental Biology, Yale University, New Haven, USA, Prof. Dr. Stephen L. Dellaporta.
- July 2006 - Oct. 2007** Research projects: ITZ, Ecology & Evolution, Stiftung Tierärztliche Hochschule Hannover, Prof. Dr. Bernd Schierwater.

Teaching Experiences

- May 2009 - May 2012** Teaching assistant: Volker Schmid Training Course "Experimental Developmental Biology of Marine Invertebrates", Station Biologique de Roscoff, France.
- Sept. 2008 - Dez 2013** Supervision of Bachelor- and Master thesis, Stiftung Tierärztliche Hochschule Hannover.
- Nov. 2007 - Dez 2013** Supervision of practical courses: Molecular ecology & evolution, Stiftung Tierärztliche Hochschule Hannover.

Grants and Fellowships

- Jan. 2010 - Dec. 2012** PhD fellowship, Evangelisches Studienwerk Villigst e.V.
- Sept. 2009** Travel grant, Boehringer Ingelheim Fonds
- Sept. 2008 - Dec. 2009** "Otto Bütschli" fellowship, Stiftung Tierärztliche Hochschule Hannover

Presentations

- von der Chevallerie K. and Schierwater B. (2009)** *Evolution of Apoptosis and Cell Proliferation in Animals: Genetic Studies on the Placozoan Trichoplax adhaerens*, International workshop: Searching for Eve - Basal Metazoans and the Evolution of Multicellular Complexity, evangelische Akademie Tutzing, Germany.
- von der Chevallerie K. and Schierwater B. (2009)** *Evolution of Apoptosis and Cell Proliferation in Animals: Genetic Studies on the Placozoan Trichoplax adhaerens*, International Workshop of the Hydrozoan Society, Lecce, Italy.
- von der Chevallerie K. and Schierwater B. (2009)** *Trichoplax adhaerens, a Model Organism not only for Evolutionary Biology*, Seminar: Northern Illinois University, Illinois, USA.
- von der Chevallerie K., Moreno, E. Schierwater, B. (2009)** *Patterns of Cell Proliferation in Trichoplax adhaerens (Placozoa)*, poster presentation "14th Annual DZG Evolution PhD Meeting 2009", Munich, Germany.
- von der Chevallerie K., Moreno E., Schierwater B. (2008)** *Trichoplax & cell proliferation*, 2nd North German Evolution and Development Symposium, Zoological Institute Christian-Albrechts- University, Kiel, Germany.
- von der Chevallerie K., Bergmann T., Schierwater B. (2007)** *Opsin genes in Trichoplax adhaerens*, 1st North German Evolution and Development Symposium, ITZ, Ecology & Evolution, Stiftung TiHo Hannover, Germany.

Acknowledgements

This thesis wouldn't have been possible without the help of various people that contributed directly or indirectly to the completion of my studies. In this section I'll now try to express my appreciation for their material and intellectual support.

First and foremost I'd like to express my deep gratitude to my supervisor Prof. Dr. Bernd Schierwater for giving me this very interesting topic to work on and also for supporting me in every possible way. He did not only help me to challenge every scientific problem I had but also provided me chances to attend meetings and courses that substantially improved my professional and personal skills.

I am furthermore thankful to Prof. Dr. Dieter Steinhagen who willingly agreed to review this thesis and to Prof. Dr. Küster for chairing the disputation.

I had a great time during my work in the ITZ, whose (present and former) team members did not only help me a lot during the time of my studies, but also created such a pleasant atmosphere that it often did not feel like work at all. Without Annkathrin Acktun, Nicole Bartkowiak, Tjard Bergmann, Jutta Bunnenberg, Dr. Sandra Damm, Dr. Michael Eitel, Angie Faust, Wiebke Feindt, PD Dr. Heike Hadrys, Rebecca Herzog, Tina Herzog, Dr. Eckhard Holtorf, Dr. Wolfgang Jakob, Ulrike Oberjatzas, Haju Osigus, Dr. Omid Paknia, Sarah Rolfes, Dr. Sven Sagasser, Dr. Dasa Schleicherova, Björn Seegebarth, Dr. Sabrina Simon and Karina Zimmer the time in the institute would have been only half as good. - Thanks a lot for the help, support and fun!

My academic and personal education would not have been the same without diverse stays abroad and fruitful international collaborations that brought me into contact with great scientists like Prof. Dr. Stephen Dellaporta, Prof. Dr. Rob DeSalle, Dr. Eduardo Moreno, Dr. Neil Blackstone and Dr. John Murray. The participation in three "Volker Schmidt" training courses in Roscoff (France) as a supervisor significantly enriched the time of my studies and I really appreciate the support and help of the people working at the "Station Biologique de Roscoff".

I'd like to thank Prof. Dr. Georgios Tsiavaliaris, Andrea Topf, Katharina Stahl and Christian Wassmann for helping me essentially with the protein expression project.

Acknowledgements

I am deeply thankful for financial support from Prof. Dr. Bernd Schierwater and the Tierärztliche Hochschule Hannover by giving me an “Otto Bütschli” scholarship. The Böhringer Ingelheim Fonds financially enabled my participation at the Cold Spring Harbor Course in 2009 and the Evangelische Studienwerk e.V. Villigst granted three years of financial support by a PhD fellowship, which made this thesis possible.

Ein großer Dank gebührt natürlich meiner Familie, die mich immer unterstützt und an mich geglaubt hat.- Ihr hattet es auch wirklich nicht immer leicht mit mir!

Vielen Dank auch meinen Freunden (besonders Anne+Andy, Sanny+Timo, Basti+Doro) die mich auch mal ablenken konnten und immer für mich da waren.

Den größten Dank verdient jedoch Dr. Hauke Horn. Er hat stets zu mir gestanden, mich immer unterstützt und manchmal einfach nur ertragen. Dankeschön!

List of Publications

Schierwater B., Eitel M., Osigus H-J, **von der Chevallerie K.**, Bergmann T., Hadrys H., Cramm M., Heck L., L.M.R., und R. DeSalle (2010) *Trichoplax and Placozoa: one of the crucial keys to understanding metazoan evolution*. page 289-326 in Key transitions in animal evolution, R. DeSalle and B. Schierwater, eds. CRC Press.

von der Chevallerie K., Eitel M., Schierwater B. (2010) *Focus on an unexpected discovery in Roscoff - a warm water species of the phylum Placozoa*. Cah Biol Mar. 212-21.

Schierwater B., Eitel M., **von der Chevallerie K.**, Jakob W. (2011) *Der Ursprung der Zelldifferenzierung in Metazoen*. Journal: Stiftung Tierärztliche Hochschule Hannover, Die Zelle: Vielfalt - Kommunikation - Wachstum 79-82.

Eitel M., Jakob W., Osigus H-J, Paknia O., **von der Chevallerie K.**, Bergmann T., Schierwater, B. (2013) *Trying to resolve the base of the Metazoa* Deep Metazoan Phylogeny, The Backbone of the Tree of Life. De Gruyter, in press.

von der Chevallerie K., Rolfes S., Schierwater B. (2013) *Inhibitors of the p53-Mdm2 interaction increase apoptosis and produce abnormal phenotypes in the placozoan Trichoplax adhaerens (F.E. Schulze)*., Development Genes and Evolution, submitted.

von der Chevallerie K., Topf A., Sagasser S., Tsiavaliaris G., Schierwater B. (2013) *The Myc/Max network at the base of the Metazoan tree of life.*, to be submitted to Molecular Biology and Evolution.

von der Chevallerie K., Kosubek, J. Schleicherova D., Eitel M., Schierwater B. (2013) *Regeneration and self/non-self recognition in the phylum Placozoa.*, in submission to Zoology.